# Measurement of charged fragments production cross sections (dσ/dE) in the interactions of C-ions with C,H,O targets

## Episode II: forward angles

IlaMi for Roma and Milano, June 2020

# Experimental SETUP

CNAO

**Thin Targets based on C,H and O elements: PMMA, Graphite and Plastic Scintillator**

- The fragments production (Z=1) has been measured as a function of the kinetic energy for 4 angles;
- The Time of Flight in thin plastic scintillators and the energy deposit in the inorganic crystals has been used for PID and kinetic energy measurements;

The thin targets (1-2 mm) do not require, as a first approximation, the implementation of a correction for the fragments absorption inside the target.

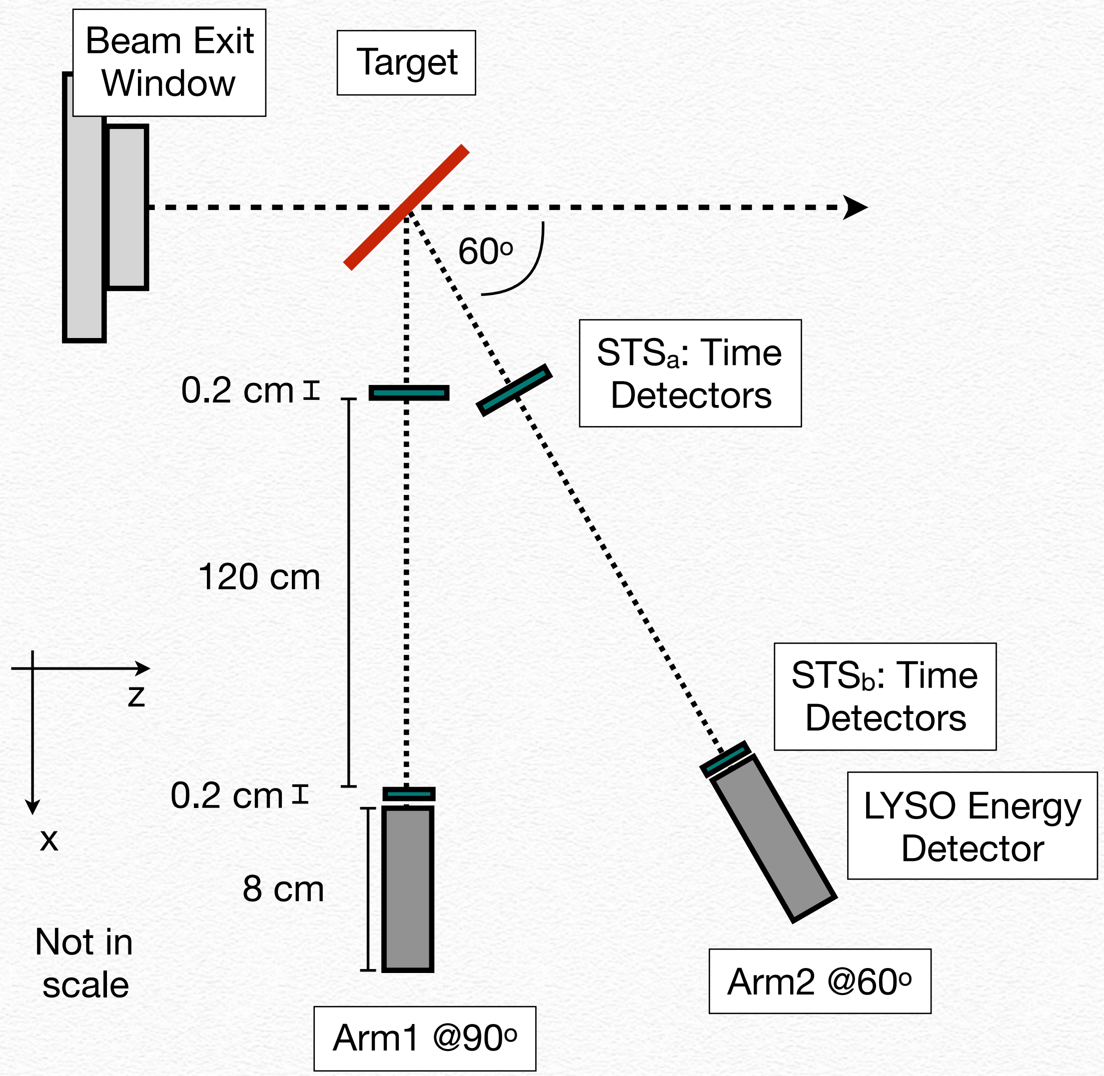


- 4 STS: thicknesses 2 mm for ToF measurements (Time Resolution ~400-600 ps) and Deposited Energy measurements (dE)
- 2 LYSO: 8 cm thick for Deposited Energy measurements (E)

**Episode I: 90/60°**

# Experimental SETUP

CNAO

**Thin Targets based on C,H and O elements: PMMA, Graphite and Plastic Scintillator**

- The fragments production (Z=1) has been measured as a function of the kinetic energy for 4 angles;
- The Time of Flight in thin plastic scintillators and the ene… use…

The thin targets (1-2 mm) do not require, as a first approximation, the implementation of a correction …bsorption …get.

**"FORWARD" ANGLES: 50° ± 2° and 32° ± 2°**

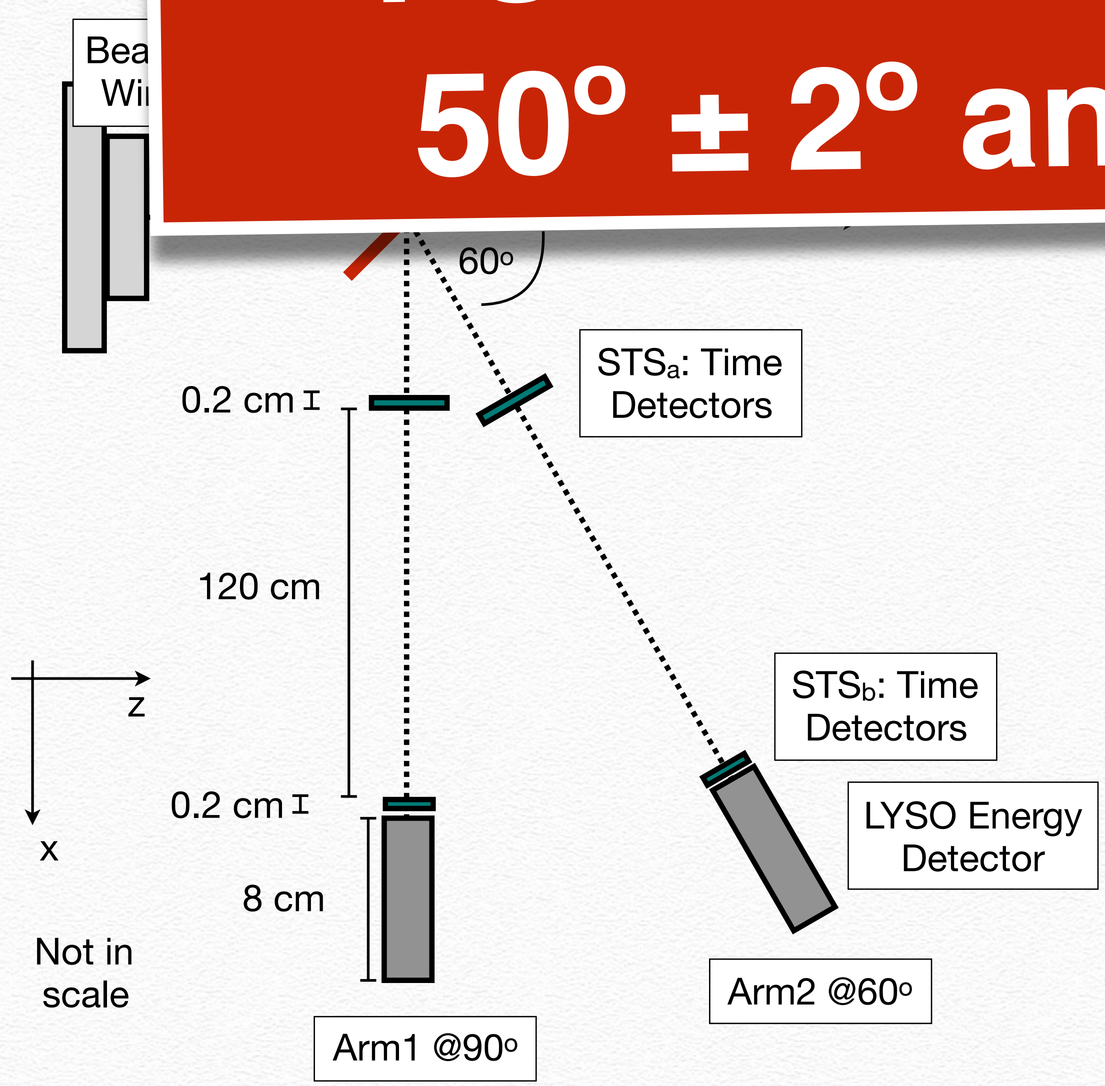


- …n for ToF measurements (Time Resolution ~400-600 ps) and Deposited Energy measurements (dE)
- 2 LYSO: 8 cm thick for Deposited Energy measurements (E)

**Episode II: 50/32°**

# Cross section

The $^{12}$C fragmentation cross sections for a $^{A}{}_{Z}$X fragment are obtained as:

$$\frac{d\sigma}{dE_k}({}^{A}_{Z}X) = \frac{N_{{}^{A}_{Z}X}(E_k)}{N_{{}^{12}C}} \cdot \frac{1}{N_Y} \cdot \frac{1}{\epsilon}$$

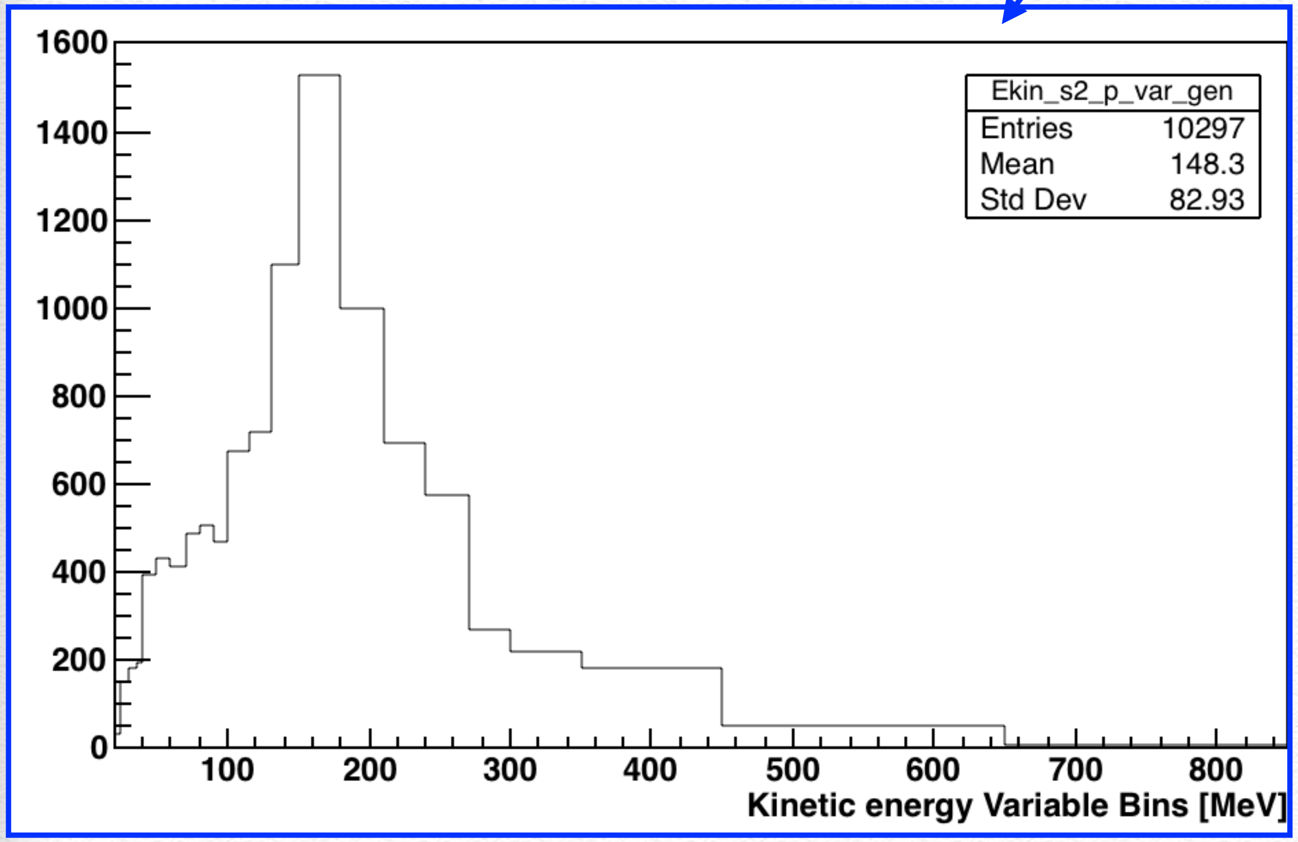


Ekin at generation

The energy loss by the fragments has been taken into account: we evaluate via MC the fragments (p,d,t) energy loss in target, air and sts1 and then we corrected the measured Ekin up to the energy at generation.

# Cross section

The $^{12}$C fragmentation cross sections for a $^{A}_{Z}$X fragment are obtained as:

$$\frac{d\sigma}{dE_k}({}^{A}_{Z}X) = \frac{N_{{}^{A}_{Z}X}(E_k)}{N_{^{12}C}} \cdot \frac{1}{N_Y} \cdot \frac{1}{\epsilon}$$

From CNAO
Dose Delivery

dose-current conversion systematic uncertainty. The relative uncertainty on $N_{^{12}C}$ (4%) is hence the convolution of the uncertainty on the stopping power determination [20] and on the dose measurements [21]. A possible additional contribution to the systematic uncertainty, coming from the monitoring system measurement stability [22], was found to be negligible

| $N_{^{12}C}$ | $\cdot 10^6$ | $\cdot 10^6$ | $\cdot 10^6$ | $\cdot 10^6$ | $\cdot 10^6$ |
|---|---|---|---|---|---|
| Target | 115 [MeV/u] | 153 [MeV/u] | 222 [MeV/u] | 281 [MeV/u] | 353 [MeV/u] |
| PMMA | 49866 | 46512 | 49395 | 49601 | 42000 |
| Graphyte | 49454 | 46583 | 47484 | 47288 | 49328 |
| Plast. Scint. | 49728 | 50600 | 49347 | 49787 | 49653 |

Information of the target composition:

| Target | Composition | Thickness $[mm]$ | Density $[g/cm^3]$ |
|---|---|---|---|
| PMMA | $C_5O_2H_8$ | 2 | 1.19 |
| Graphite | C | 1 | 0.94 |
| Plas.Scint. | $C_bH_a$ | 2 | 1.024 |

$$N_Y = \frac{\rho_Y \cdot th_Y \cdot N_A}{A_Y}$$

thy=thy*sqrt(2)

# Cross section

The $^{12}$C fragmentation cross sections for a $^{A}_{Z}X$ fragment are obtained as:

$$\frac{d\sigma}{dE_k}(^{A}_{Z}X) = \frac{N_{^{A}_{Z}X}(E_k)}{N_{^{12}C}} \cdot \frac{1}{N_Y} \cdot \frac{1}{\epsilon}$$

Solid angle and efficiencies

$$\epsilon = \epsilon_{Det} \cdot \epsilon_{Sel} \cdot \epsilon_{DT}$$

Protons, deutons and tritons impinged on the experimental setup to calculate the geometrical acceptance and the trigger+detection efficiency

Full simulation (C on Targets and fragments production). On the E (and dE) vs ToF distributions application of the PID selections tuned from data: evaluation of fragments (p, d, t) mis-identification.

Measurements of the DAQ dead time for each run (rate dependent)

# Particle Identification

Protons Deutons and tritons have been selected from all other particles exploiting **deposited Energy vs ToF**, Edep vs 1/ToF, dE vs E and dE vs ToF information.

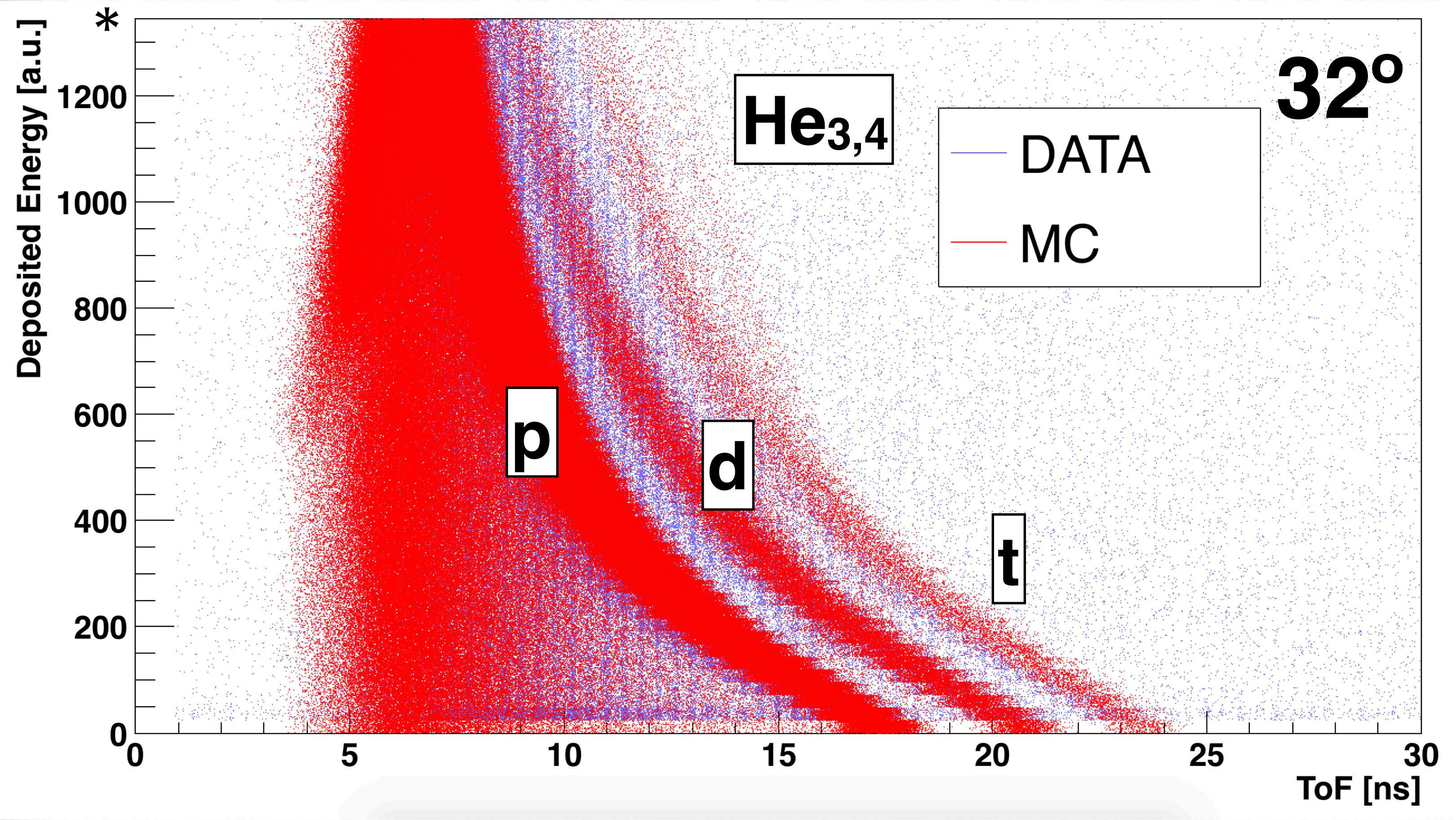


The use of MC allows to clearly identify the fragments and define our identification strategy.

The He contribution is visible.. see next slide for the Z>2 separation.

***QDC saturation @ 1350pC**

The deposited energy in the LYSO crystal is shown as a function of the time of flight of the measured particles for data and MC-data. For the data and the MC, the deposited energy is in arbitrary units. The fragments identity is shown in order to confirm the described data selection strategy.

# Particle Identification

Protons Deutons and tritons have been selected from all other particles exploiting deposited Energy vs ToF, Edep vs 1/ToF, dE vs E and **dE vs ToF** information.

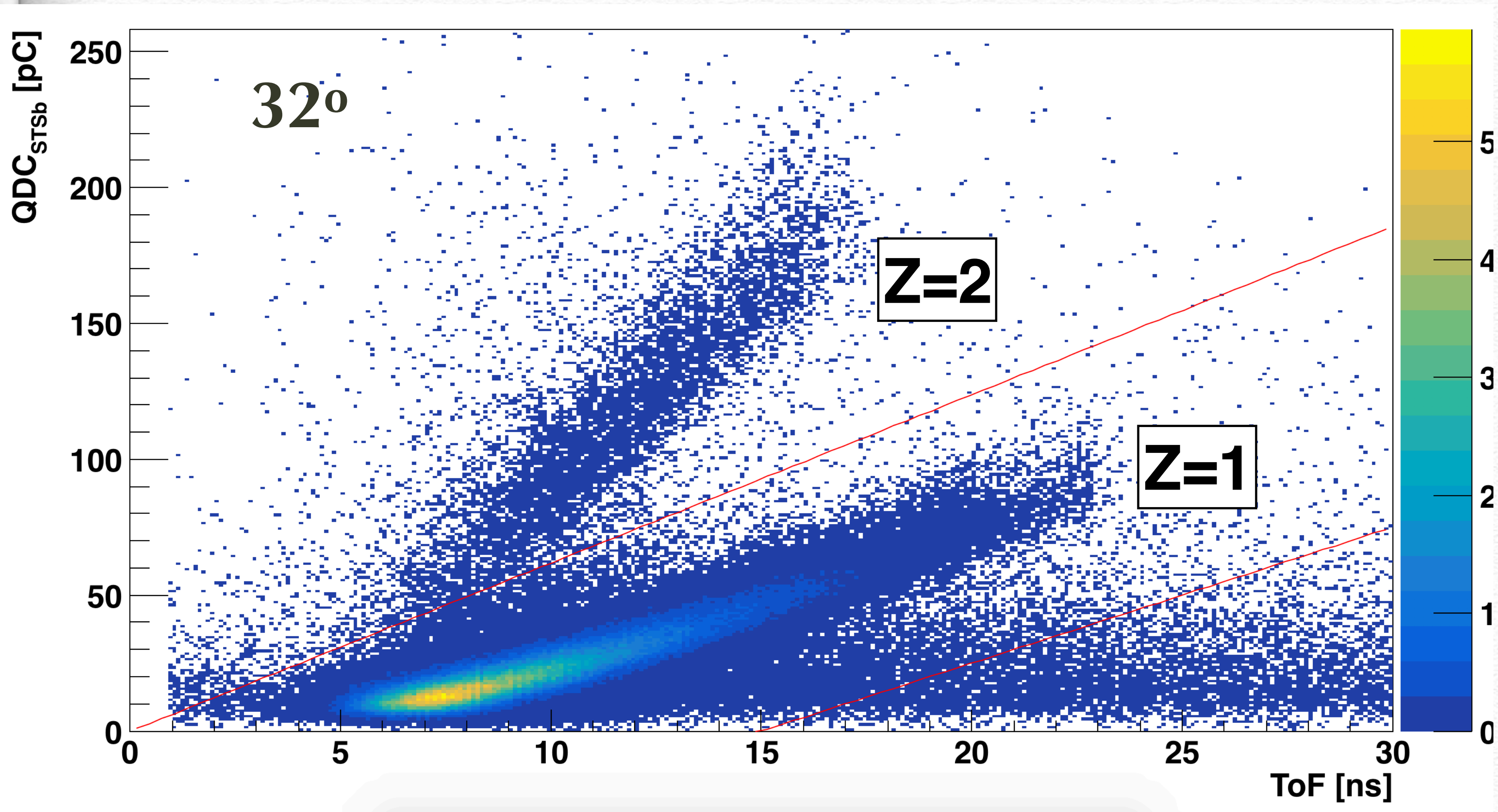


The energy loss in the STSb (in pC) is shown as a function of the time of flight of the measured particles. The populations of Z=1 and Z=2 at 32 degrees are clearly separated by the red line.

**The helium fragments, as well as tritons, do not represent a statistically significant sample: only about 2% of the fragments are Z=2, at 32°. No cross section analysis has been performed for Z>1 fragments. They have been removed from the analysed data sample.**

# Particle Identification

**32°**

Protons Deutons and tritons have been selected from all other particles exploiting deposited Energy vs ToF, **Edep vs 1/ToF**, dE vs E and **dE vs ToF** information.

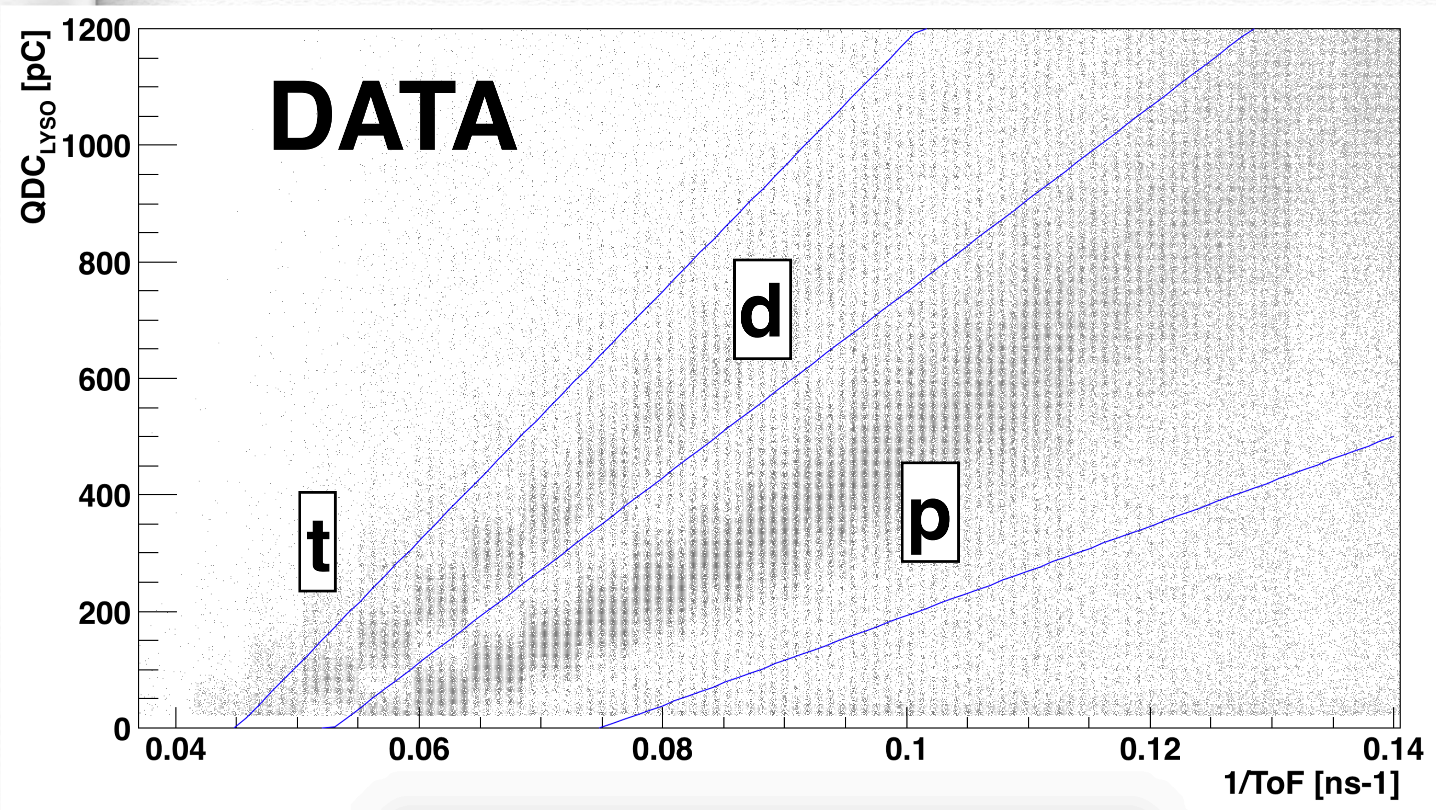


**Protons and deuterons are reasonably abundant in all the specific data sets: about 80% and 20% of the fragments respectively at 32°.**

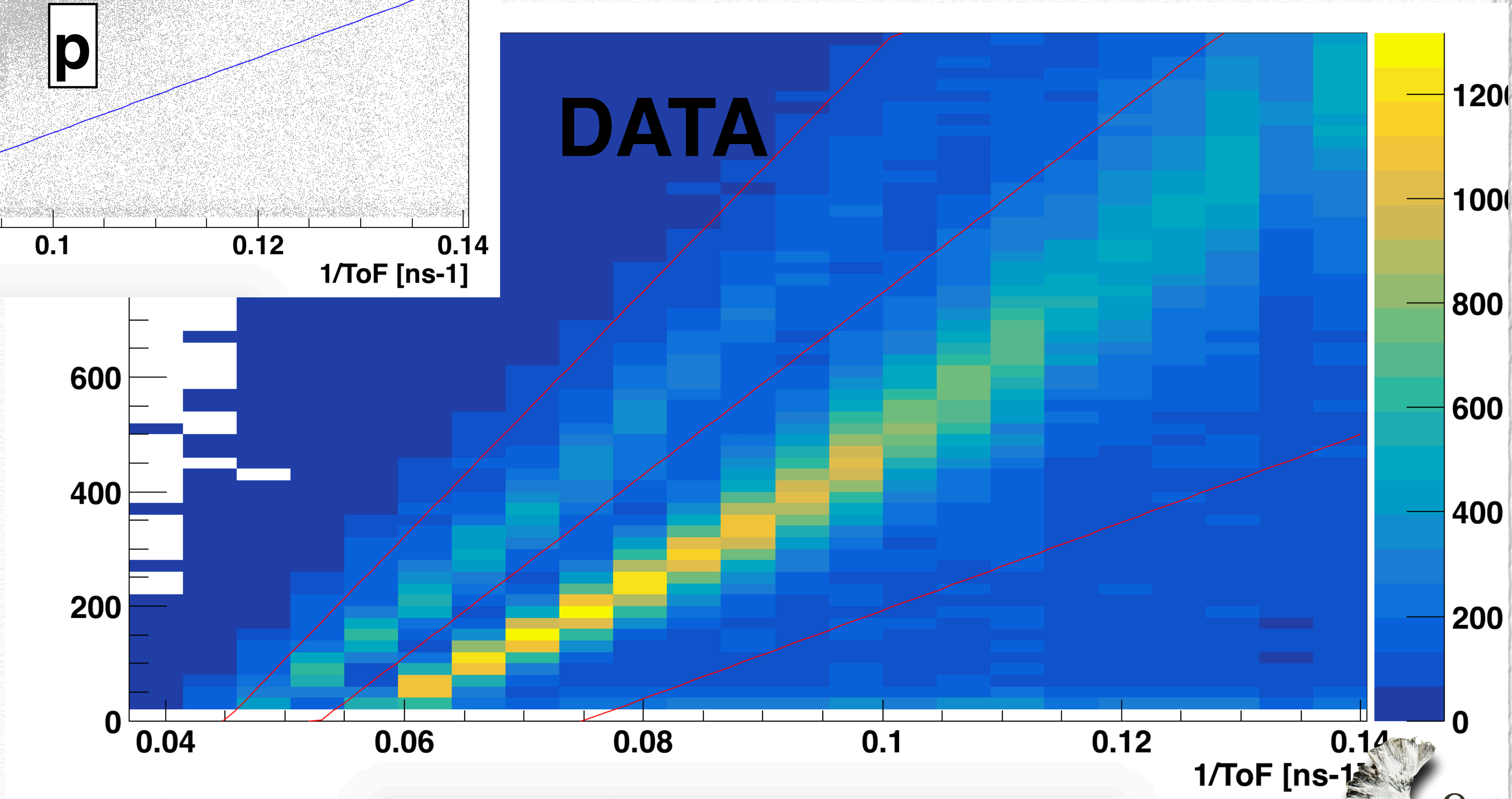

# Kinetic Energy Spectra

Time of Flight distribution of protons is shown in the top plot and converted in the kinetic energy distribution as shown in the bottom plot. Data refer to Arm2, graphite target with C-ion beam at 352 MeV/u:

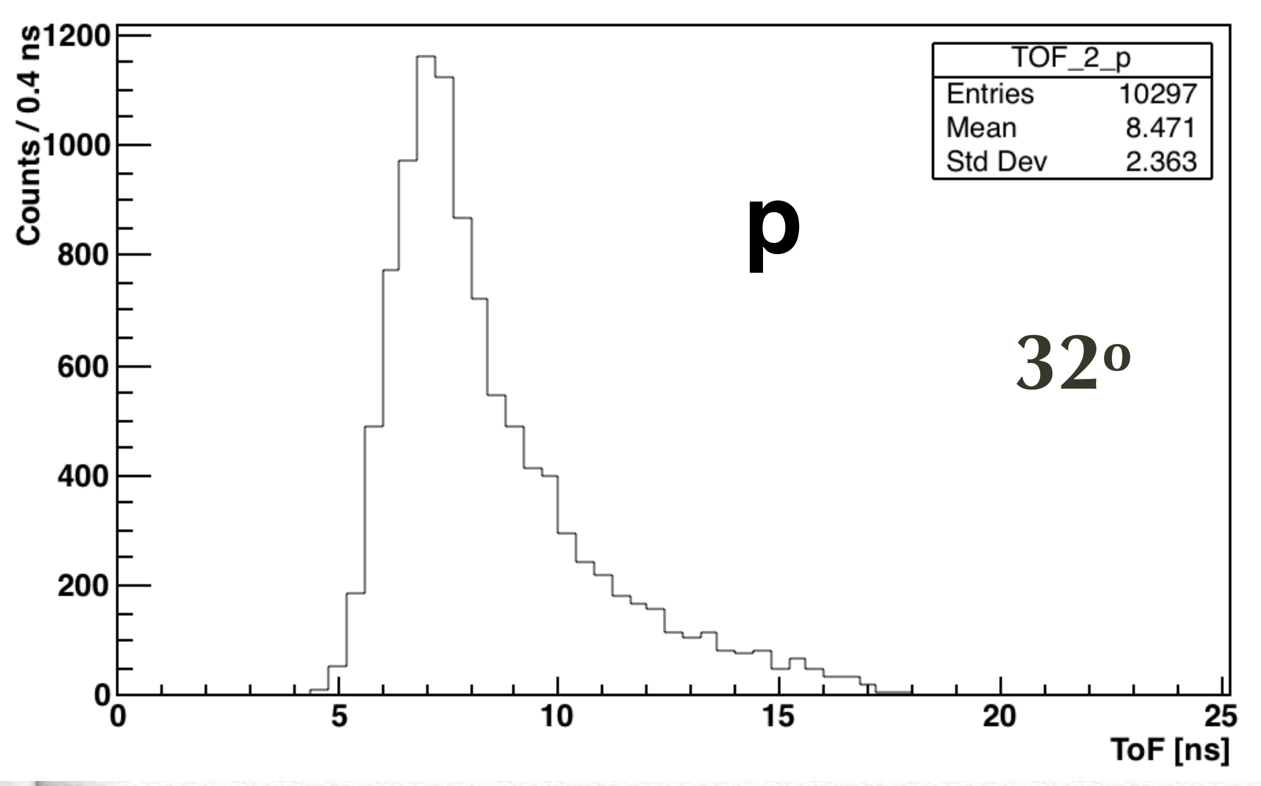


Time resolution evaluated from dedicated run:

- 50º: 720 ps
- 32º: 370 ps

$$\beta_i = L/(ToF_i \cdot c)$$

$$E_{kin} = m_i \cdot (\gamma - 1)$$

Energy resolution as a function of proton kinetic energy ranges from **12% (5%) up to 35% (20%)** for 50º (32º) (worsening with increasing energy).

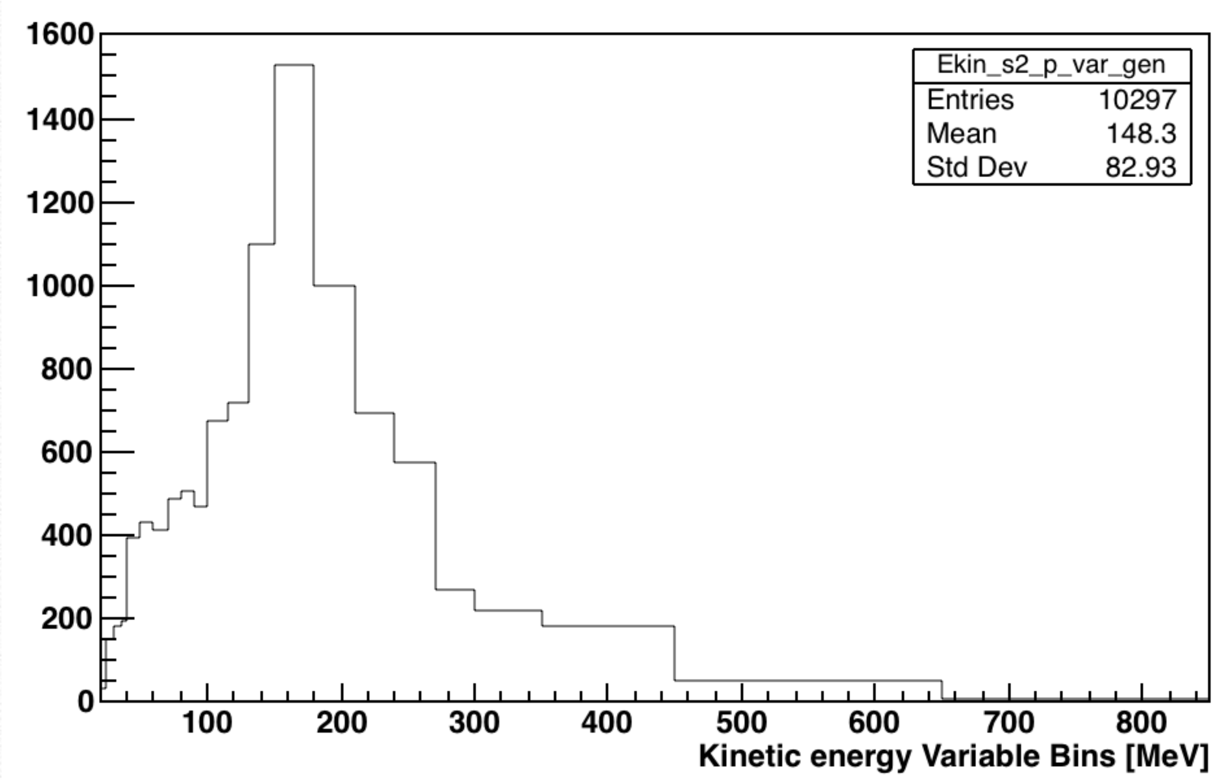


The kinetic energy has been reconstructed in variable size bins that have been chosen as a compromise between the **energy resolution and the available statistics** in each bin (in the final differential cross section evaluation).

# Kinetic Energy Spectra

Time of Flight distribution of protons is shown in the top plot and converted in the kinetic energy distribution as shown in the bottom plot. Data refer to Arm2, graphite target with C-ion beam at 352 MeV/u:

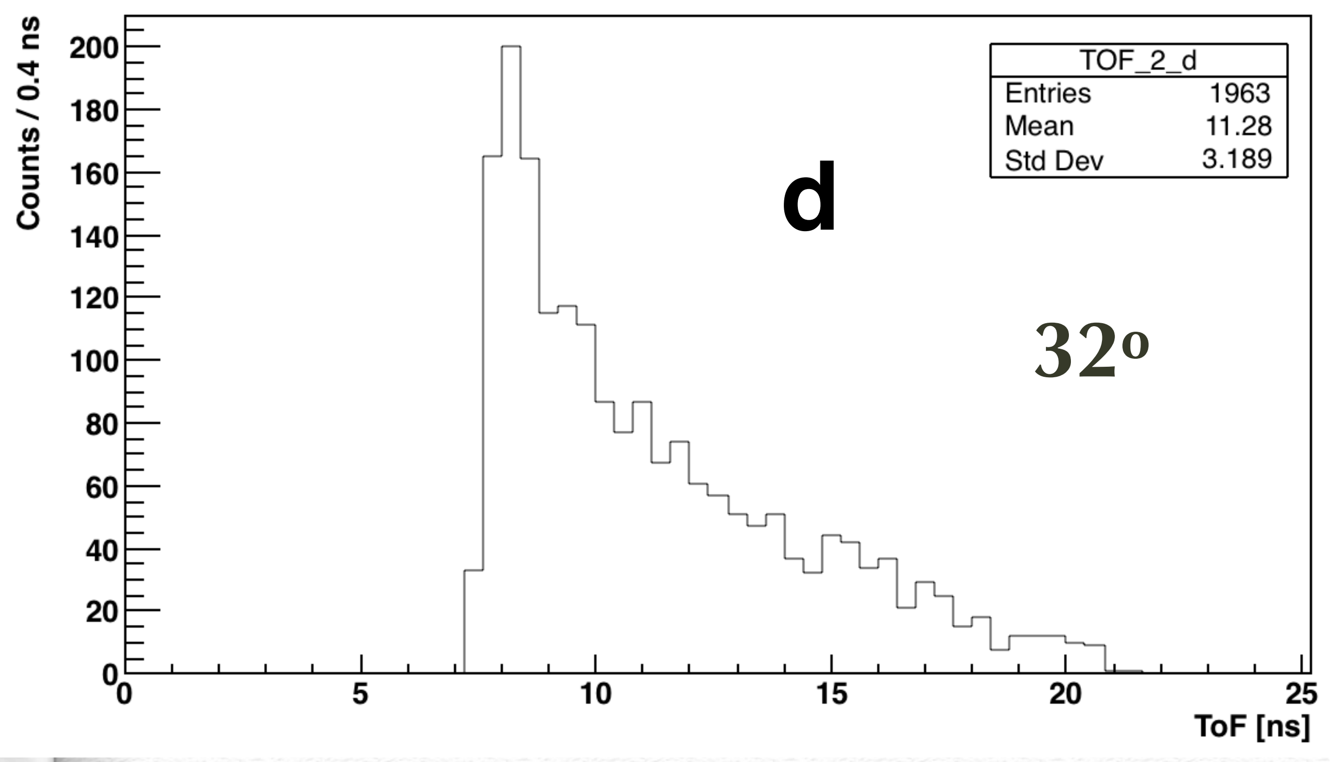


Time resolution evaluated from dedicated run:

- 50º: 720 ps
- 32º: 370 ps

$$\beta_i = L/(ToF_i \cdot c)$$

$$E_{kin} = m_i \cdot (\gamma - 1)$$

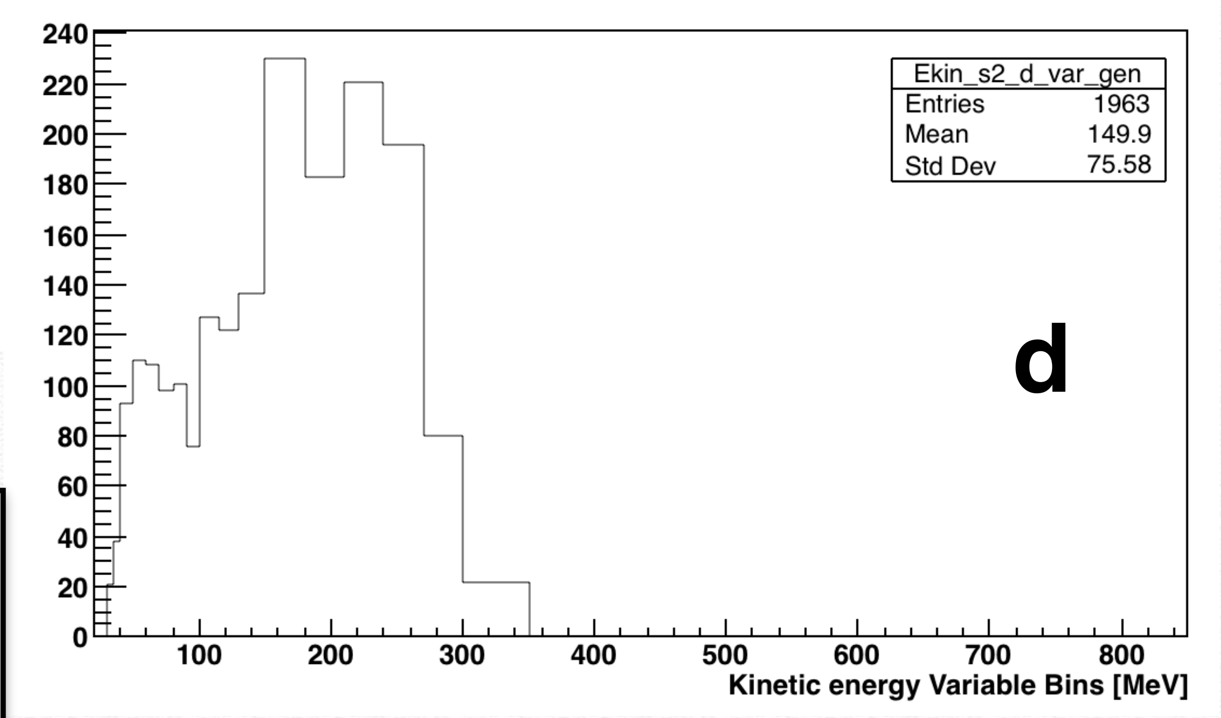


Energy resolution as a function of deuteron kinetic energy ranges from **8% (4%) up to 28% (11%)** for 50º (32º) (worsening with increasing energy).

The kinetic energy has been reconstructed in variable size bins that have been chosen as a compromise between the **energy resolution and the available statistics** in each bin (in the final differential cross section evaluation).

# Efficiency evaluation:

$$\epsilon = \epsilon_{Det} \cdot \epsilon_{Sel} \cdot \epsilon_{DT}$$

The efficiency $\epsilon_{Det}(E_{kin})$ and $\epsilon_{Sel}$ have been evaluated using dedicated Monte Carlo simulations developed with the FLUKA code.

- To evaluate $\epsilon_{Det}(E_{kin})$: detector, angular, trigger, signal selection efficiency = > MC FLAT (no triggered MC: all events recorded): p, d, t sources, 4π production

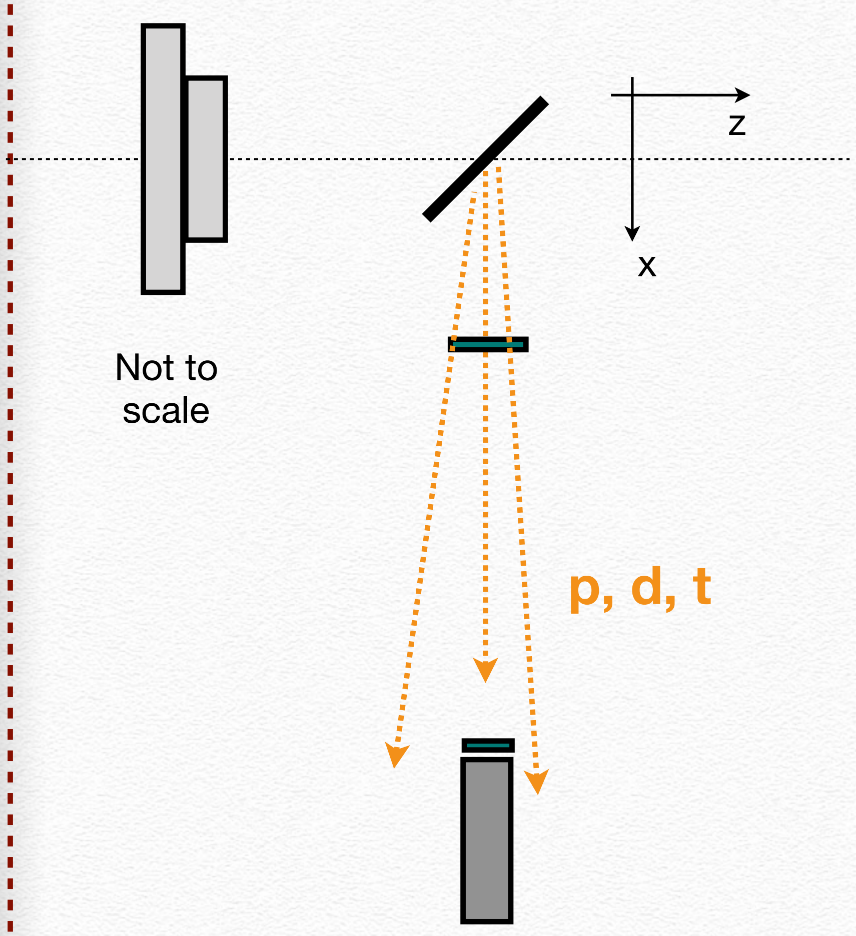

# Efficiency evaluation:

$$\epsilon = \epsilon_{Det} \cdot \epsilon_{Sel} \cdot \epsilon_{DT}$$

The efficiency $\epsilon_{Det}(E_{kin})$ and $\epsilon_{Sel}$ have been evaluated using dedicated Monte Carlo simulations developed with the FLUKA code.

- To evaluate $\epsilon_{Det}(E_{kin})$: detector, angular, trigger, signal selection efficiency = > MC FLAT (no triggered MC: all events recorded): p, d, t sources, 4π production

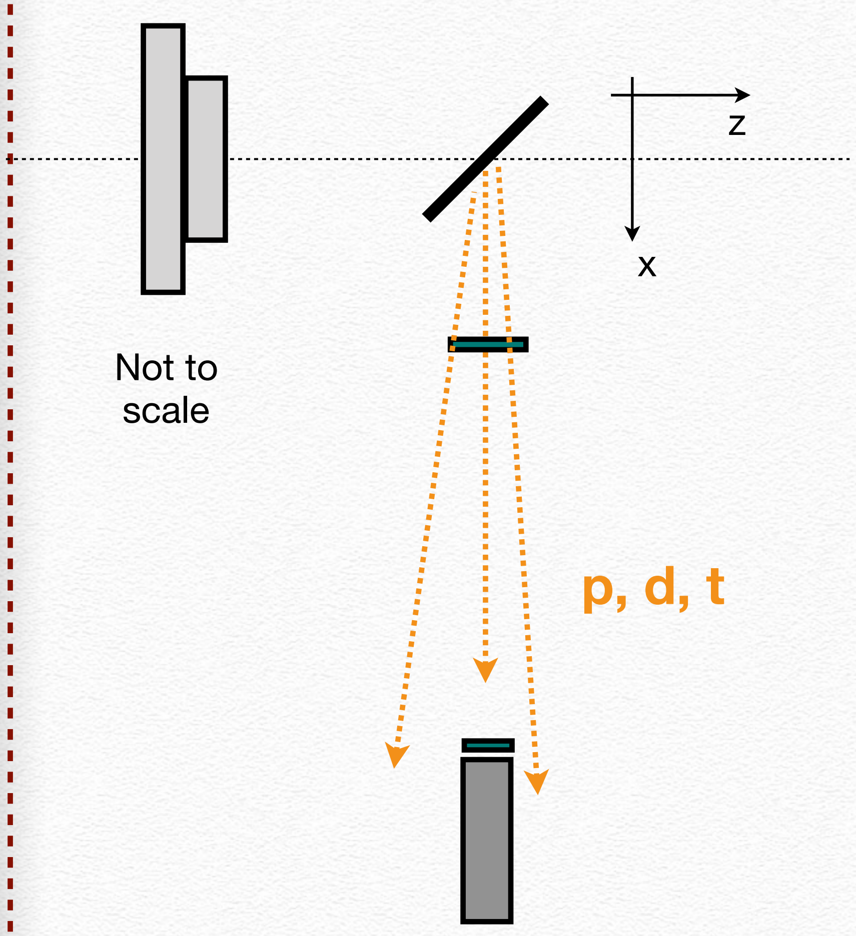


- To evaluate $\epsilon_{Sel}$: p, d, t identification efficiency using the PID bands = > MC FULL (target, beam, etc..)

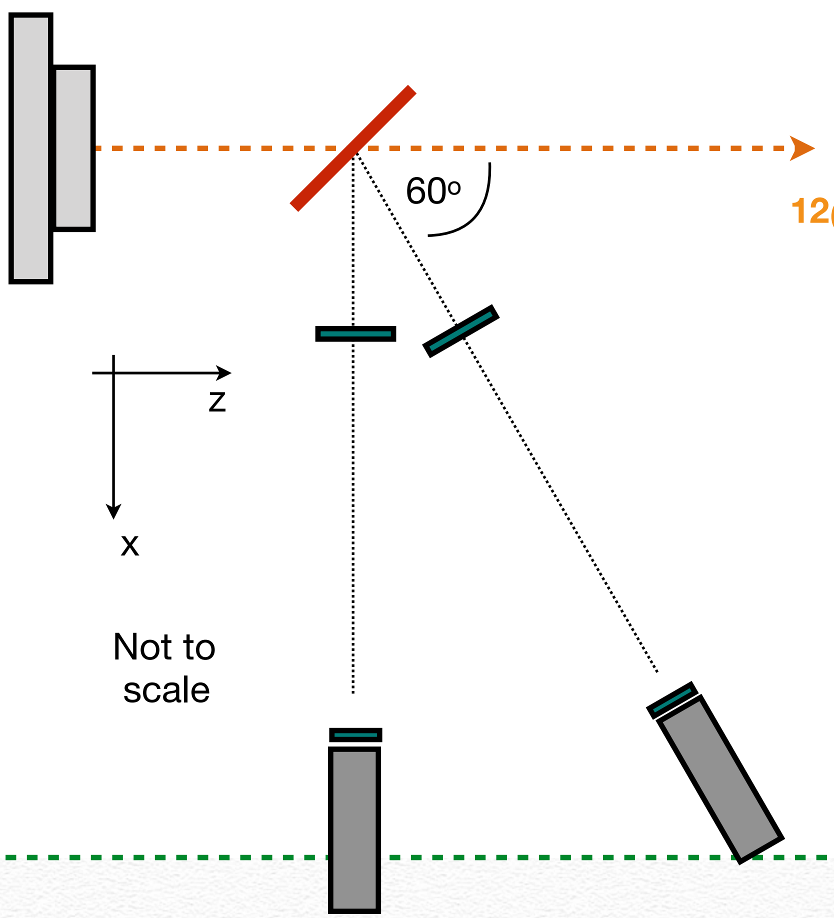

# Det Efficiency: Trig + Det + Geo

**Probability that a fragment of type *u* is measured by our detectors ( *u* = *p, d, t*)**

$$\epsilon^{u}_{Det}(E_{kin})_i = \left(\frac{N^u_{meas}}{N^u_{gen}}\right)_i$$

**Simulation no trig of p (d, t) produced 4π with FLAT Ekin = [5 MeV - 1 GeV] (x2 if d) (x3 if t)**

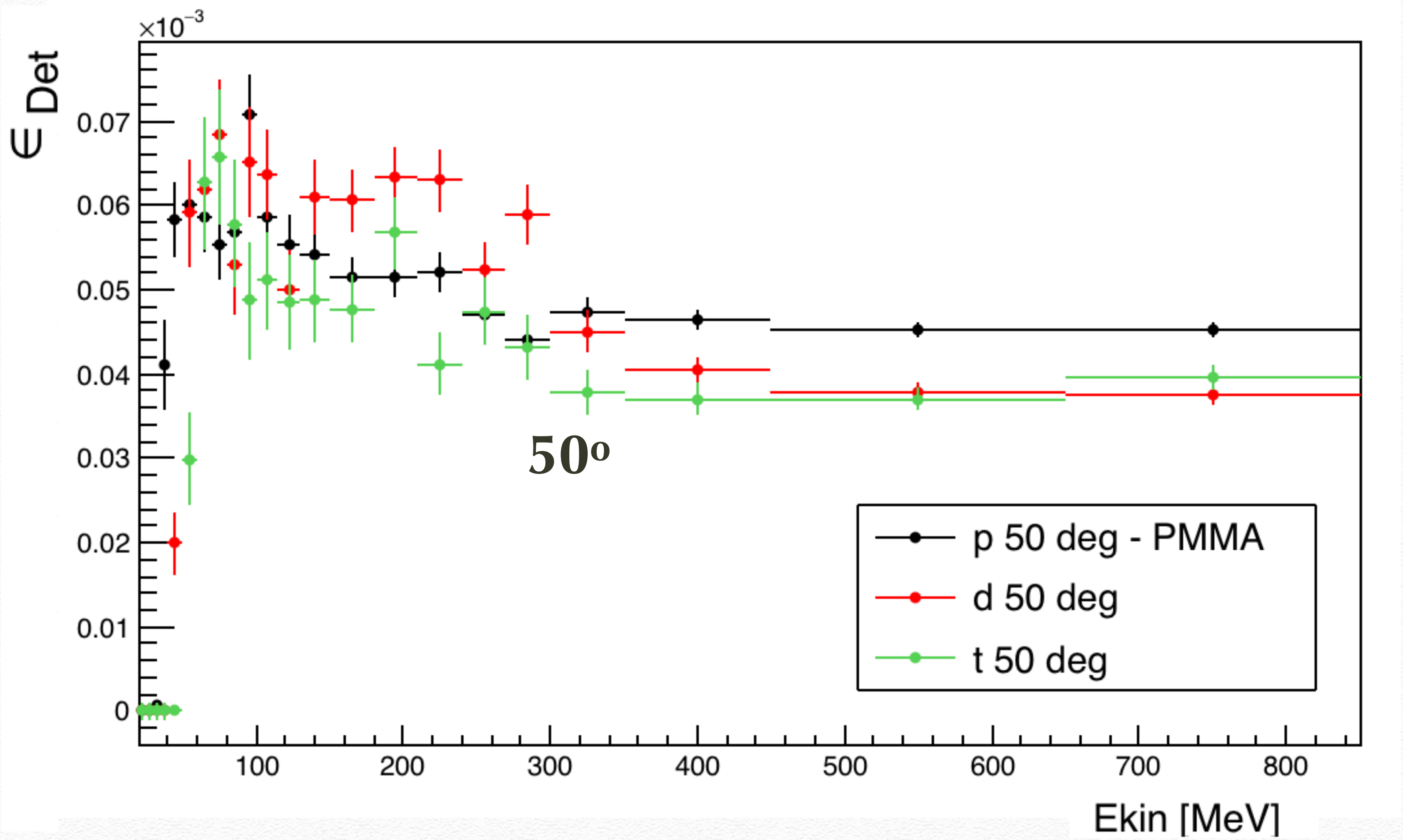

# Det Efficiency: Trig + Det + Geo

**Probability that a fragment of type *u* is measured by our detectors ( *u = p, d, t*)**

$$\epsilon^{u}_{Det}(E_{kin})_i = \left(\frac{N^u_{meas}}{N^u_{gen}}\right)_i$$

**Simulation no trig of p (d, t) produced 4π with FLAT Ekin = [5 MeV - 1 GeV] (x2 if d) (x3 if t)**

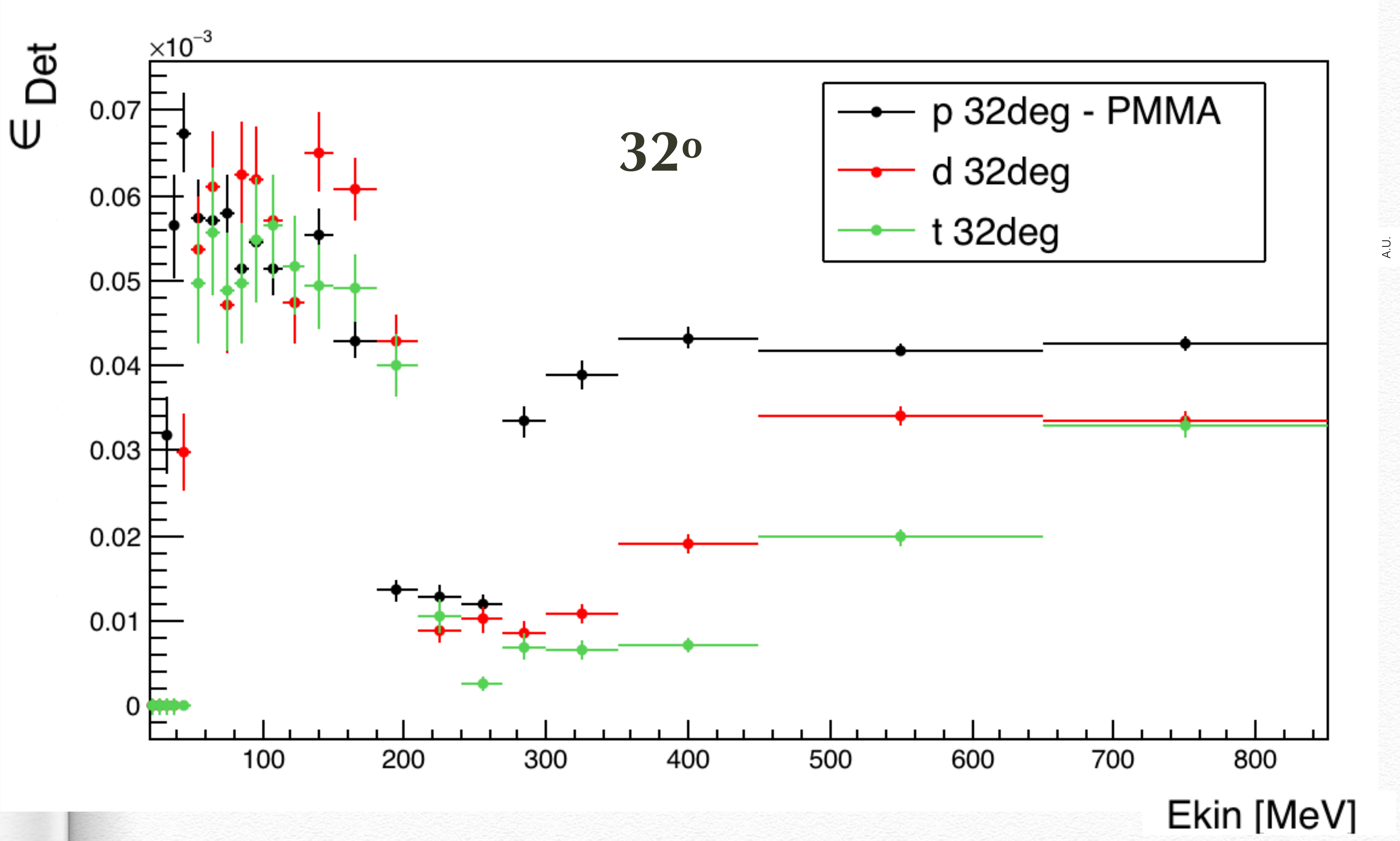

# Det Efficiency: Trig + Det + Geo

**Probability that a fragment of type *u* is measured by our detectors ( *u* = *p*, *d*, *t*)**

$$\epsilon^u_{Det}(E_{kin})_i = \left(\frac{N^u_{meas}}{N^u_{gen}}\right)_i$$

**Simulation no trig of p (d, t) produced 4π with FLAT Ekin = [5 MeV - 1 GeV] (x2 if d) (x3 if t)**

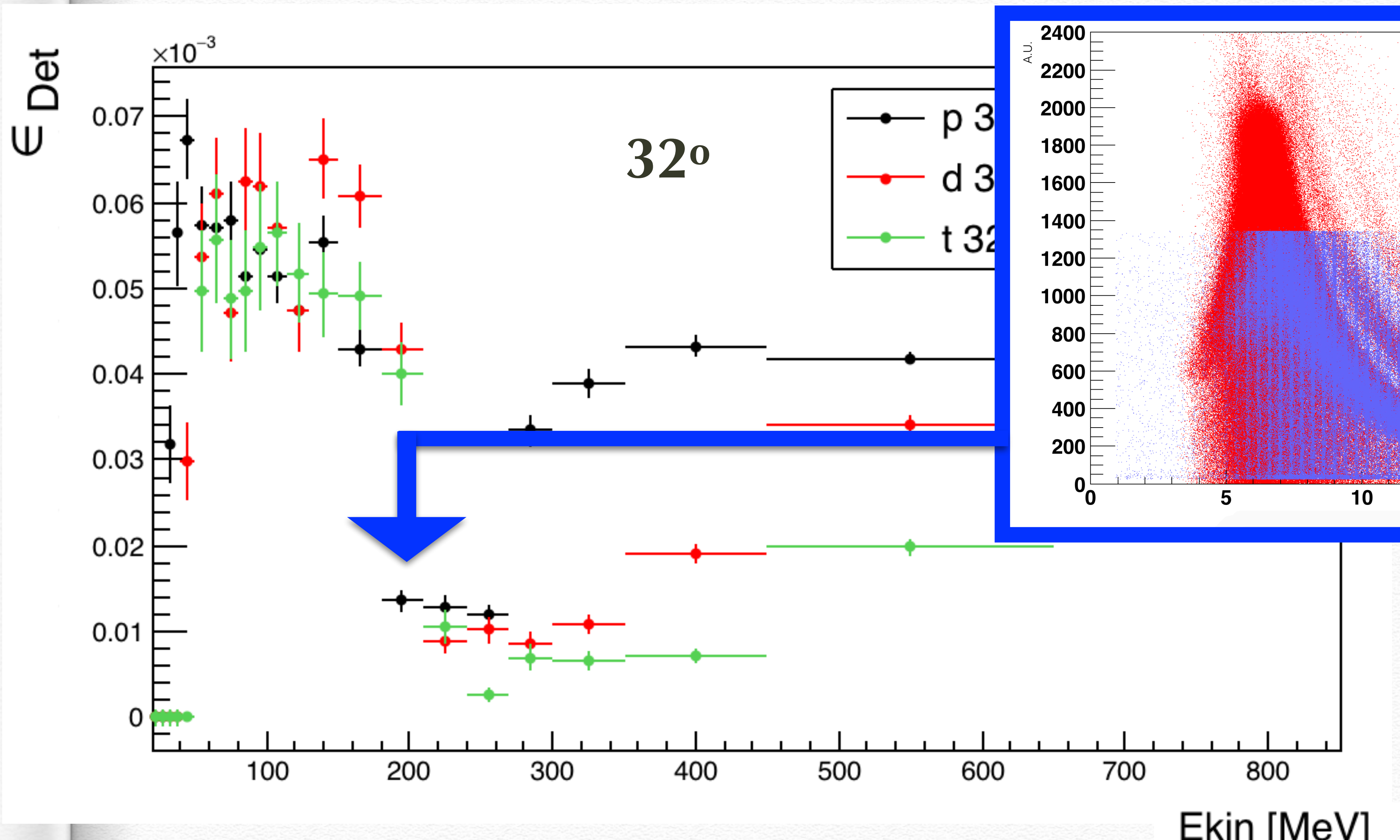


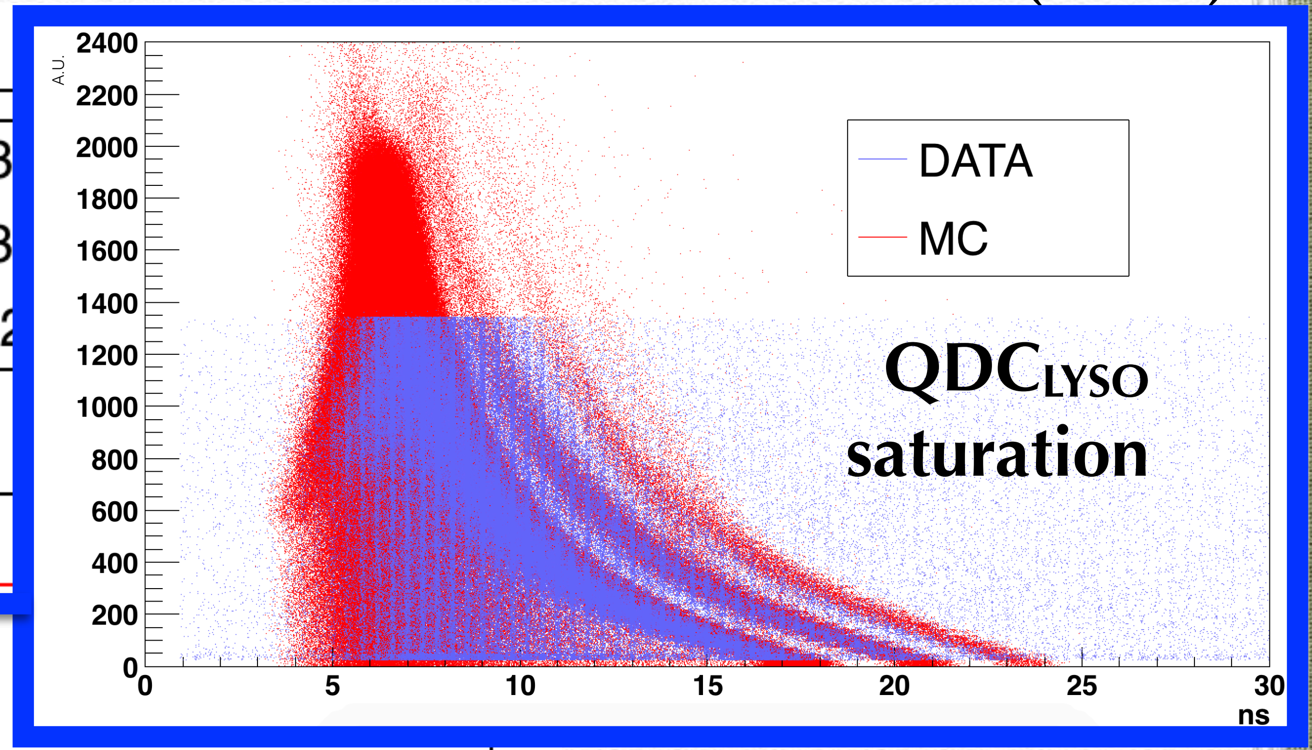

# Mixing Efficiency

Probability that a fragment of type *u* is measured in the region *v* ( *u*, *v* = *p*, *d*, *t* )

$$\epsilon^{uv}_{mix} = \frac{N^{uv}}{N^{u}}$$

**FULL simulation of 12C ion beam impinging over a PMMA target.**

$$\epsilon_{mix} = \begin{pmatrix} \epsilon^{pp} & \epsilon^{pd} & \epsilon^{pt} \\ \epsilon^{dp} & \epsilon^{dd} & \epsilon^{dt} \\ \epsilon^{tp} & \epsilon^{td} & \epsilon^{tt} \end{pmatrix}$$

$\epsilon_{Sel}$

| $E^{C}_{kin}$ $[MeV/u]$ | $\epsilon^{pp}$ [%] | $\epsilon^{dd}$ [%] | $\epsilon^{tt}$ [%] |
|---|---|---|---|
| **50º** | | | |
| 115 | 95 ± 5 | 89 ± 9 | 85 ± 12 |
| 153 | 95 ± 5 | 85 ± 14 | 91 ± 6 |
| 221 | 94 ± 5 | 85 ± 12 | 86 ± 10 |
| 281 | 94 ± 5 | 84 ± 12 | 71 ± 31 |
| 353 | 94 ± 5 | 84 ± 14 | 81 ± 15 |
| **32º** | | | |
| 115 | 95 ± 4 | 78 ± 21 | 76 ± 32 |
| 153 | 95 ± 5 | 77 ± 22 | 83 ± 17 |
| 221 | 95 ± 5 | 75 ± 23 | 73 ± 32 |
| 281 | 95 ± 5 | 75 ± 24 | 76 ± 26 |
| 353 | 94 ± 5 | 75 ± 24 | 69 ± 37 |

| $E^{C}_{kin}$ $[MeV/u]$ | $\epsilon^{dp}$ [%] | $\epsilon^{tp}$ [%] | $\epsilon^{pd}$ [%] | $\epsilon^{td}$ [%] | $\epsilon^{dt}$ [%] |
|---|---|---|---|---|---|
| **50º** | | | | | |
| 115 | 6 ± 7 | - | 2 ± 2 | 12 ± 13 | 5 ± 7 |
| 153 | 10 ± 15 | 2 ± 3 | 1 ± 2 | 5 ± 4 | 4 ± 5 |
| 221 | 4 ± 4 | 3 ± 4 | 2 ± 3 | 11 ± 10 | 7 ± 6 |
| 281 | 5 ± 3 | 2 ± 2 | 2 ± 3 | 8 ± 6 | 8 ± 7 |
| 353 | 4 ± 2 | 1 ± 1 | 2 ± 2 | 10 ± 10 | 7 ± 7 |
| **32º** | | | | | |
| 115 | 4 ± 3 | 2 ± 2 | 1 ± 2 | 3 ± 4 | 13 ± 13 |
| 153 | 4 ± 2 | 2 ± 2 | 1 ± 2 | 2 ± 2 | 16 ± 16 |
| 221 | 4 ± 4 | 2 ± 2 | 1 ± 2 | 8 ± 14 | 17 ± 17 |
| 281 | 4 ± 3 | 3 ± 3 | 1 ± 2 | 10 ± 19 | 16 ± 16 |
| 353 | 4 ± 3 | 5 ± 6 | 2 ± 3 | 10 ± 14 | 17 ± 17 |

**The d and t contribution to the $XSec_p$ has been subtracted and viceversa:**

$$XSec_{p\_final} = XSec_p - (eps_{dp}/eps_{pp}) * XSec_d - (eps_{tp}/eps_{pp}) * XSec_t$$

# Ekin Spectra (Data - FLUKA) Protons :: 50 - 32 :: PMMA

**Absolute Normalization**

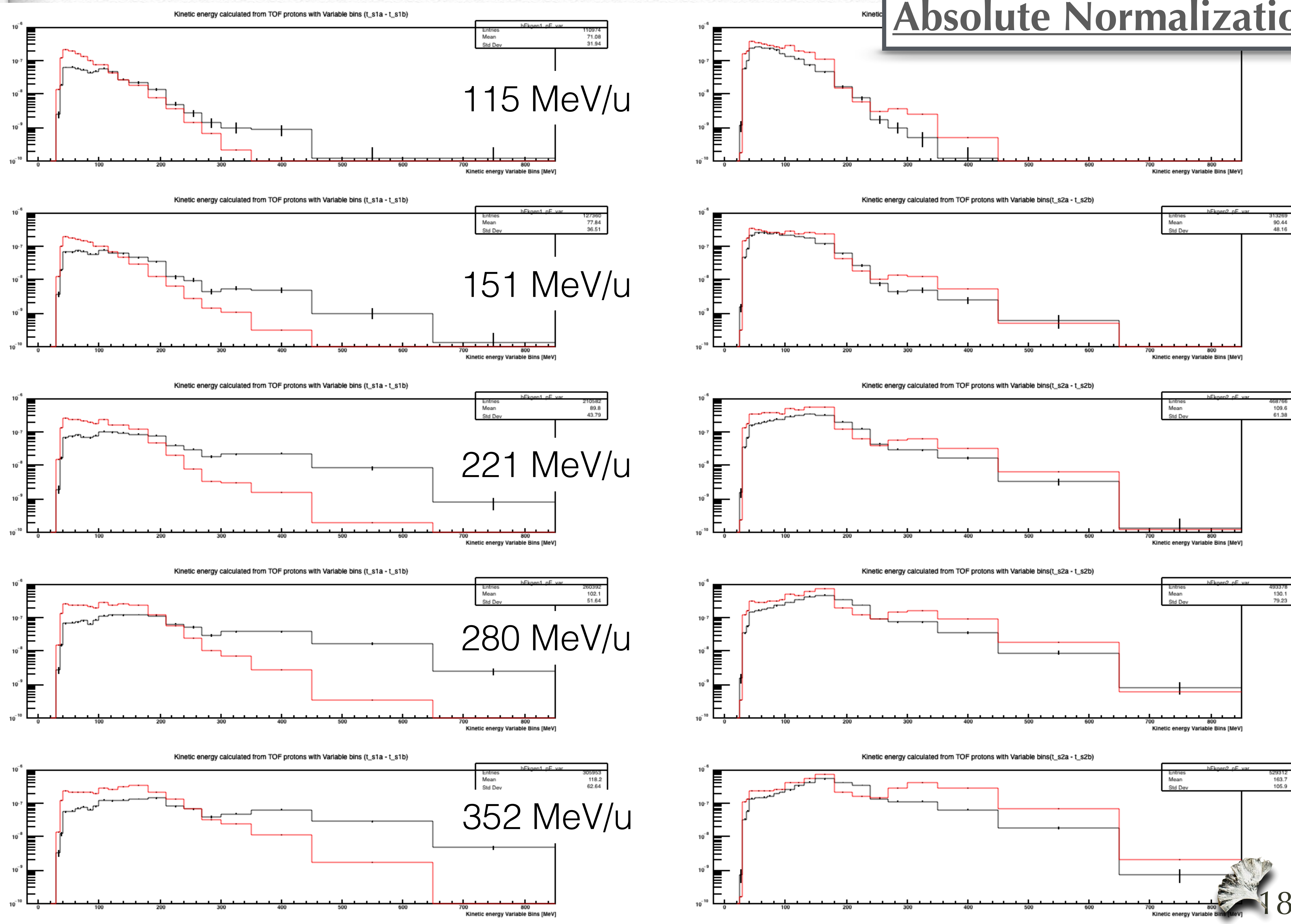

# Ekin Spectra (Data - FLUKA) Protons :: 50 - 32 :: PMMA

**Absolute Normalization**

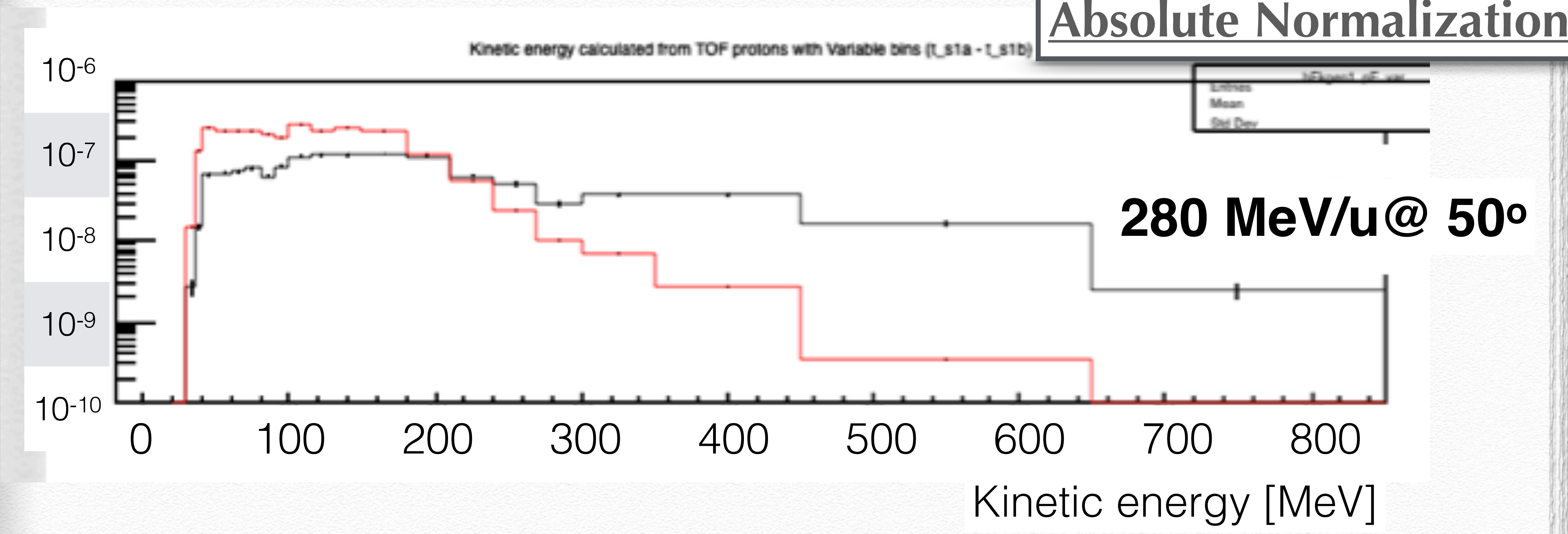


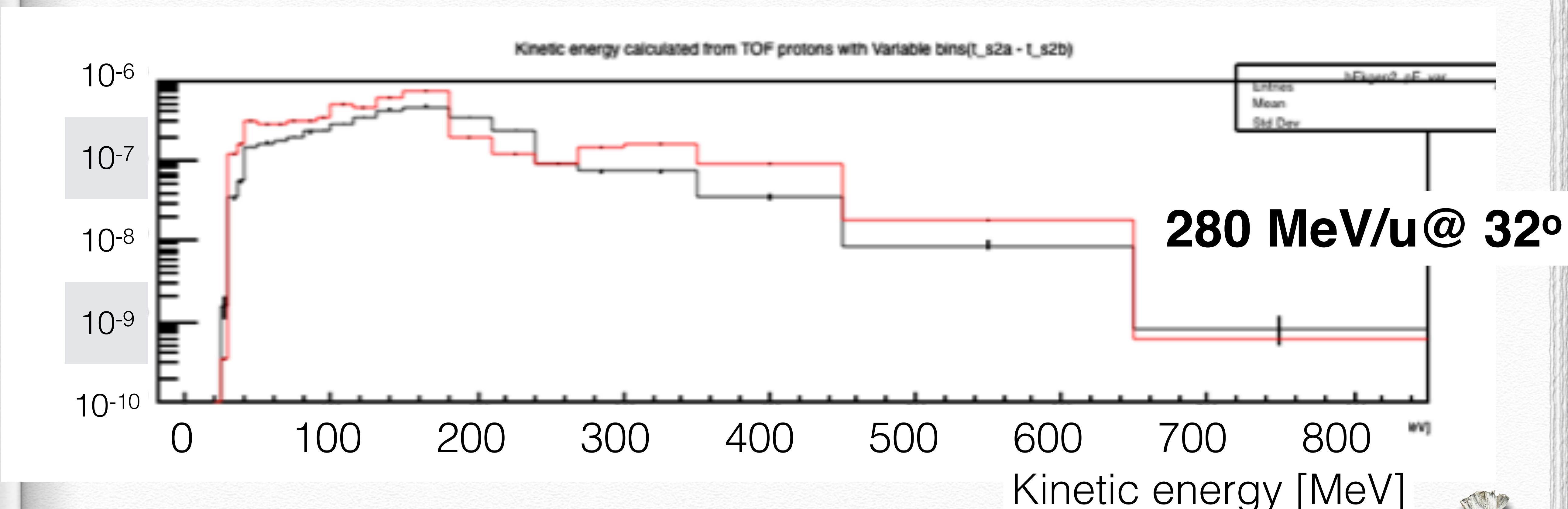

# Ekin Spectra (Data - FLUKA) Deuterons :: 50 - 32 :: PMMA

**Absolute Normalization**

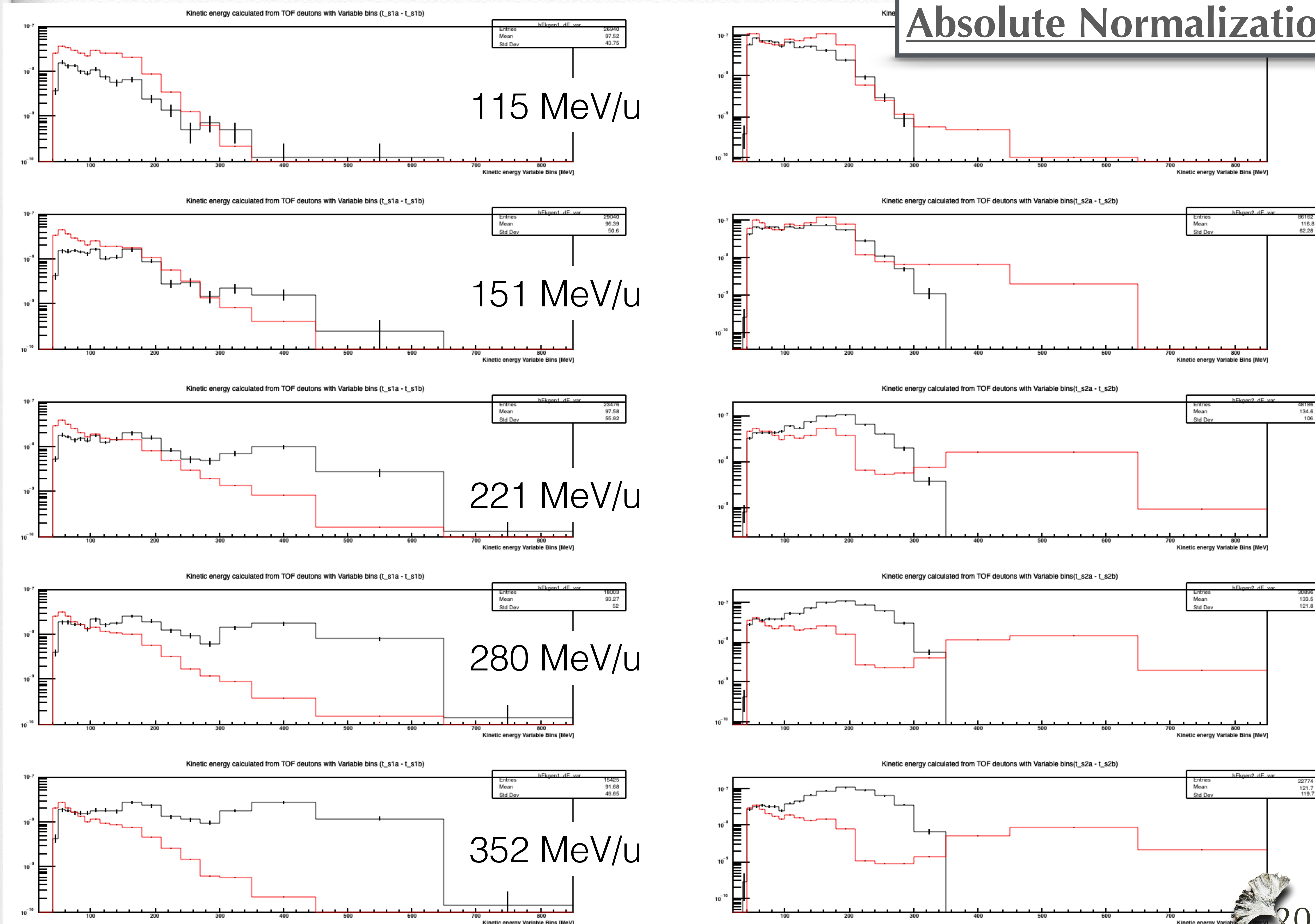

# Ekin Spectra (Data - FLUKA) Protons :: 50 - 32 :: Grafite

**Absolute Normalization**

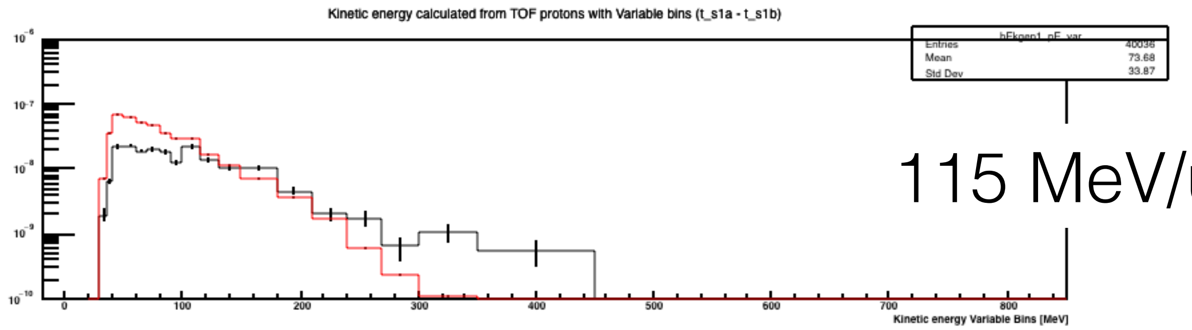


115 MeV/u

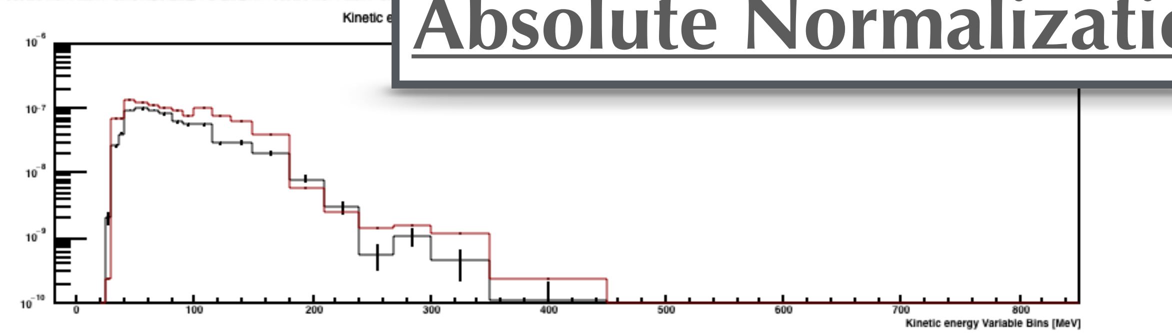


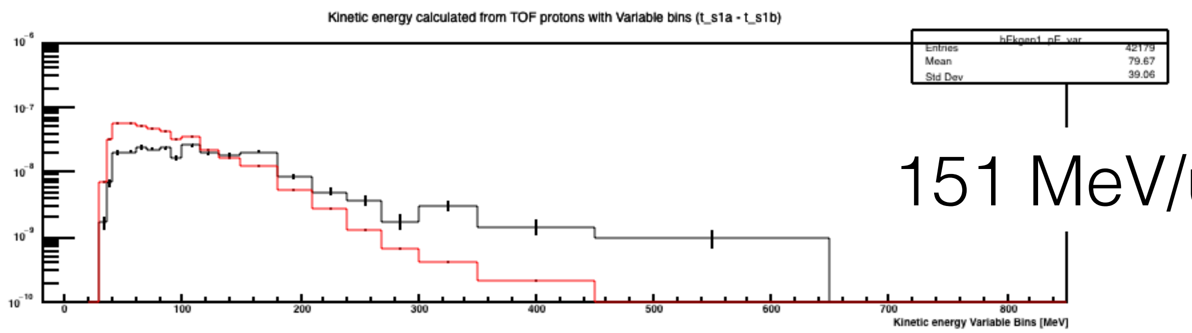


151 MeV/u

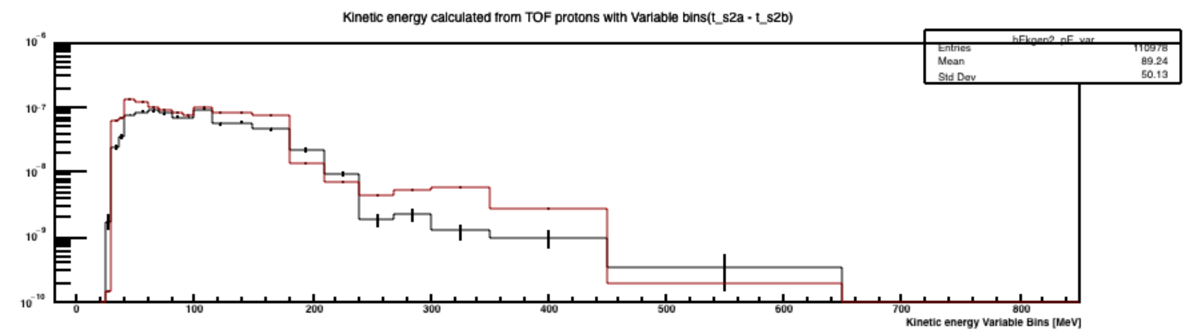


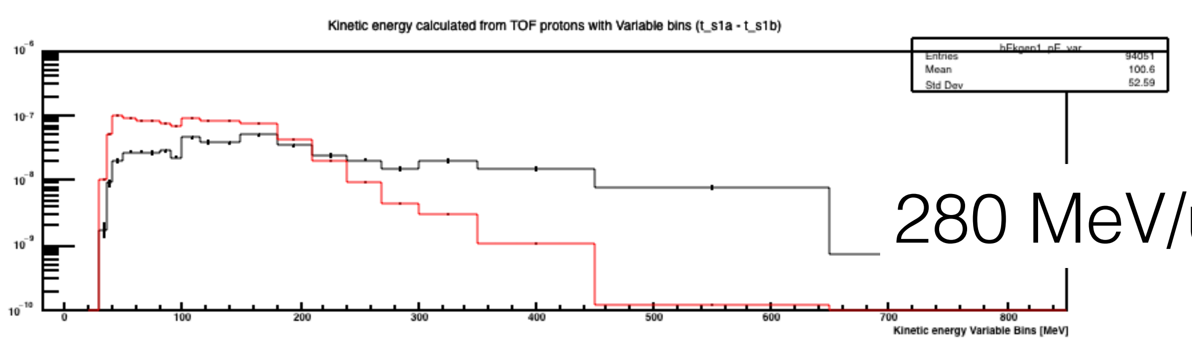


280 MeV/u

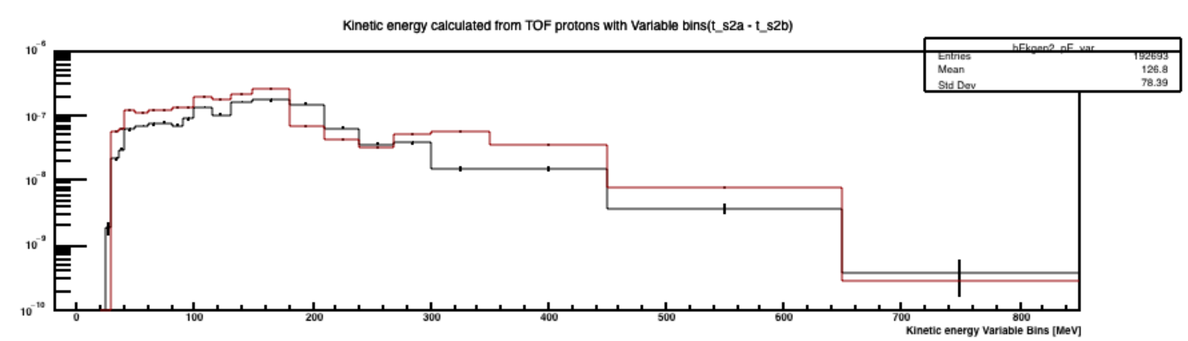


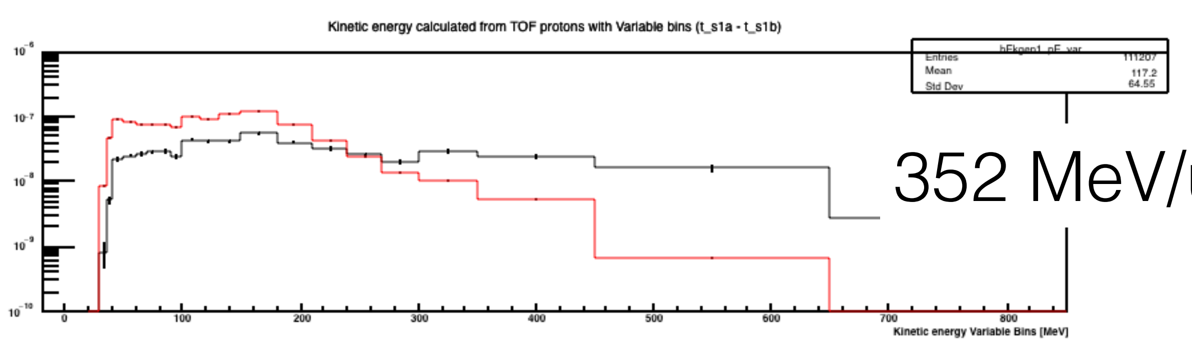


352 MeV/u

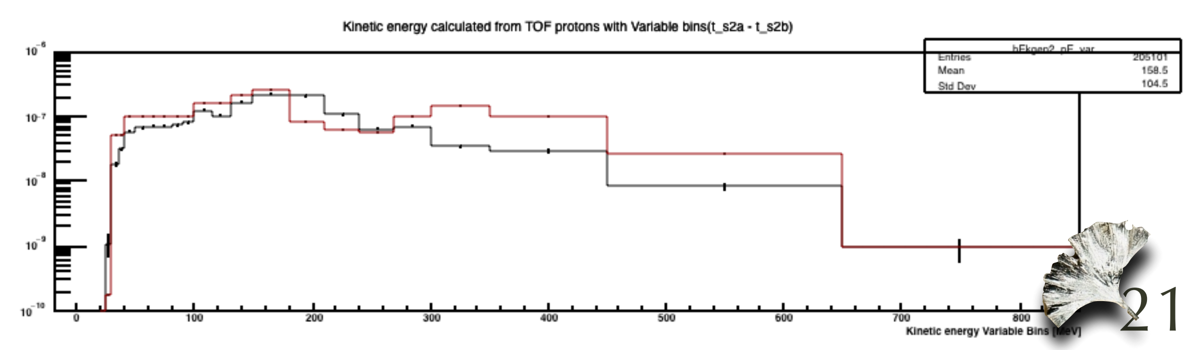

# Ekin Spectra (Data - FLUKA)Deuterons :: 50 - 32 :: Grafite

**Absolute Normalization**

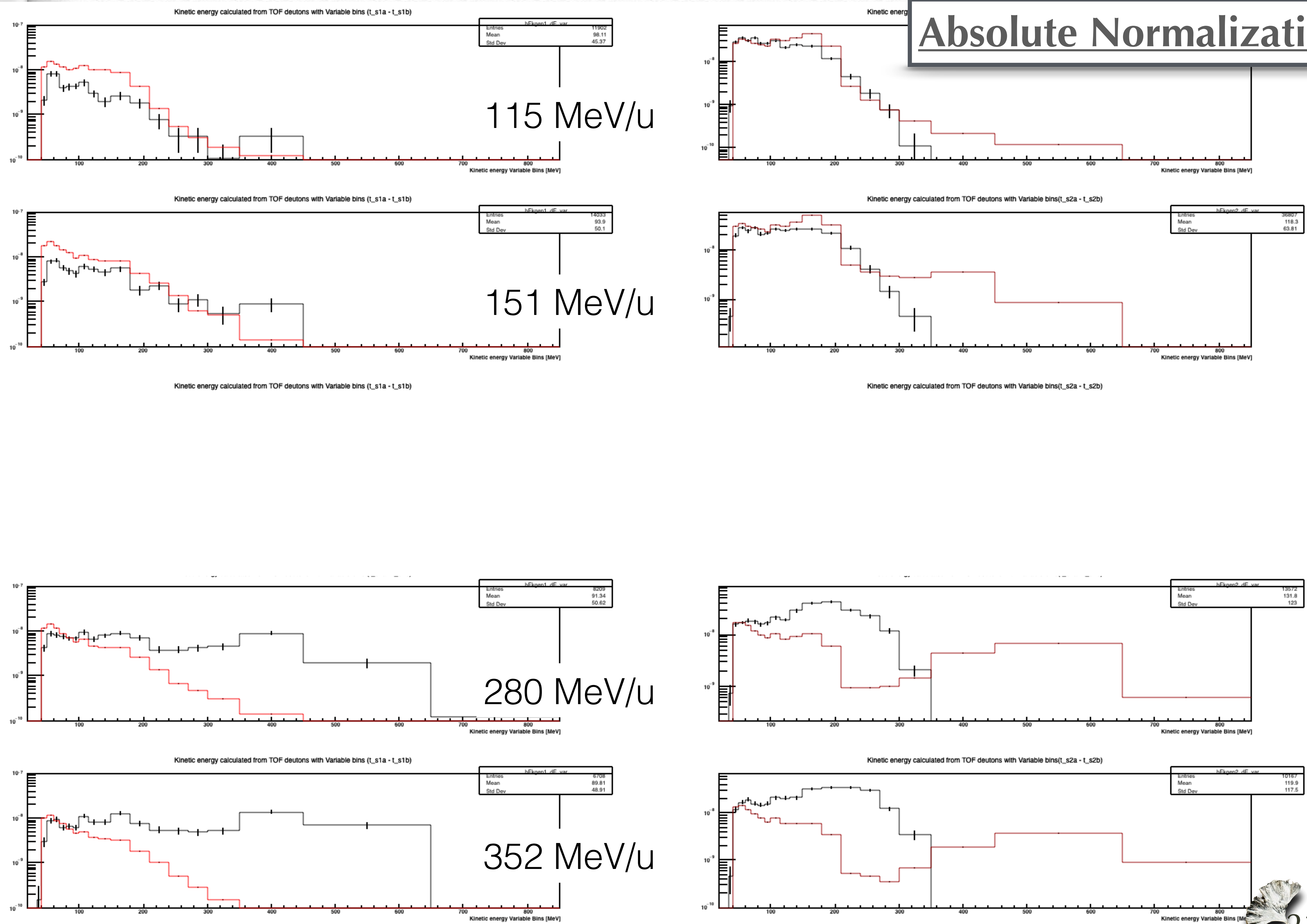

# Ekin Spectra (Data - FLUKA) Protons :: 50 - 32 :: Scint

Absolute Normalization

115 MeV/u

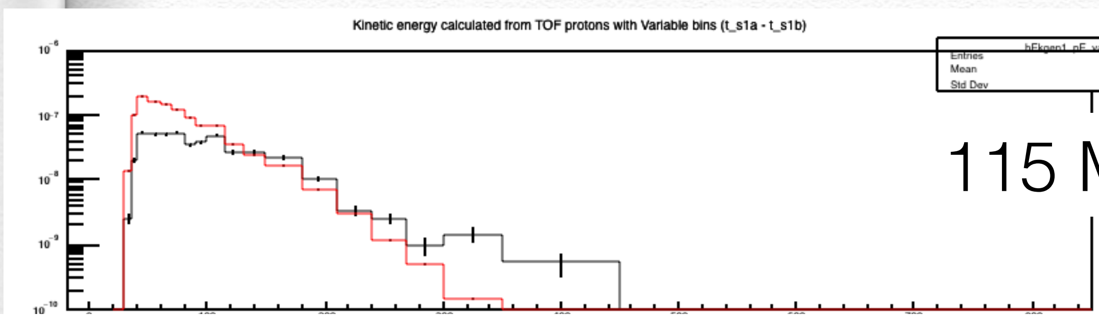


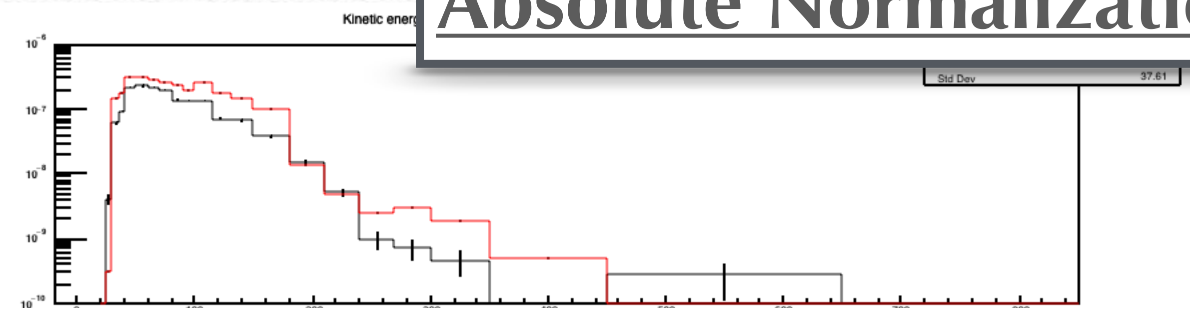


280 MeV/u

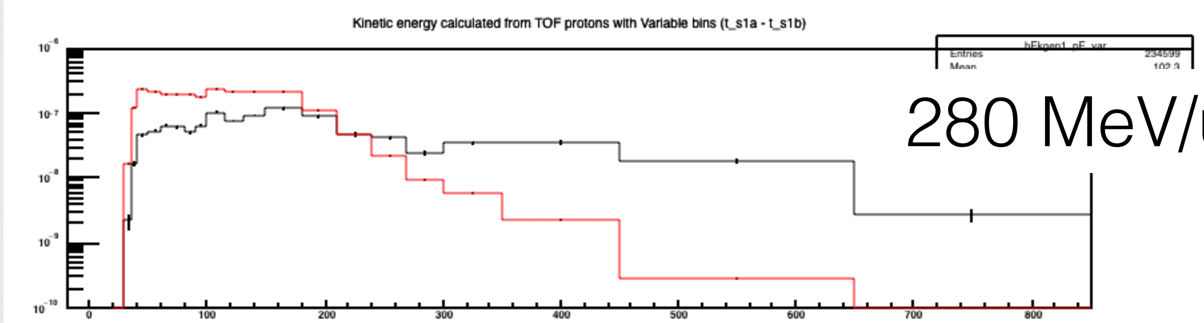


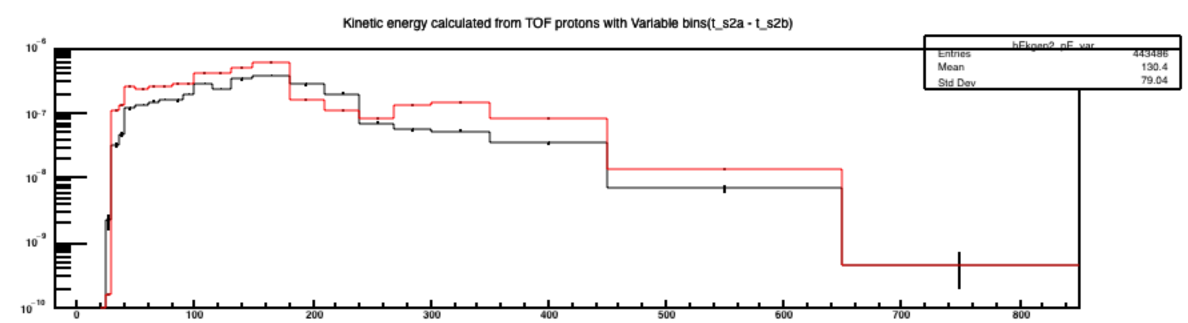


352 MeV/u

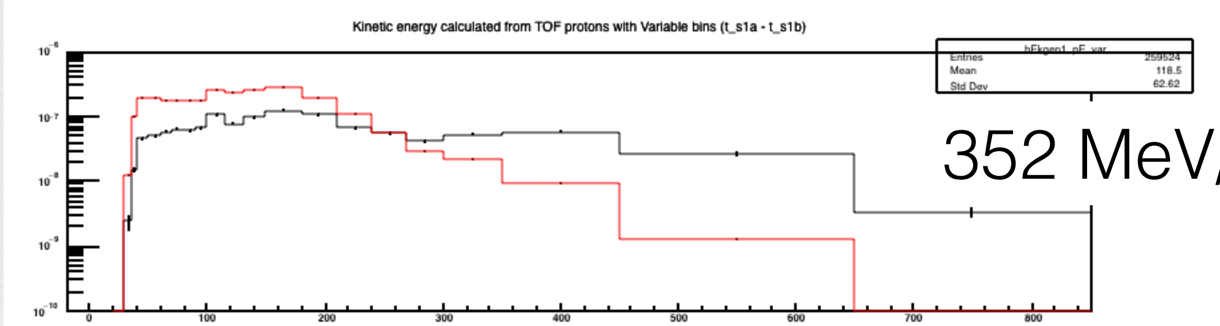


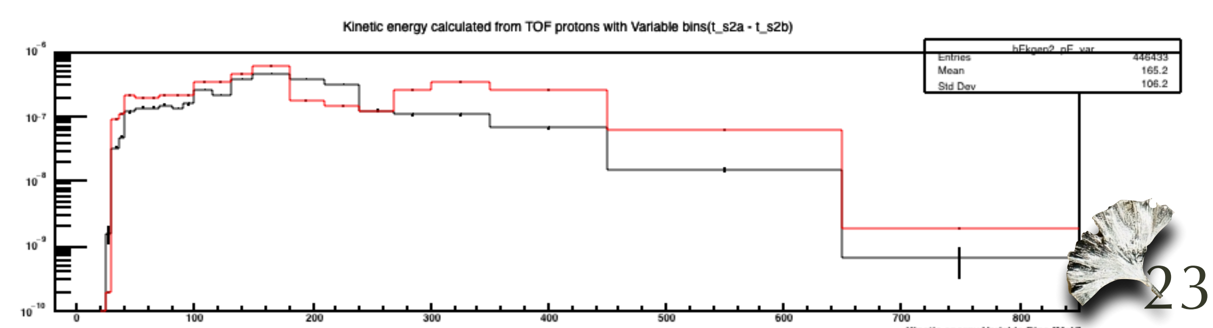

# Ekin Spectra (Data - FLUKA) Deuterons :: 50 - 32 :: Scint

**Absolute Normalization**

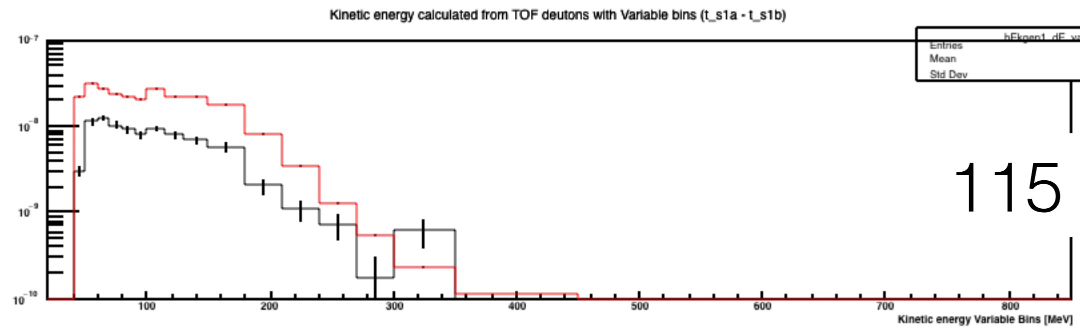


115 MeV/u

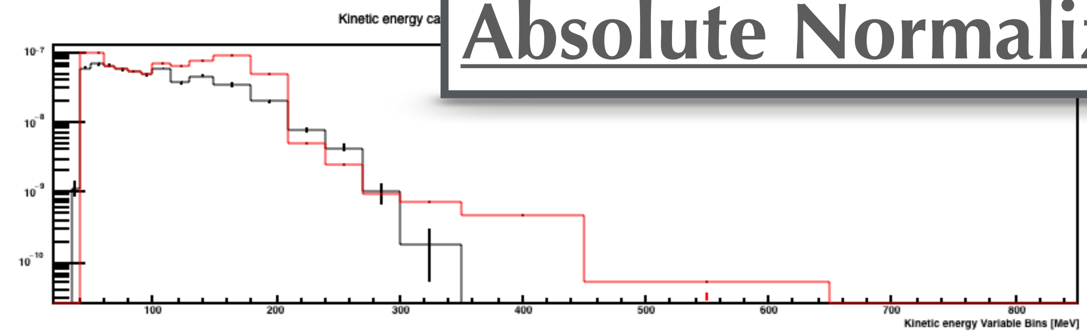


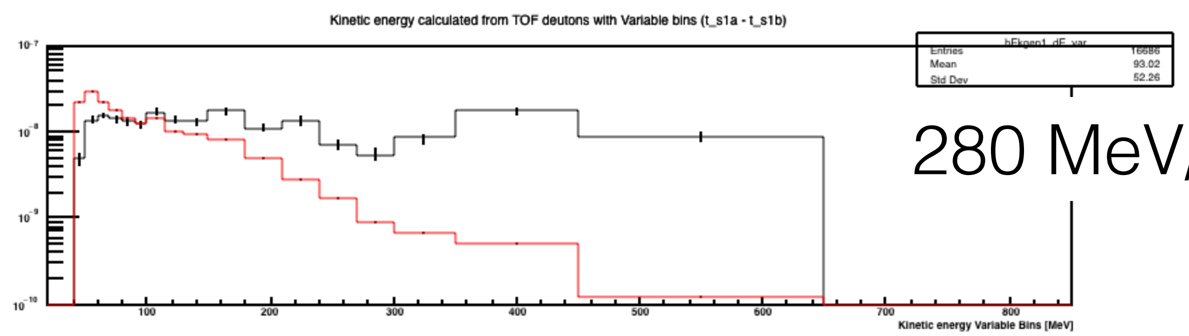


280 MeV/u

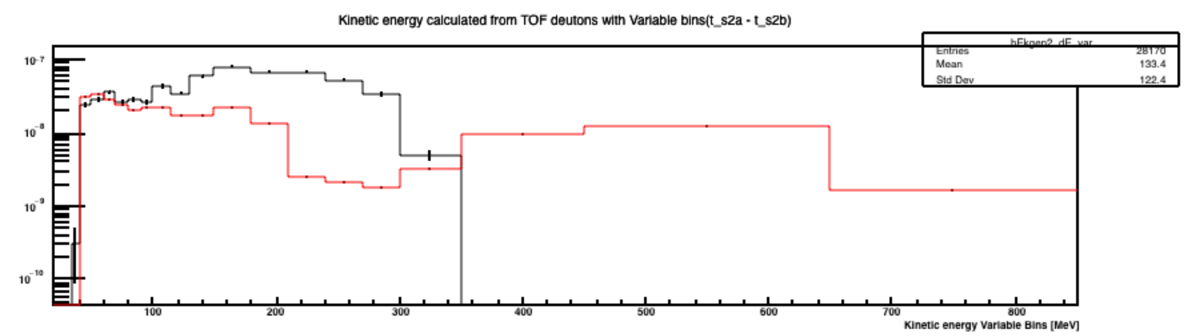


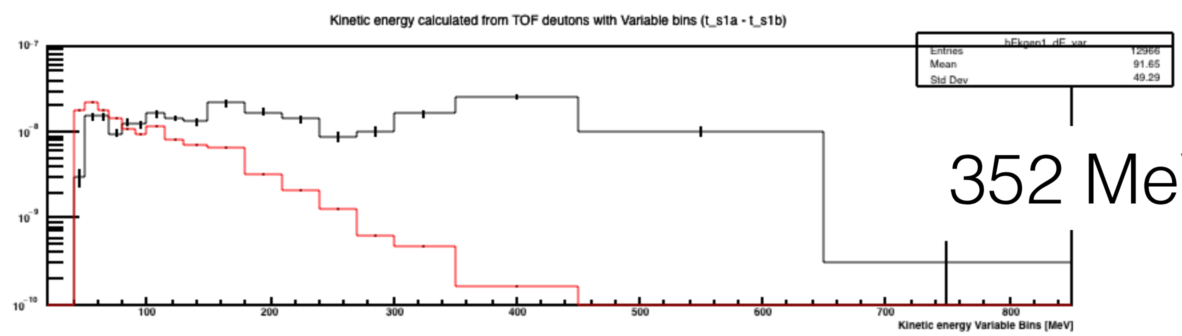


352 MeV/u

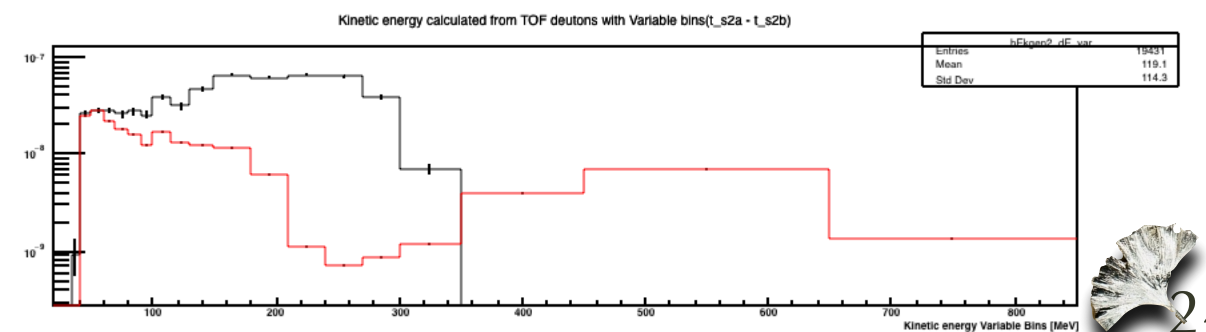

# Cross section on TARGET

*Only statistical uncertainties

PMMA, Graphite and Plastic scintillator. All efficiencies included.

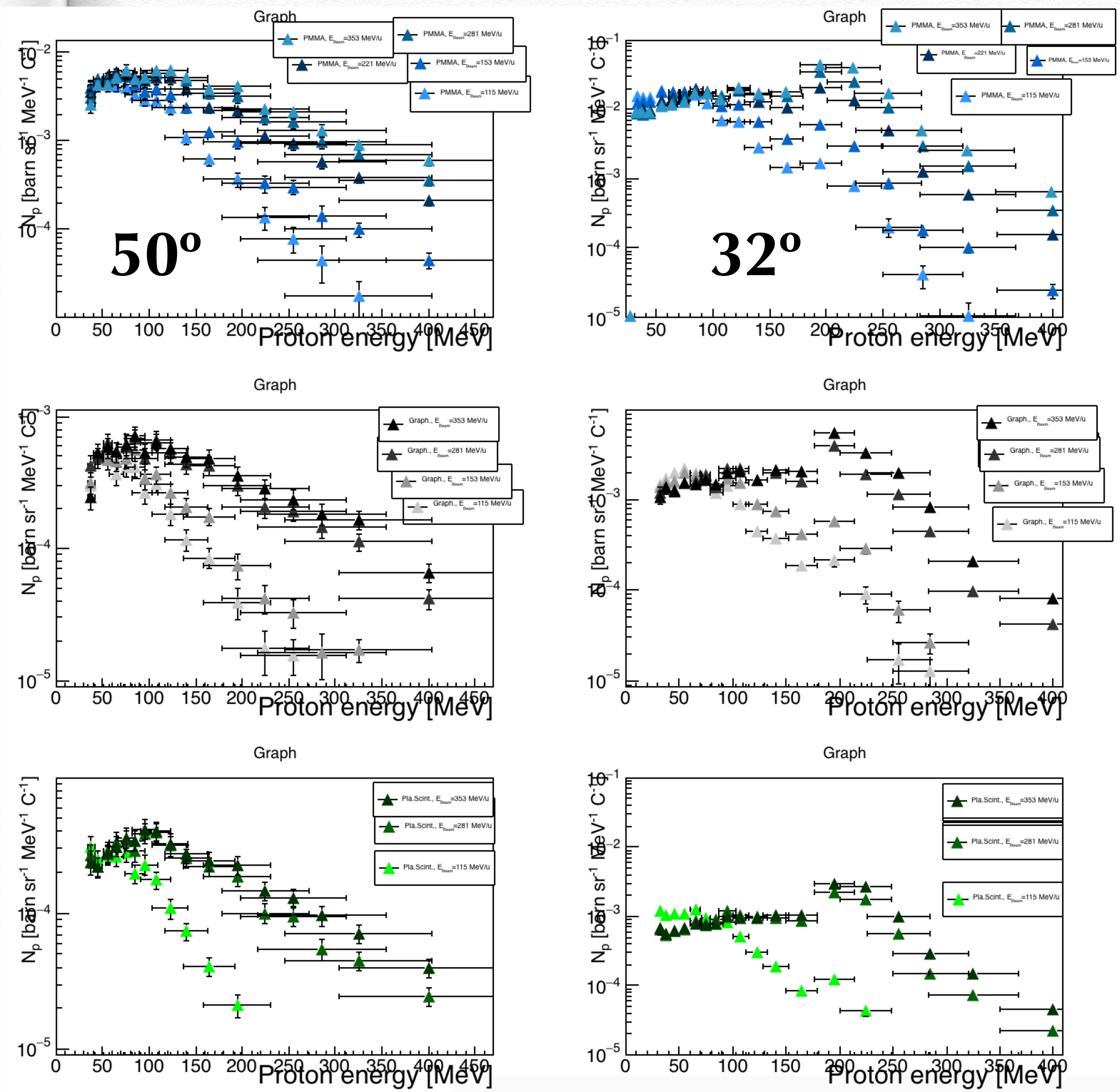


**PROTONS**

**$N_p$** [barn sr$^{-1}$ MeV$^{-1}$ C$^{-1}$]
**vs Proton Energy** [MeV]
($10^{-5} \div 10^{-1}$) / (0 ÷ 400)

- PMMA = $C_5O_2H_8$
- Graphite = C
- EJ-212 = $C_bH_a$

**Beam Energy**
**C 115**
**C 150**
**C 220**
**C 279**
**C 351**

# Cross section on TARGET

*Only statistical uncertainties

PMMA, Graphite and Plastic scintillator. All efficiencies included.

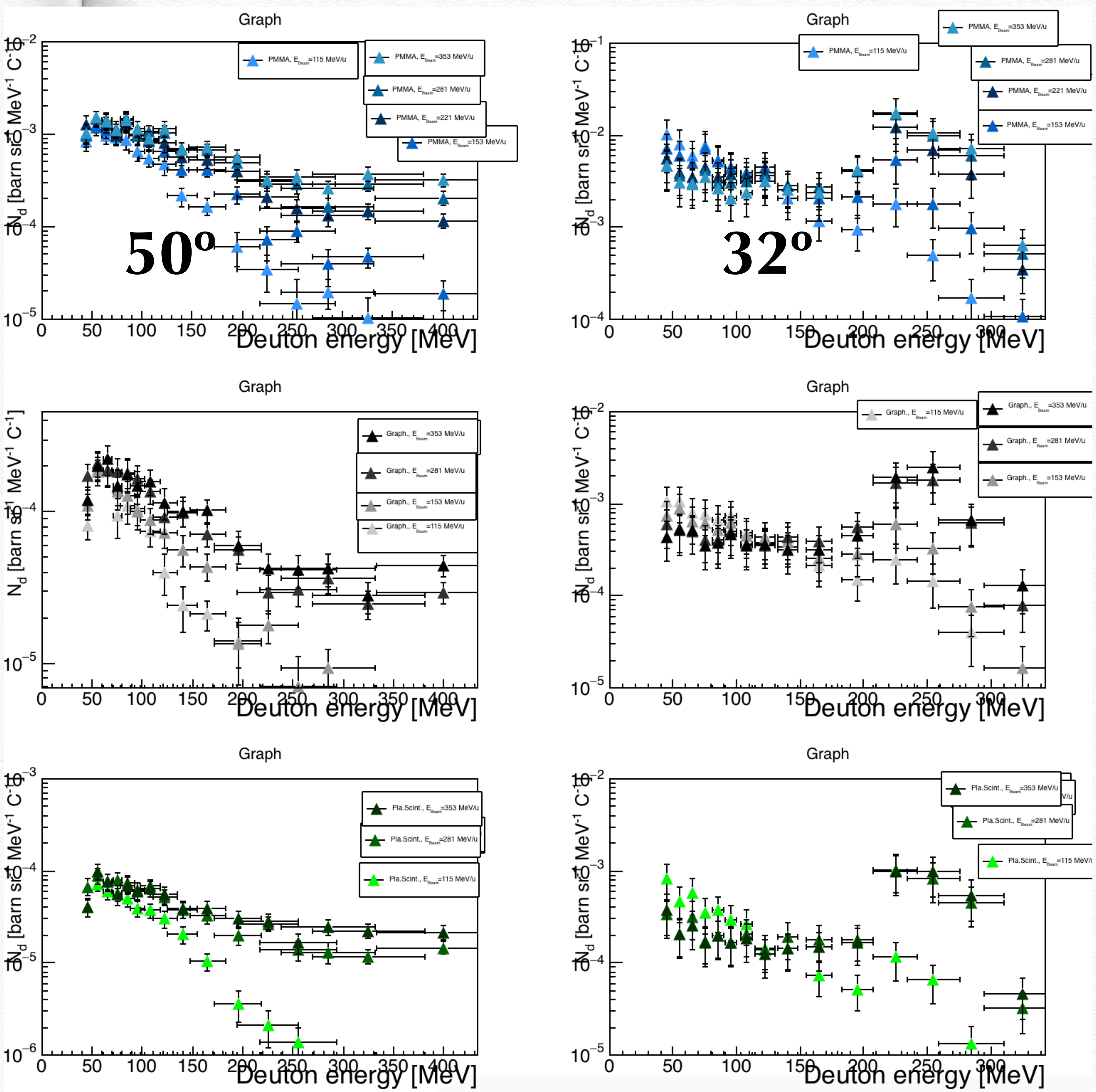


## DEUTERONS

**$N_d$** [barn sr$^{-1}$ MeV$^{-1}$ C$^{-1}$]
**vs Deuteron Energy** [MeV]
($10^{-5}$÷$10^{-1}$) / (0 ÷ 400)

- PMMA = $C_5O_2H_8$
- Graphite = C
- EJ-212 = $C_bH_a$

**Beam Energy**
**C 115**
**C 150**
**C 220**
**C 279**
**C 351**

**XSec:** From the combination of the different targets (subtraction of C from C2H4 and of C and H from C5O2H8) we obtain the C, O, H proton production cross-sections as a function of the kinetic energy, at 90º and 60º.

# PROTONS

• Graphite = **C**

$$\frac{d\sigma_C}{dE_k} = \frac{d\sigma^{Graphite}}{dE_k}$$

• EJ-212 = $C_b$**H**$_a$

$$\frac{d\sigma_H}{dE_k} = \frac{1}{0.524} \cdot [\frac{d\sigma^{PS}}{dE_k} - 0.476 \cdot \frac{d\sigma_C}{dE_k}]$$

• PMMA = $C_5$**O**$_2H_8$

$$\frac{d\sigma_O}{dE_k} = \frac{1}{2} \cdot [\frac{d\sigma^{PMMA}}{dE_k} - 8 \cdot \frac{d\sigma_H}{dE_k} - 5 \cdot \frac{d\sigma_C}{dE_k}]$$

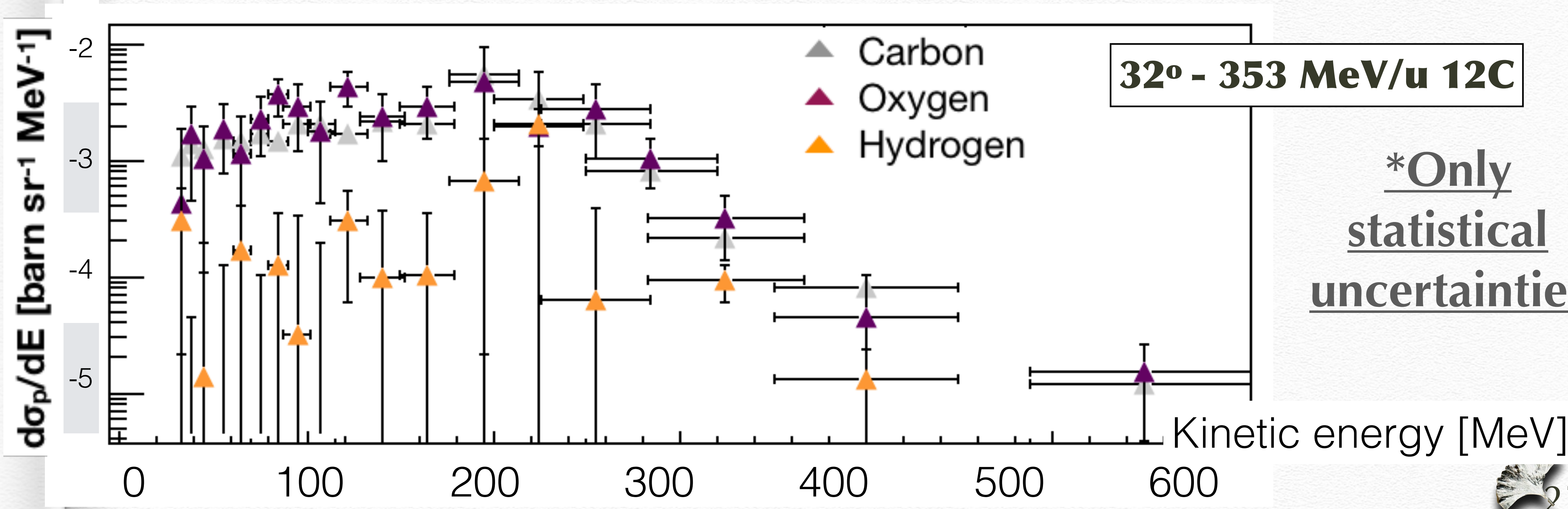


**32º - 353 MeV/u 12C**

***Only statistical uncertainties**

**XSec:** From the combination of the different targets (subtraction of C from C2H4 and of C and H from C5O2H8) we obtain the C, O, H proton production cross-sections as a function of the kinetic energy, at 90º and 60º.

# DEUTERONS

- Graphite = **C**

$$\frac{d\sigma_C}{dE_k} = \frac{d\sigma^{Graphite}}{dE_k}$$

- EJ-212 = $C_bH_a$

$$\frac{d\sigma_H}{dE_k} = \frac{1}{0.524} \cdot [\frac{d\sigma^{PS}}{dE_k} - 0.476 \cdot \frac{d\sigma_C}{dE_k}]$$

- PMMA = $C_5O_2H_8$

$$\frac{d\sigma_O}{dE_k} = \frac{1}{2} \cdot [\frac{d\sigma^{PMMA}}{dE_k} - 8 \cdot \frac{d\sigma_H}{dE_k} - 5 \cdot \frac{d\sigma_C}{dE_k}]$$

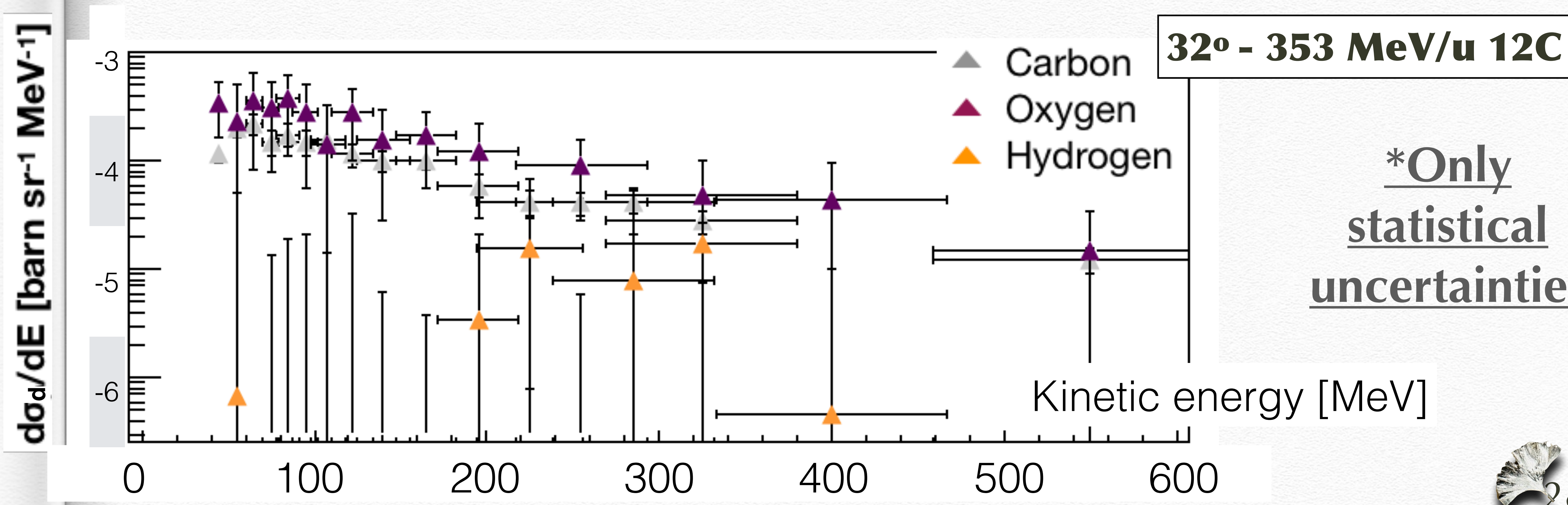


*Only statistical uncertainties

# Comparison with GANIL & FLUKA

*Only statistical uncertainties

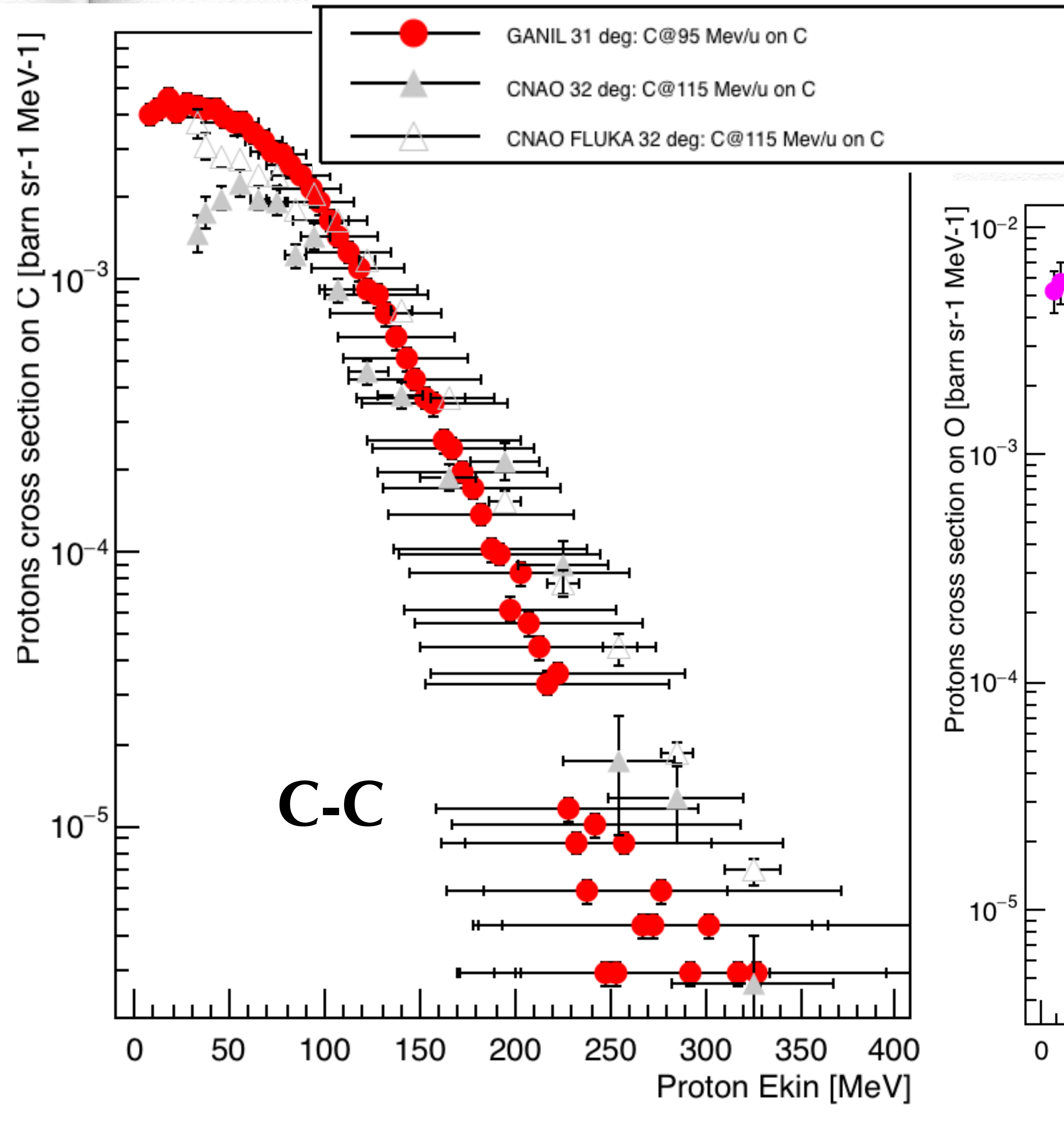


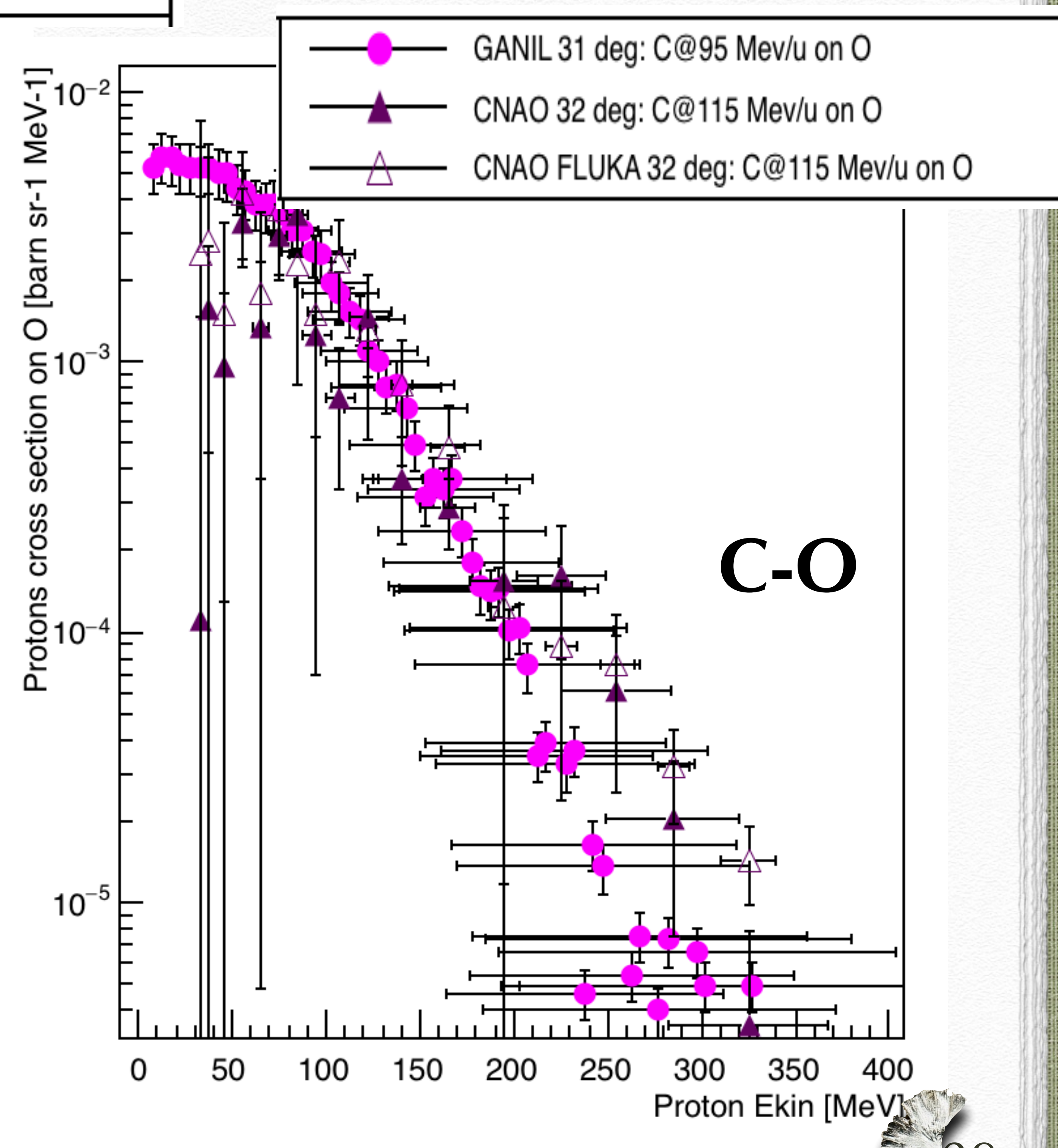

# Comparison with GANIL & FLUKA

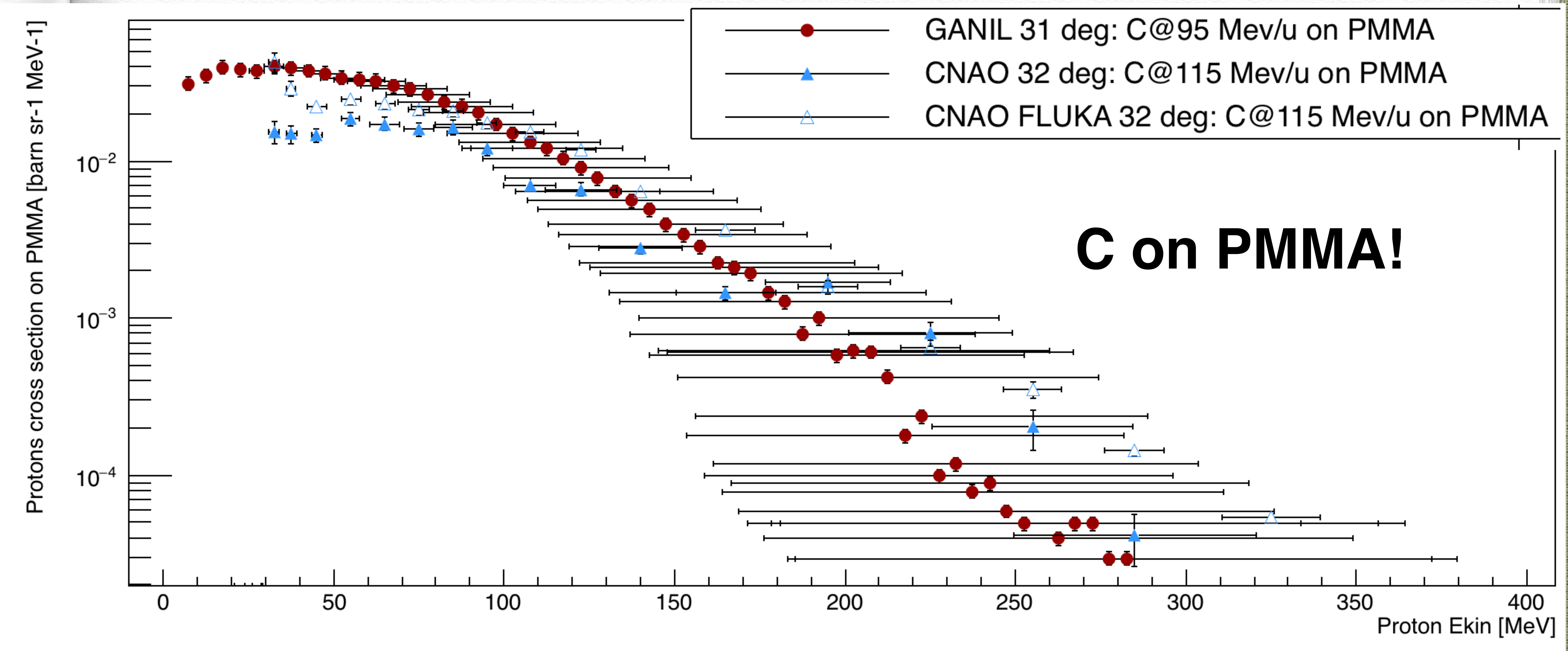


*Only statistical uncertainties

# TOTAL XSec vs Beam Energy

*Stat+Sys err

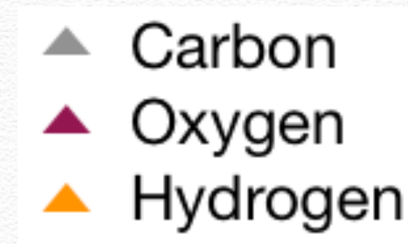


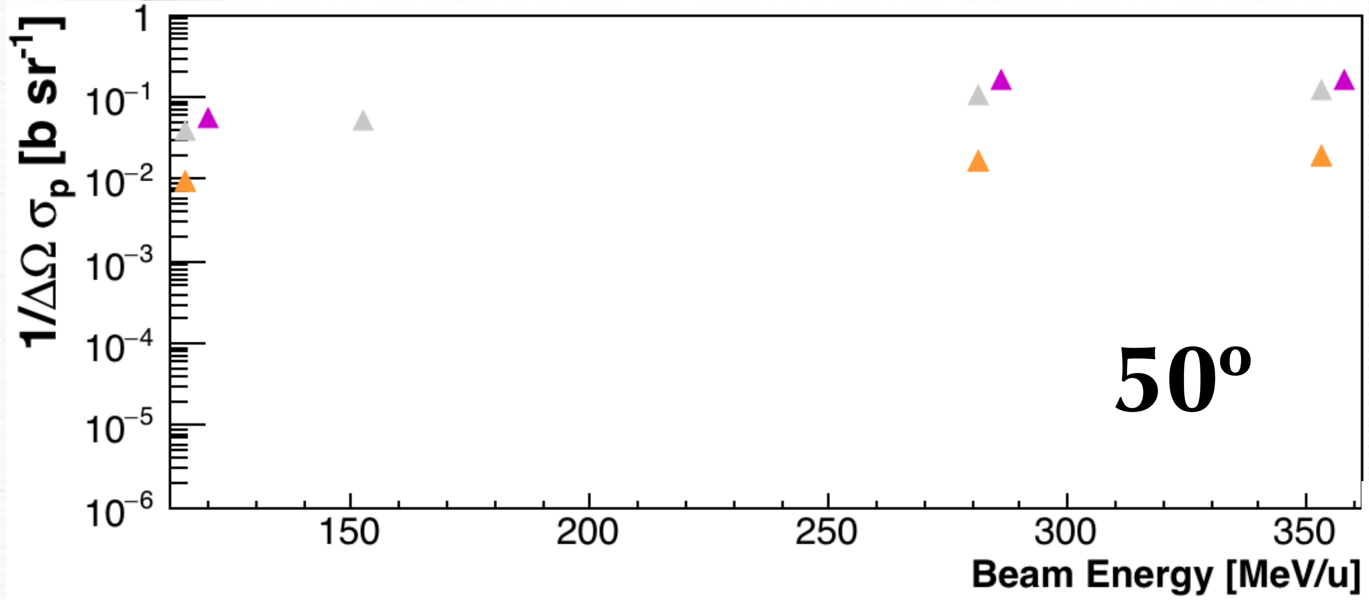


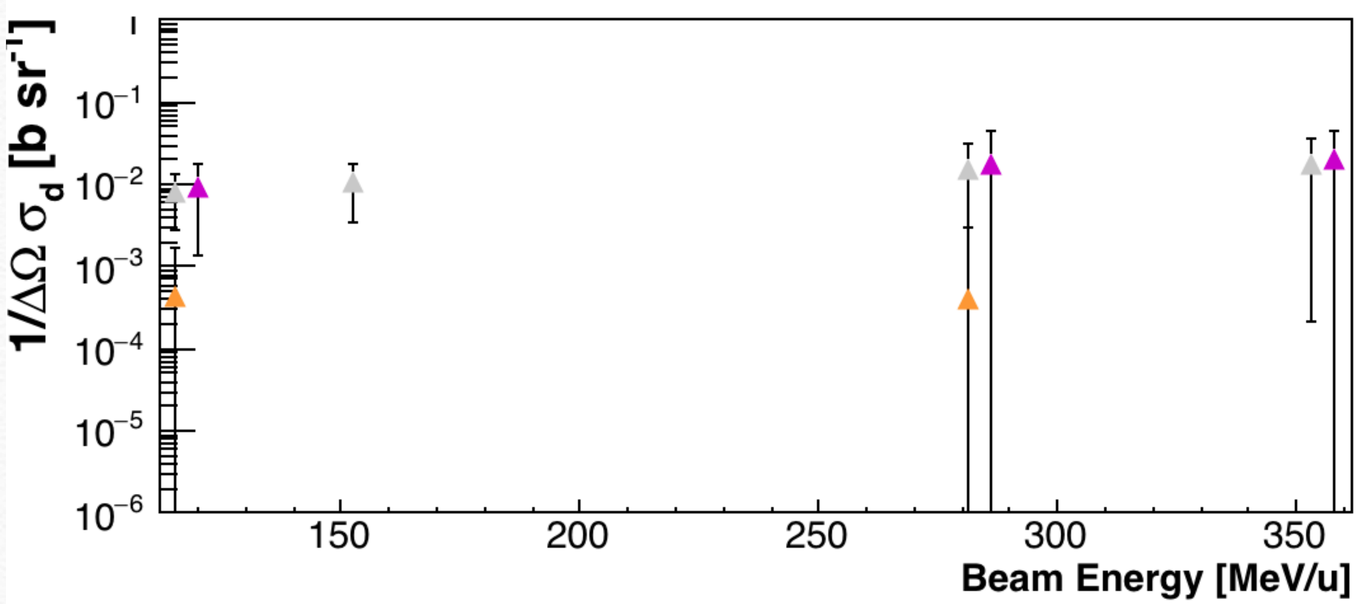


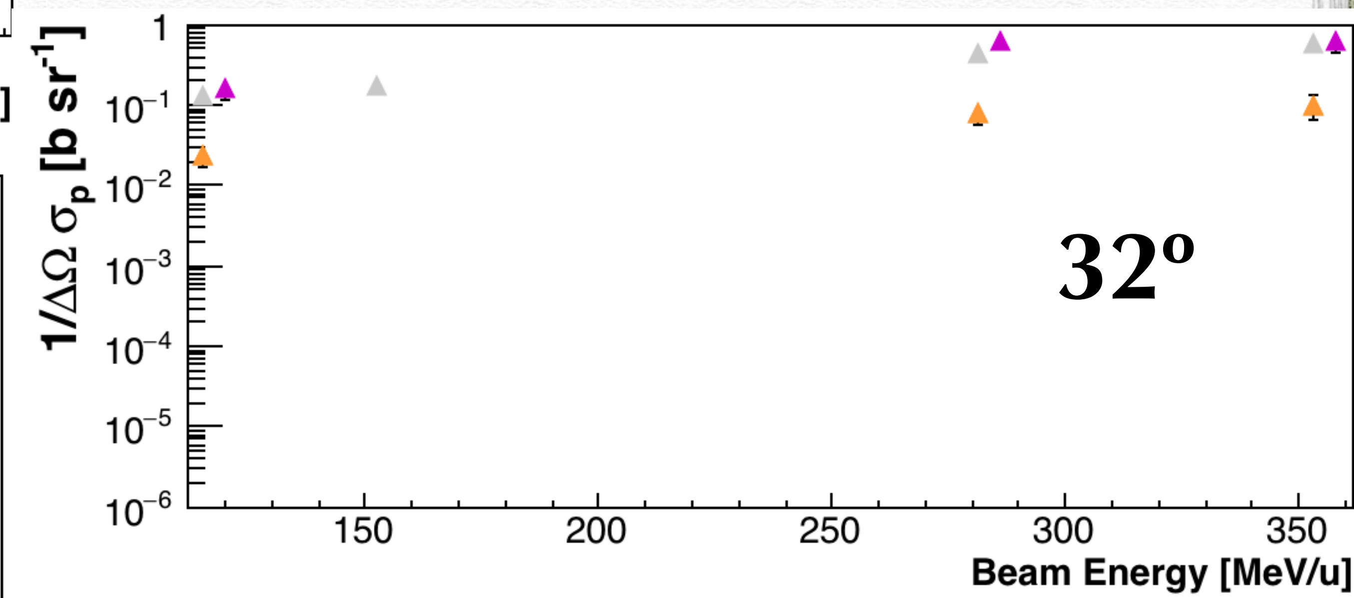


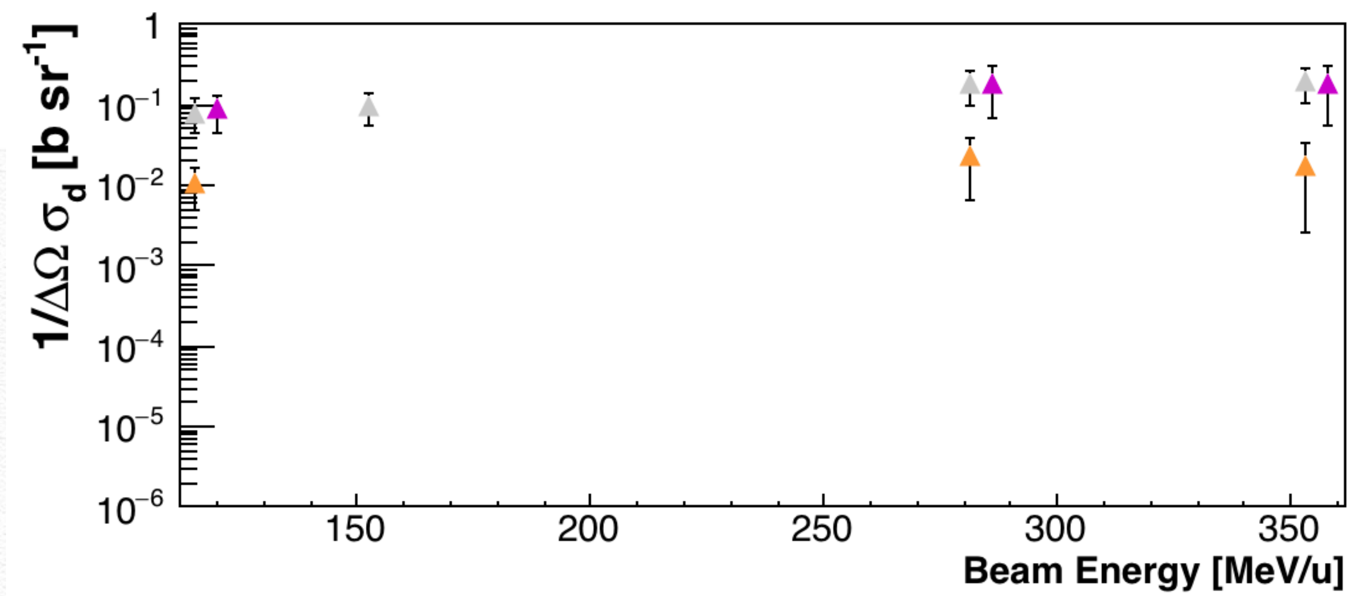


**In the TOTAL Xsec, DATA are corrected for the contamination of deuterons in the proton signal**

# TOTAL XSec vs Angle

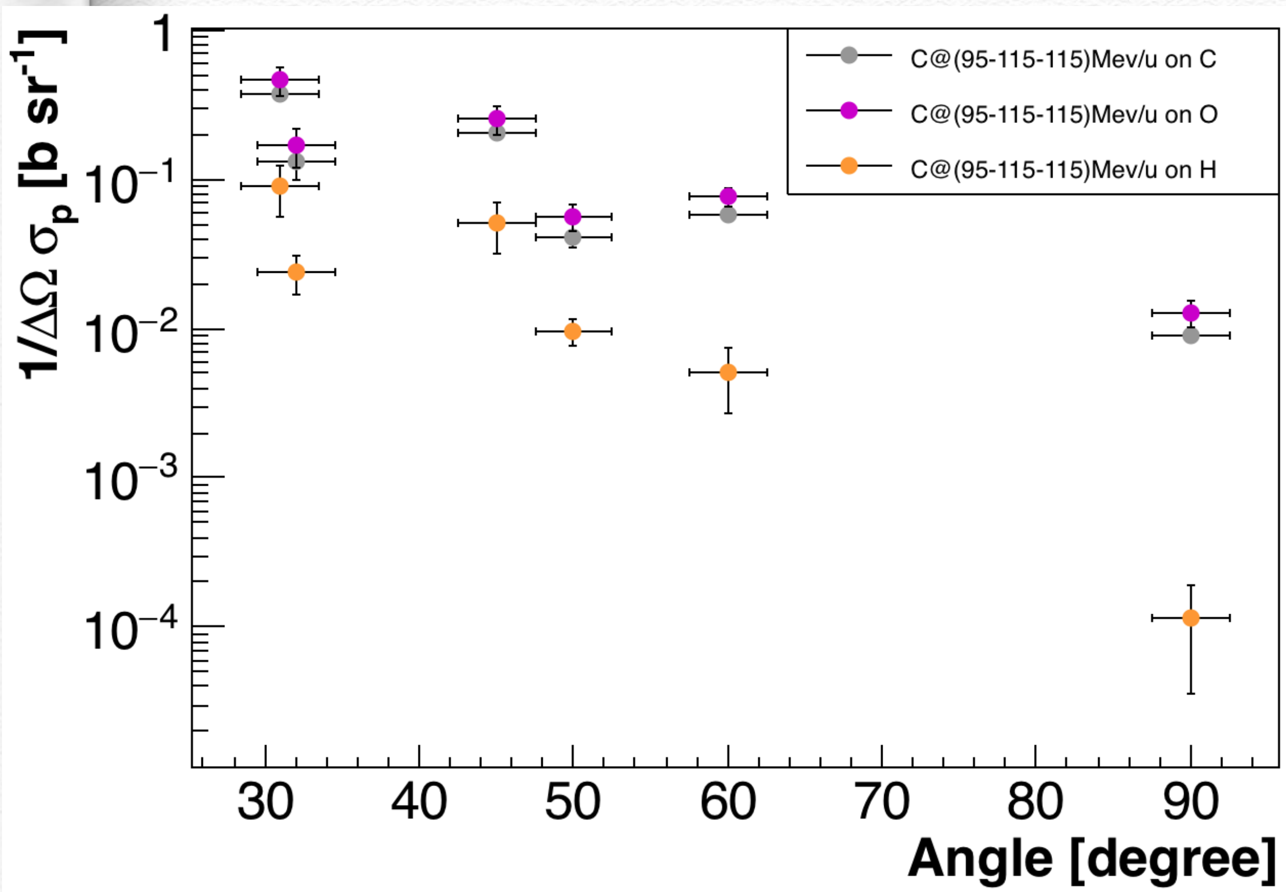


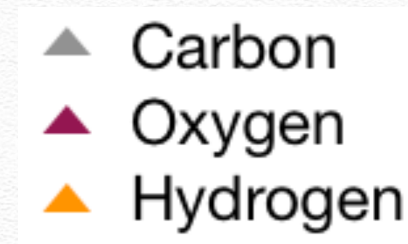


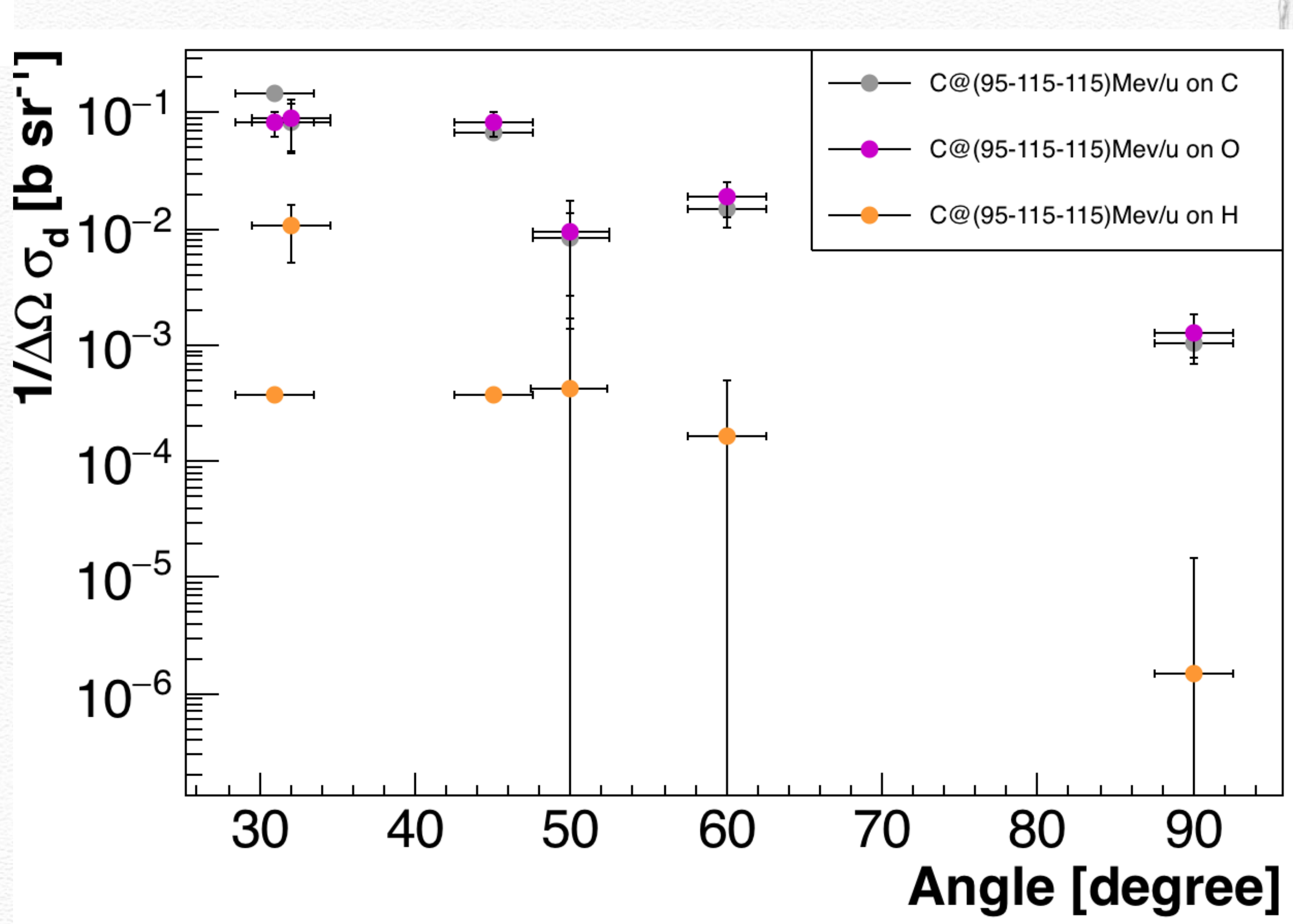

# Conclusions

- The experimental data analysis is at its conclusion (tritons included). We have to investigate more the underestimation of the detection efficiency computed from the flat simulation at 32º.

- The DATA-FLUKA comparison has been studied at 90º and 60º and it is encouraging regarding the models status (see backup slides). The analysis strategy has to be changed in order to take into account the mixing efficiency dependency to the fragment kinetic energy.

- Our aim is to publish also the DATA-FLUKA comparison at all 4 angles as a FOOT collaboration paper.

backup

# Particle Identification

Protons and Deutons have been selected from all other particles exploiting **deposited Energy vs ToF,** Edep vs 1/ToF, dE vs E and dE vs ToF information.

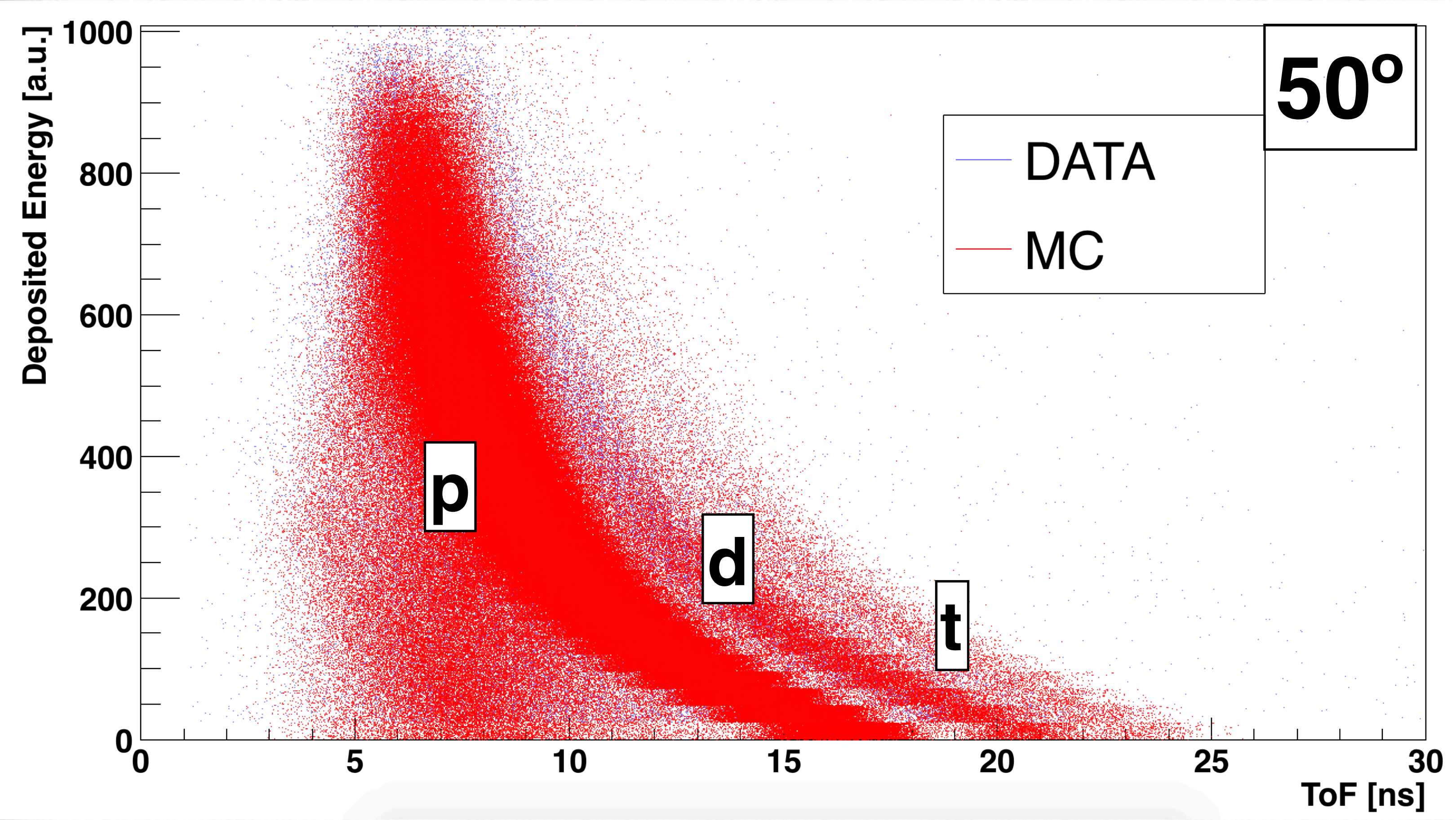


The use of MC allows to clearly identify the fragments and define our identification strategy. In the plot the separation lines that are applied on data to separate in mass the fragments are reported.

The deposited energy in the LYSO crystal is shown as a function of the time of flight of the measured particles for data and MC-data. For the data and the MC, the deposited energy is in arbitrary units. The fragments identity is shown in order to confirm the described data selection strategy.

# Particle Identification

**50°**

Protons Deutons and tritons have been selected from all other particles exploiting deposited Energy vs ToF, **Edep vs 1/ToF**, dE vs E and **dE vs ToF** information.

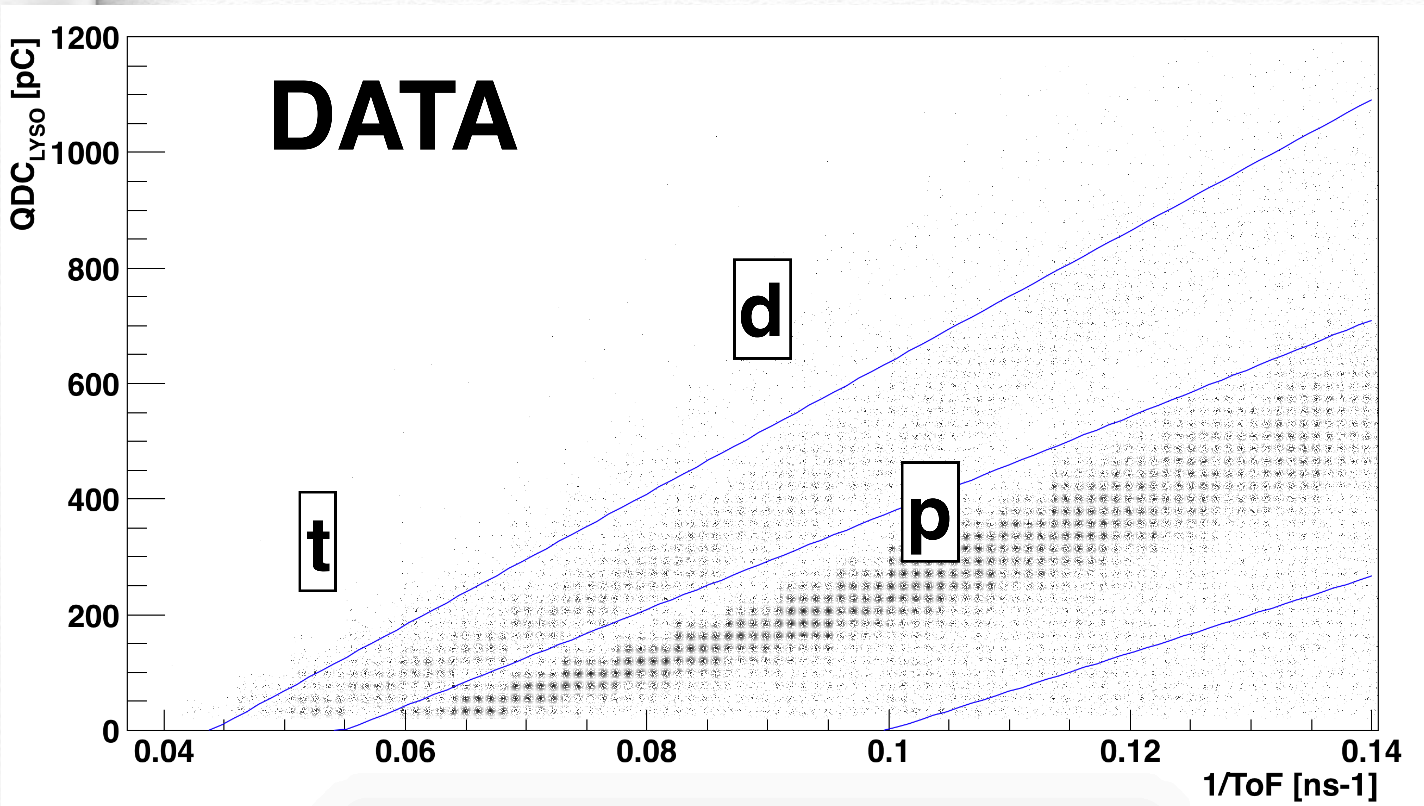


**Protons and deuterons are reasonably abundant in all the specific data sets: about 80% and 20% of the fragments respectively at 32°.**

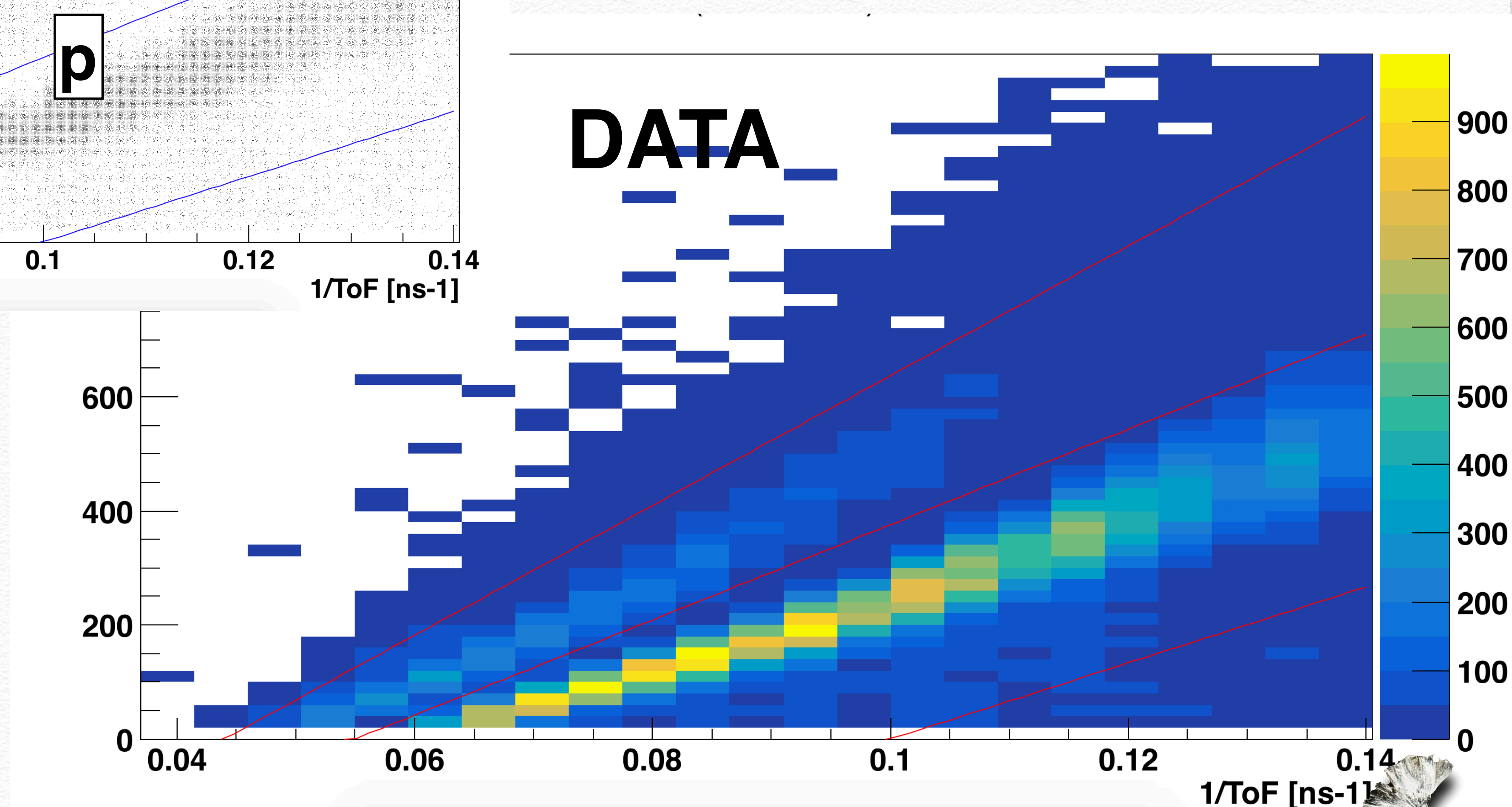


In this presentation we show the proton analysis

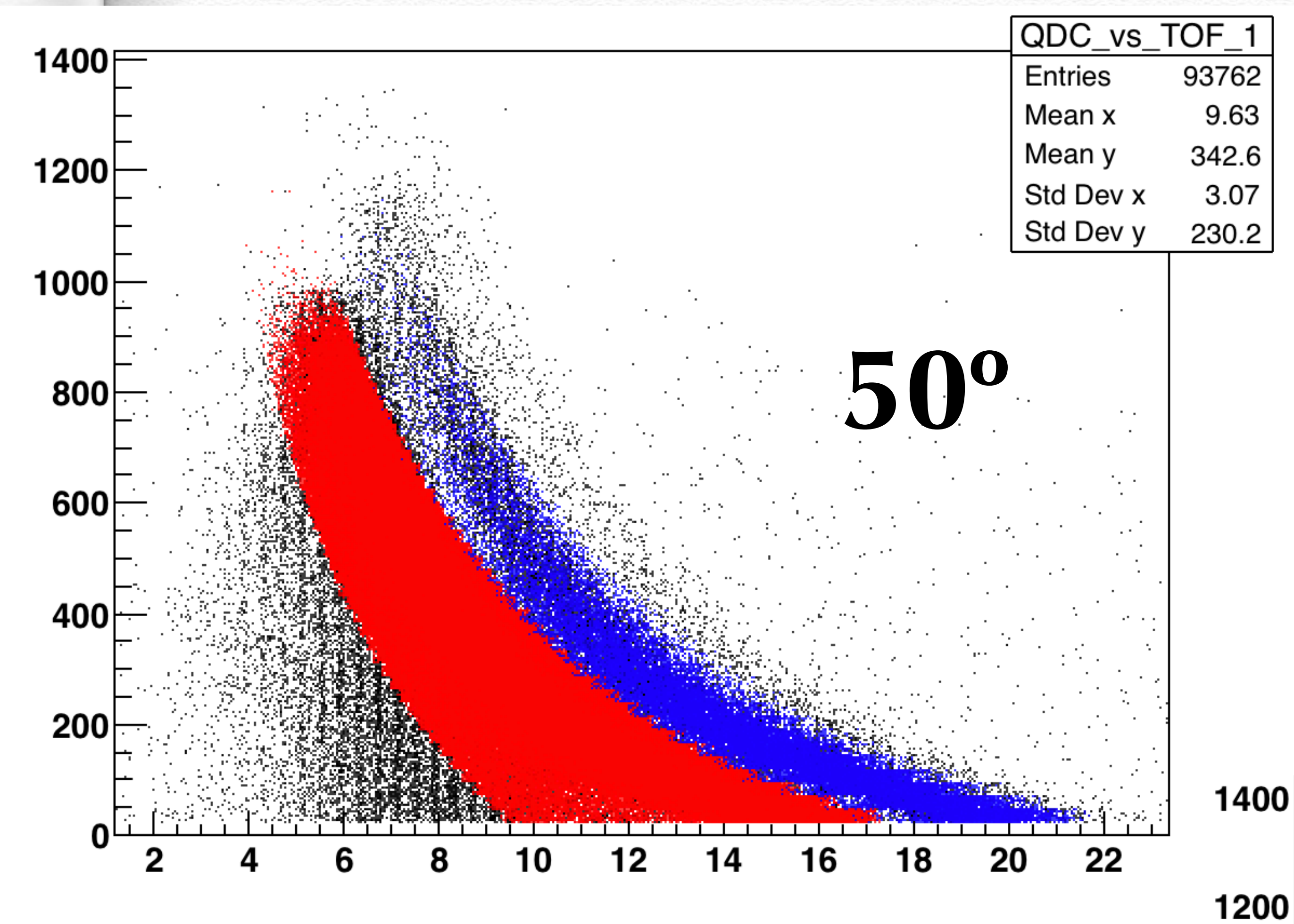
QDC_vs_TOF_1
Entries 93762
Mean x 9.63
Mean y 342.6
Std Dev x 3.07
Std Dev y 230.2
50°
0
200
400
600
800
1000
1200
1400
2
4
6
8
10
12
14
16
18
20
22

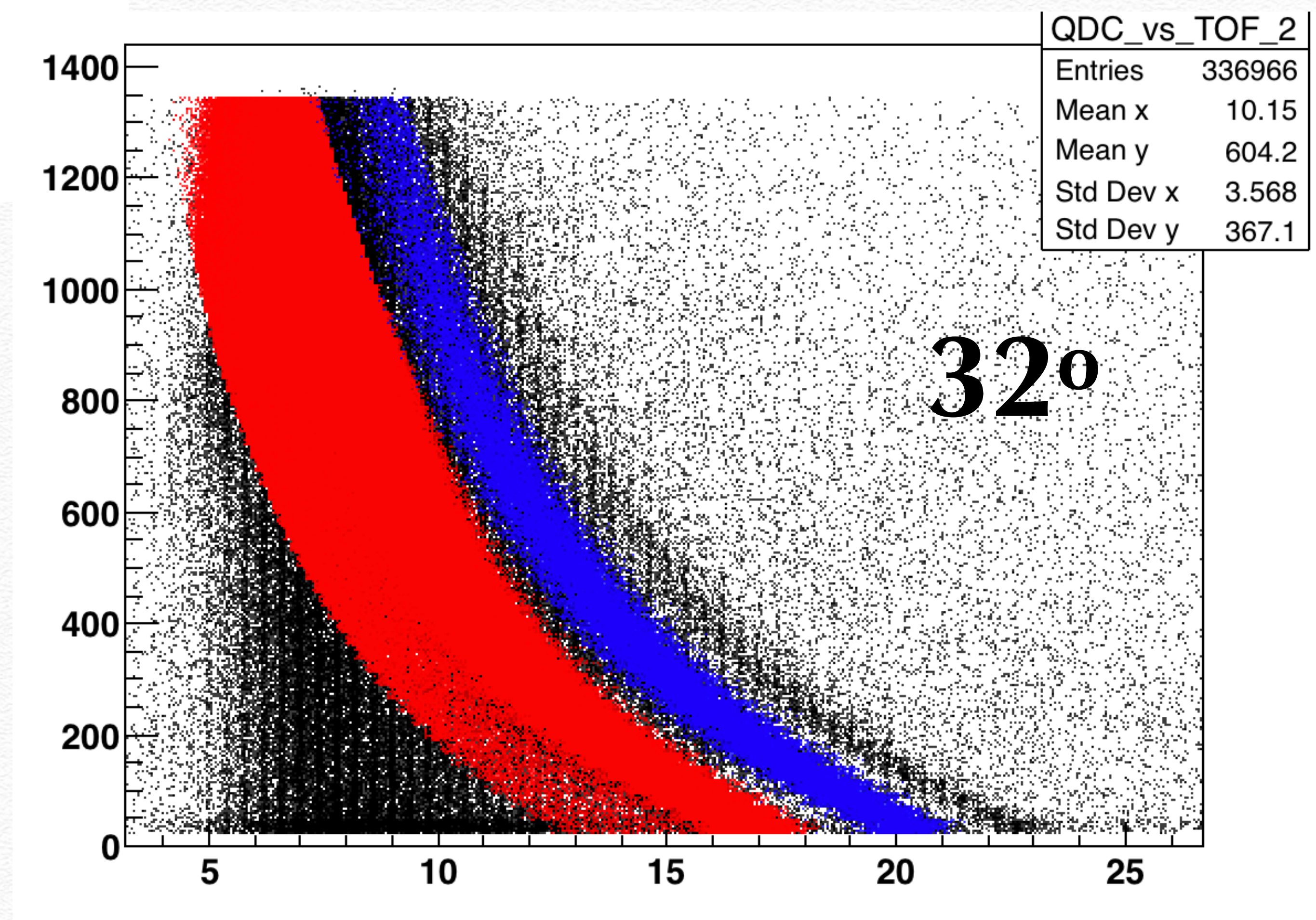
QDC_vs_TOF_2
Entries 336966
Mean x 10.15
Mean y 604.2
Std Dev x 3.568
Std Dev y 367.1
32°
0
200
400
600
800
1000
1200
1400
5
10
15
20
25

# Cr

C350

The 12 … e obtained as:

$$\ldots k) \cdot \frac{1}{N_Y} \cdot \frac{1}{\epsilon}$$

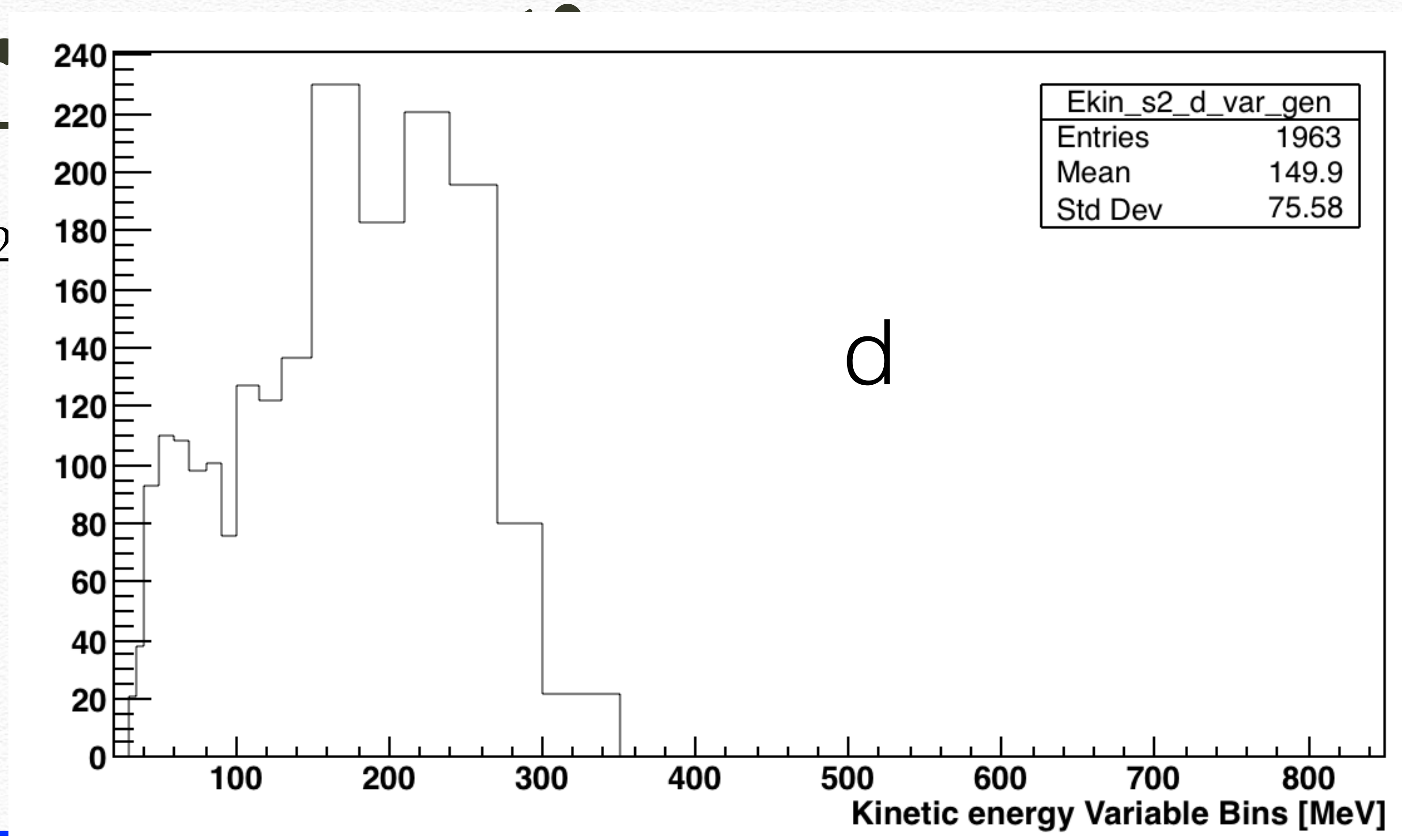


The energy loss by the

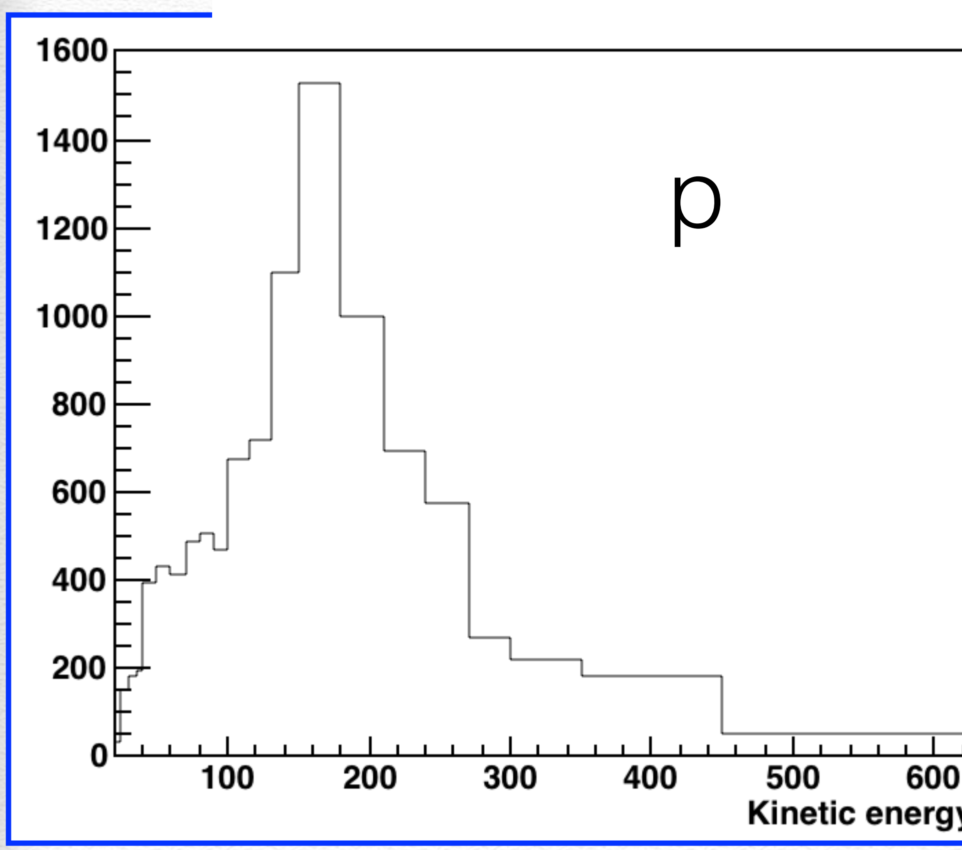


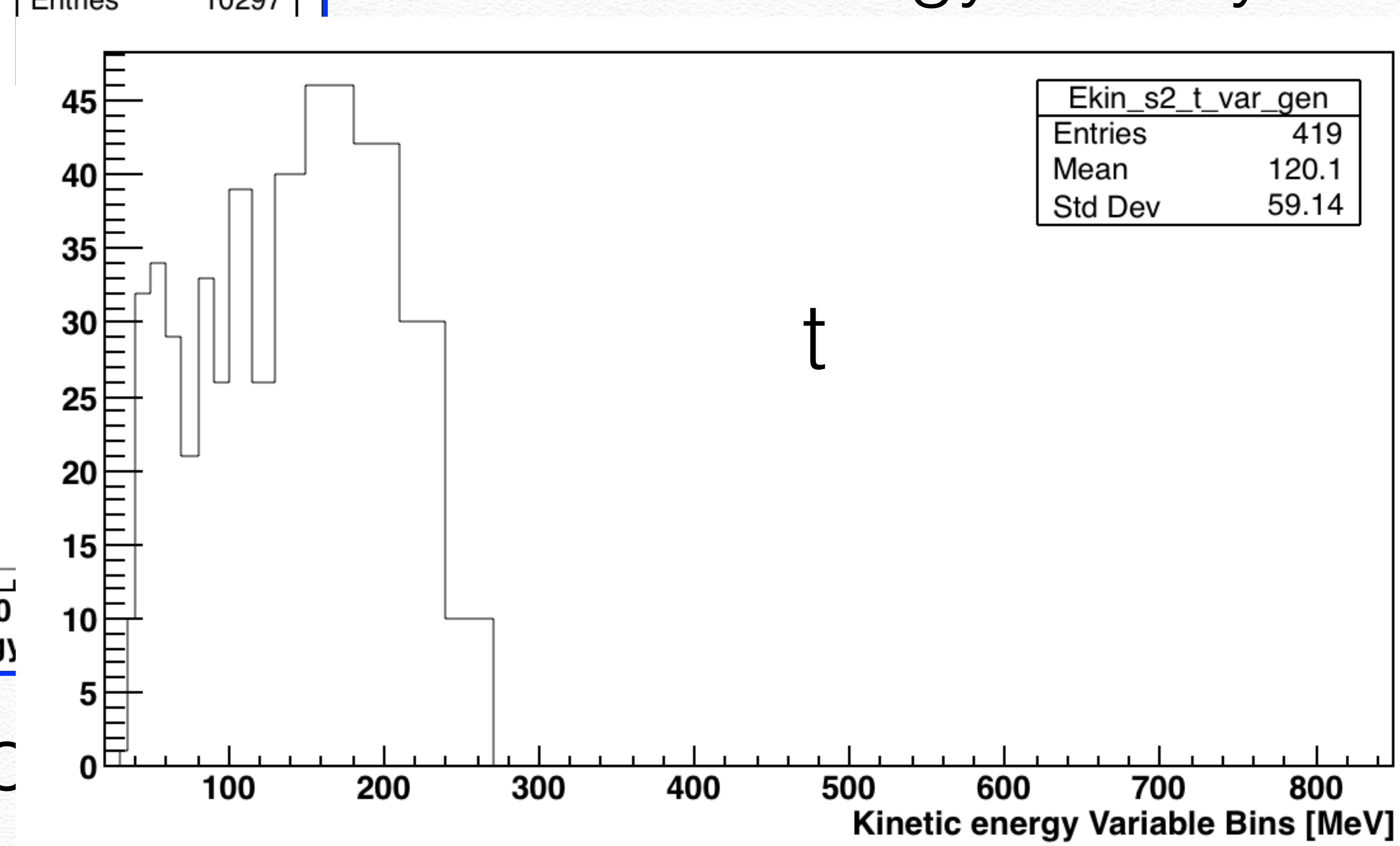


Ekin at generatio

# C350

e top plot and converted in the kinetic
ta refer to Arm2, graphite target with C-ion

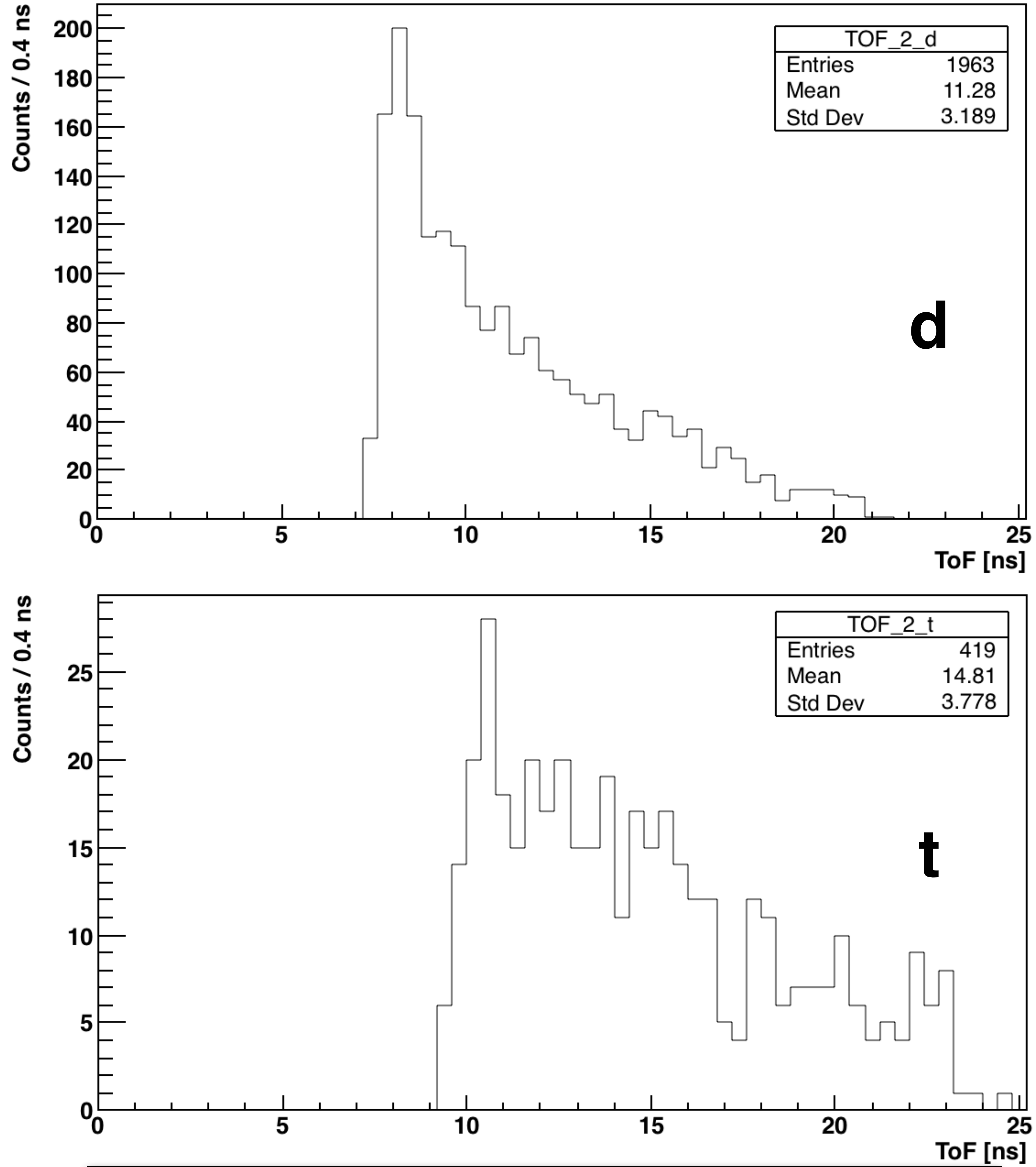


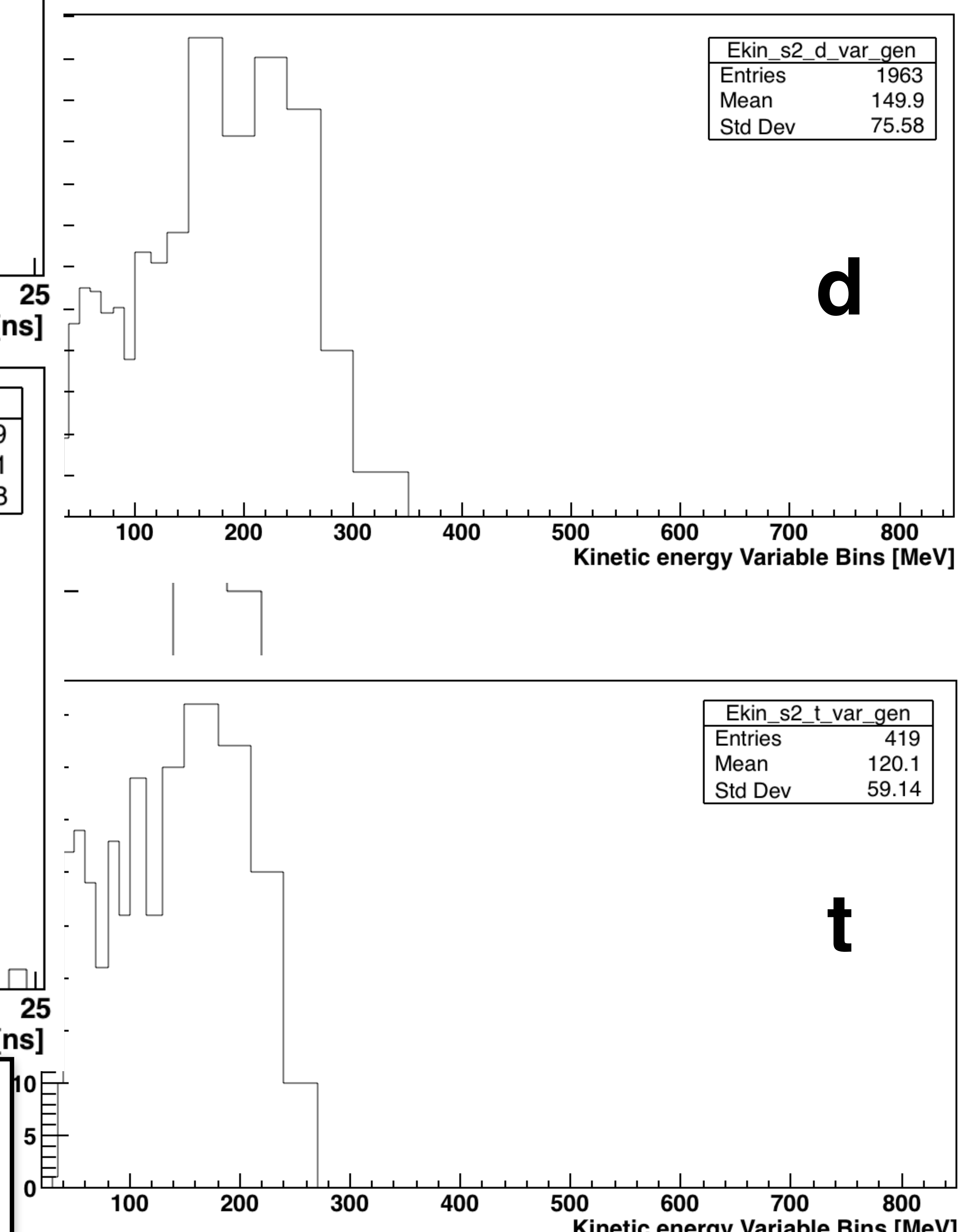


Energy resolution as a function of deuteron kinetic energy ranges from **8% (4%) up to 28% (11%)** for 50$^{o}$ (32$^{o}$) (worsening with increasing energy).

# OLD FLUKA vs NEW FLUKA

**@90º,60º**

## OLD

Table III
PARTICLE IDENTIFICATION EFFICIENCY: SELECTION EFFICIENCIES EVALUATED FOR BOTH 90° AND 60° DETECTION CONFIGURATIONS.

| $E^{C}_{kin}$ $[MeV/u]$ | $\epsilon^{pp}$ [%] | $\epsilon^{dd}$ [%] | $\epsilon^{tt}$ [%] |
|---|---|---|---|
| $90^o$ | | | |
| 115 | 95 ± 5 | 89 ± 9 | 85 ± 12 |
| 153 | 95 ± 5 | 85 ± 14 | 91 ± 6 |
| 221 | 94 ± 5 | 85 ± 12 | 86 ± 10 |
| 281 | 94 ± 5 | 84 ± 12 | 71 ± 31 |
| 353 | 94 ± 5 | 84 ± 14 | 81 ± 15 |
| $60^o$ | | | |
| 115 | 95 ± 4 | 78 ± 21 | 76 ± 32 |
| 153 | 95 ± 5 | 77 ± 22 | 83 ± 17 |
| 221 | 95 ± 5 | 75 ± 23 | 73 ± 32 |
| 281 | 95 ± 5 | 75 ± 24 | 76 ± 26 |
| 353 | 94 ± 5 | 75 ± 24 | 69 ± 37 |

Table IV
PARTICLE IDENTIFICATION EFFICIENCY: OFF DIAGONAL ELEMENTS EVALUATED FOR BOTH THE 90° AND 60° DETECTION CONFIGURATIONS.

| $E^{C}_{kin}$ $[MeV/u]$ | $\epsilon^{dp}$ [%] | $\epsilon^{tp}$ [%] | $\epsilon^{pd}$ [%] | $\epsilon^{td}$ [%] | $\epsilon^{dt}$ [%] |
|---|---|---|---|---|---|
| $90^o$ | | | | | |
| 115 | 6 ± 7 | - | 2 ± 2 | 12 ± 13 | 5 ± 7 |
| 153 | 10 ± 15 | 2 ± 3 | 1 ± 2 | 5 ± 4 | 4 ± 5 |
| 221 | 4 ± 4 | 3 ± 4 | 2 ± 3 | 11 ± 10 | 7 ± 6 |
| 281 | 5 ± 3 | 2 ± 2 | 2 ± 3 | 8 ± 6 | 8 ± 7 |
| 353 | 4 ± 2 | 1 ± 1 | 2 ± 2 | 10 ± 10 | 7 ± 7 |
| $60^o$ | | | | | |
| 115 | 4 ± 3 | 2 ± 2 | 1 ± 2 | 3 ± 4 | 13 ± 13 |
| 153 | 4 ± 2 | 2 ± 2 | 1 ± 2 | 2 ± 2 | 16 ± 16 |
| 221 | 4 ± 4 | 2 ± 2 | 1 ± 2 | 8 ± 14 | 17 ± 17 |
| 281 | 4 ± 3 | 3 ± 3 | 1 ± 2 | 10 ± 19 | 16 ± 16 |
| 353 | 4 ± 3 | 5 ± 6 | 2 ± 3 | 10 ± 14 | 17 ± 17 |

## NEW

Table III
PARTICLE IDENTIFICATION EFFICIENCY: SELECTION EFFICIENCIES EVALUATED FOR BOTH 90° AND 60° DETECTION CONFIGURATIONS.

| $E^{C}_{kin}$ $[MeV/u]$ | $\epsilon^{pp}$ [%] | $\epsilon^{dd}$ [%] | $\epsilon^{tt}$ [%] |
|---|---|---|---|
| $50^o$ | | | |
| 115 | 95 ± 5 | 88 ± 12 | 86 ± 19 |
| 150 | 95 ± 5 | 81 ± 21 | 89 ± 7 |
| 221 | 94 ± 5 | 86 ± 12 | 91 ± 6.1 |
| 279 | 95 ± 5 | 85 ± 11 | 91 ± 6.3 |
| 351 | 95 ± 5 | 85 ± 13 | 83 ± 21 |
| $32^o$ | | | |
| 115 | 95 ± 5 | 79 ± 20 | 81 ± 30 |
| 150 | 95 ± 4.8 | 78 ± 22 | 79 ± 30 |
| 221 | 95 ± 4.6 | 76 ± 23 | 86 ± 14 |
| 279 | 95 ± 4.7 | 76 ± 24 | 83 ± 18 |
| 351 | 94 ± 5.4 | 76 ± 23 | 82 ± 23 |

Table IV
PARTICLE IDENTIFICATION EFFICIENCY: OFF DIAGONAL ELEMENTS EVALUATED FOR BOTH THE 90° AND 60° DETECTION CONFIGURATIONS.

| $E^{C}_{kin}$ $[MeV/u]$ | $\epsilon^{dp}$ [%] | $\epsilon^{tp}$ [%] | $\epsilon^{pd}$ [%] | $\epsilon^{td}$ [%] | $\epsilon^{dt}$ [%] |
|---|---|---|---|---|---|
| $90^o$ | | | | | |
| 115 | 4 ± 7 | 1 ± 2 | 1 ± 1 | 10 ± 18 | 6 ± 12 |
| 150 | 7 ± 8 | 0.4 ± 1 | 2 ± 2 | 9 ± 8 | 5 ± 6 |
| 221 | 4 ± 4 | 1 ± 2 | 2 ± 3 | 6 ± 6 | 7 ± 9 |
| 279 | 5 ± 4 | 0.5 ± 1 | 2 ± 2 | 6 ± 6 | 7 ± 7 |
| 351 | 5 ± 4 | 1 ± 2 | 2 ± 2 | 11 ± 10 | 8 ± 8 |
| $60^o$ | | | | | |
| 115 | 4 ± 4 | 1 ± 1 | 1 ± 2 | 3 ± 3 | 13 ± 13 |
| 150 | 4 ± 3 | 2 ± 3 | 1 ± 2 | 3 ± 2 | 15 ± 16 |
| 221 | 4 ± 4 | 2 ± 2 | 1 ± 2 | 3 ± 3 | 16 ± 16 |
| 279 | 4 ± 3 | 2 ± 3 | 1 ± 2 | 3 ± 2 | 16 ± 16 |
| 351 | 4 ± 3 | 5 ± 7 | 2 ± 3 | 3 ± 3 | 15 ± 15 |

# OLD FLUKA vs NEW FLUKA

**@90°,60°**

**Nothing has changed in view of the published PAPER results**

## OLD

Table III

PARTICLE IDENTIFICATION EFFICIENCY: SELECTION EFFICIENCIES EVALUATED FOR BOTH 90° AND 60° DETECTION CONFIGURATIONS.

| $E^{C}_{kin}$ $[MeV/u]$ | $\epsilon^{pp}$ [%] | $\epsilon^{dd}$ [%] | $\epsilon^{tt}$ [%] |
|---|---|---|---|
| $90^o$ | | | |
| 115 | 95 ± 5 | 89 ± 9 | 85 ± 12 |
| 153 | 95 ± 5 | 85 ± 14 | 91 ± 6 |
| 221 | 94 ± 5 | 85 ± 12 | 86 ± 10 |
| 281 | 94 ± 5 | 84 ± 12 | 71 ± 31 |
| 353 | 94 ± 5 | 84 ± 14 | 81 ± 15 |
| $60^o$ | | | |
| 115 | 95 ± 4 | 78 ± 21 | 76 ± 32 |
| 153 | 95 ± 5 | 77 ± 22 | 83 ± 17 |
| 221 | 95 ± 5 | 75 ± 23 | 73 ± 32 |
| 281 | 95 ± 5 | 75 ± 24 | 76 ± 26 |
| 353 | 94 ± 5 | 75 ± 24 | [illegible] |

T[…]

PARTICLE IDENTIFICATI[…] EVALUATED FOR BO[…]NS.

| $E^{C}_{kin}$ $[MeV/u]$ | [illegible] | [illegible] | [illegible] | [illegible] [%] | $\epsilon^{dt}$ [%] |
|---|---|---|---|---|---|
| $90^o$ | | | | | |
| 115 | 6 ± [illegible] | [illegible] | 2 ± 2 | 12 ± 13 | 5 ± 7 |
| 153 | 10 ± [illegible] | 2 ± 3 | 1 ± 2 | 5 ± 4 | 4 ± 5 |
| 221 | 4 ± 4 | 3 ± 4 | 2 ± 3 | 11 ± 10 | 7 ± 6 |
| 281 | 5 ± 3 | 2 ± 2 | 2 ± 3 | 8 ± 6 | 8 ± 7 |
| 353 | 4 ± 2 | 1 ± 1 | 2 ± 2 | 10 ± 10 | 7 ± 7 |
| $60^o$ | | | | | |
| 115 | 4 ± 3 | 2 ± 2 | 1 ± 2 | 3 ± 4 | 13 ± 13 |
| 153 | 4 ± 2 | 2 ± 2 | 1 ± 2 | 2 ± 2 | 16 ± 16 |
| 221 | 4 ± 4 | 2 ± 2 | 1 ± 2 | 8 ± 14 | 17 ± 17 |
| 281 | 4 ± 3 | 3 ± 3 | 1 ± 2 | 10 ± 19 | 16 ± 16 |
| 353 | 4 ± 3 | 5 ± 6 | 2 ± 3 | 10 ± 14 | 17 ± 17 |

## NEW

Table III

PARTICLE IDENTIFICATION EFFICIENCY: SELECTION EFFICIENCIES EVALUATED FOR BOTH 90° AND 60° DETECTION CONFIGURATIONS.

| $E^{C}_{kin}$ $[MeV/u]$ | $\epsilon^{pp}$ [%] | $\epsilon^{dd}$ [%] | $\epsilon^{tt}$ [%] |
|---|---|---|---|
| $50^o$ | | | |
| 115 | 95 [illegible] | [illegible] 12 | 86 ± 19 |
| 150 | [illegible] | [illegible] 21 | 89 ± 7 |
| [illegible] | [illegible] | [illegible] 12 | 91 ± 6.1 |
| [illegible] | [illegible] | [illegible] 11 | 91 ± 6.3 |
| [illegible] | [illegible] | [illegible] | 83 ± 21 |
| [illegible] | | | |
| [illegible] | [illegible] | 79 ± 20 | 81 ± 30 |
| [illegible] | [illegible] ± 4.8 | 78 ± 22 | 79 ± 30 |
| [illegible] | 95 ± 4.6 | 76 ± 23 | 86 ± 14 |
| [illegible] | 95 ± 4.7 | 76 ± 24 | 83 ± 18 |
| 351 | 94 ± 5.4 | 76 ± 23 | 82 ± 23 |

Table IV

PARTICLE IDENTIFICATION EFFICIENCY: OFF DIAGONAL ELEMENTS EVALUATED FOR BOTH THE 90° AND 60° DETECTION CONFIGURATIONS.

| $E^{C}_{kin}$ $[MeV/u]$ | $\epsilon^{dp}$ [%] | $\epsilon^{tp}$ [%] | $\epsilon^{pd}$ [%] | $\epsilon^{td}$ [%] | $\epsilon^{dt}$ [%] |
|---|---|---|---|---|---|
| $90^o$ | | | | | |
| 115 | 4 ± 7 | 1 ± 2 | 1 ± 1 | 10 ± 18 | 6 ± 12 |
| 150 | 7 ± 8 | 0.4 ± 1 | 2 ± 2 | 9 ± 8 | 5 ± 6 |
| 221 | 4 ± 4 | 1 ± 2 | 2 ± 3 | 6 ± 6 | 7 ± 9 |
| 279 | 5 ± 4 | 0.5 ± 1 | 2 ± 2 | 6 ± 6 | 7 ± 7 |
| 351 | 5 ± 4 | 1 ± 2 | 2 ± 2 | 11 ± 10 | 8 ± 8 |
| $60^o$ | | | | | |
| 115 | 4 ± 4 | 1 ± 1 | 1 ± 2 | 3 ± 3 | 13 ± 13 |
| 150 | 4 ± 3 | 2 ± 3 | 1 ± 2 | 3 ± 2 | 15 ± 16 |
| 221 | 4 ± 4 | 2 ± 2 | 1 ± 2 | 3 ± 3 | 16 ± 16 |
| 279 | 4 ± 3 | 2 ± 3 | 1 ± 2 | 3 ± 2 | 16 ± 16 |
| 351 | 4 ± 3 | 5 ± 7 | 2 ± 3 | 3 ± 3 | 15 ± 15 |

# Differential cross section for proton production from C on PMMA, CH, C vs Eprotons
## - FLUKA (open) vs DATA (filled) -

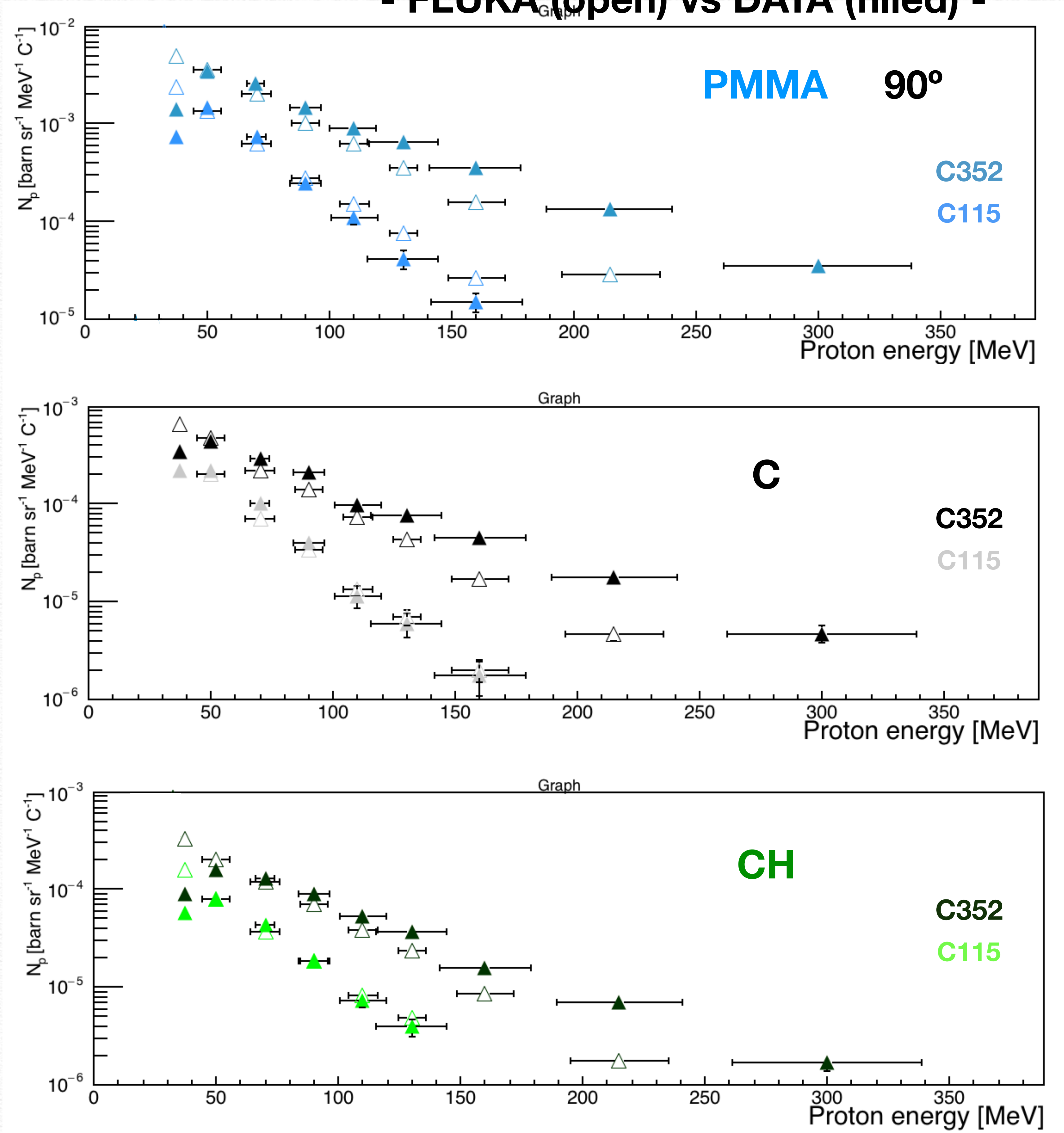


**In DATA there is the contamination of deuterons in the proton signal, especially at large Ekin**

## Differential cross section for proton production from C on PMMA, CH, C vs Eprotons - FLUKA (open) vs DATA (filled) -

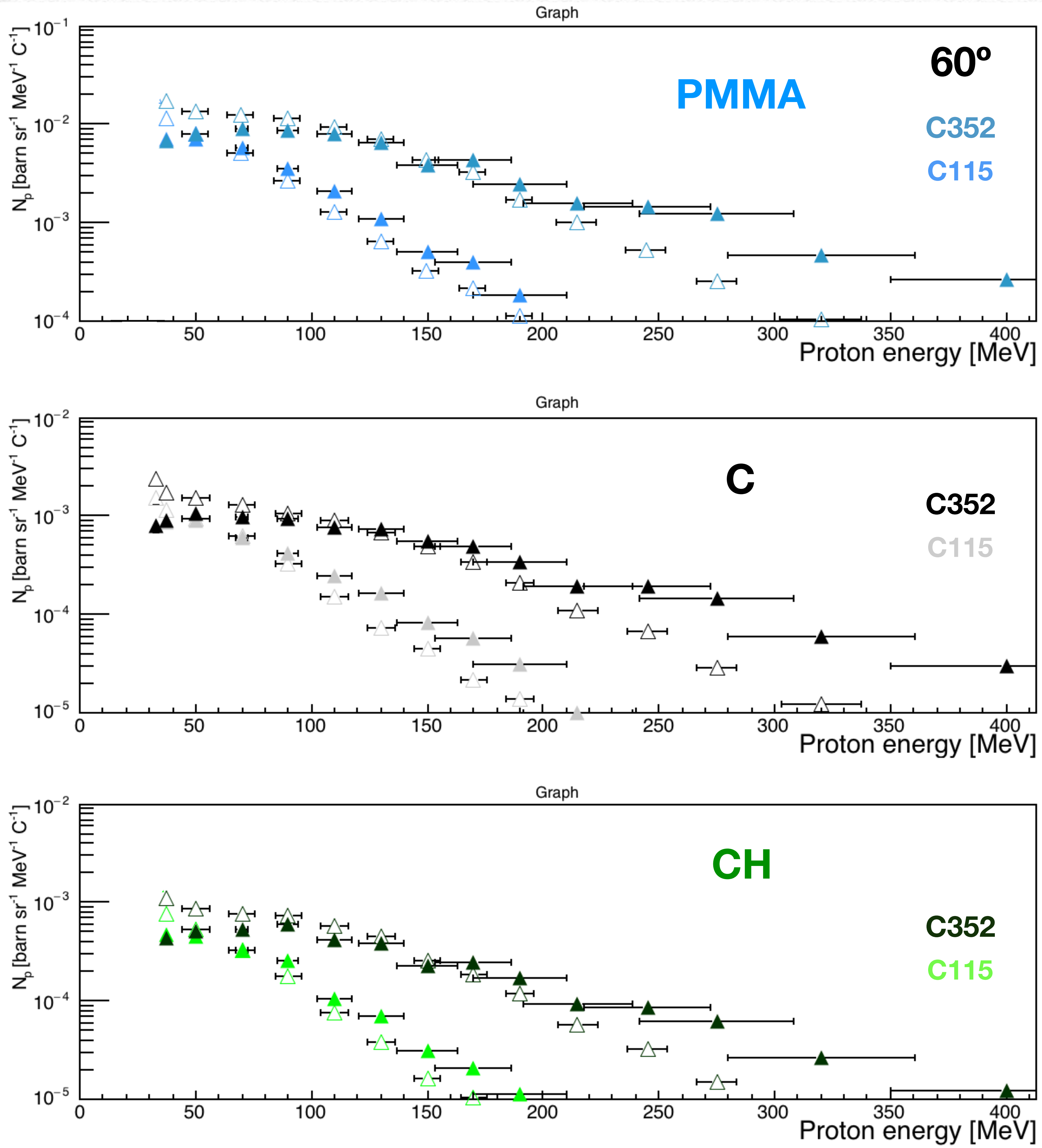


The comparison seems more in agreement at 115 MeV/u wrt 352 MeV/u but it could be due to the deuterons and tritons contamination at high energies (low ToF) and/or to the BME-rQMD models transition => to be investigated

## Differential Cross Section for proton production from C on O, H, C vs Eproton

## - FLUKA (open) vs DATA (filled) -

**C**

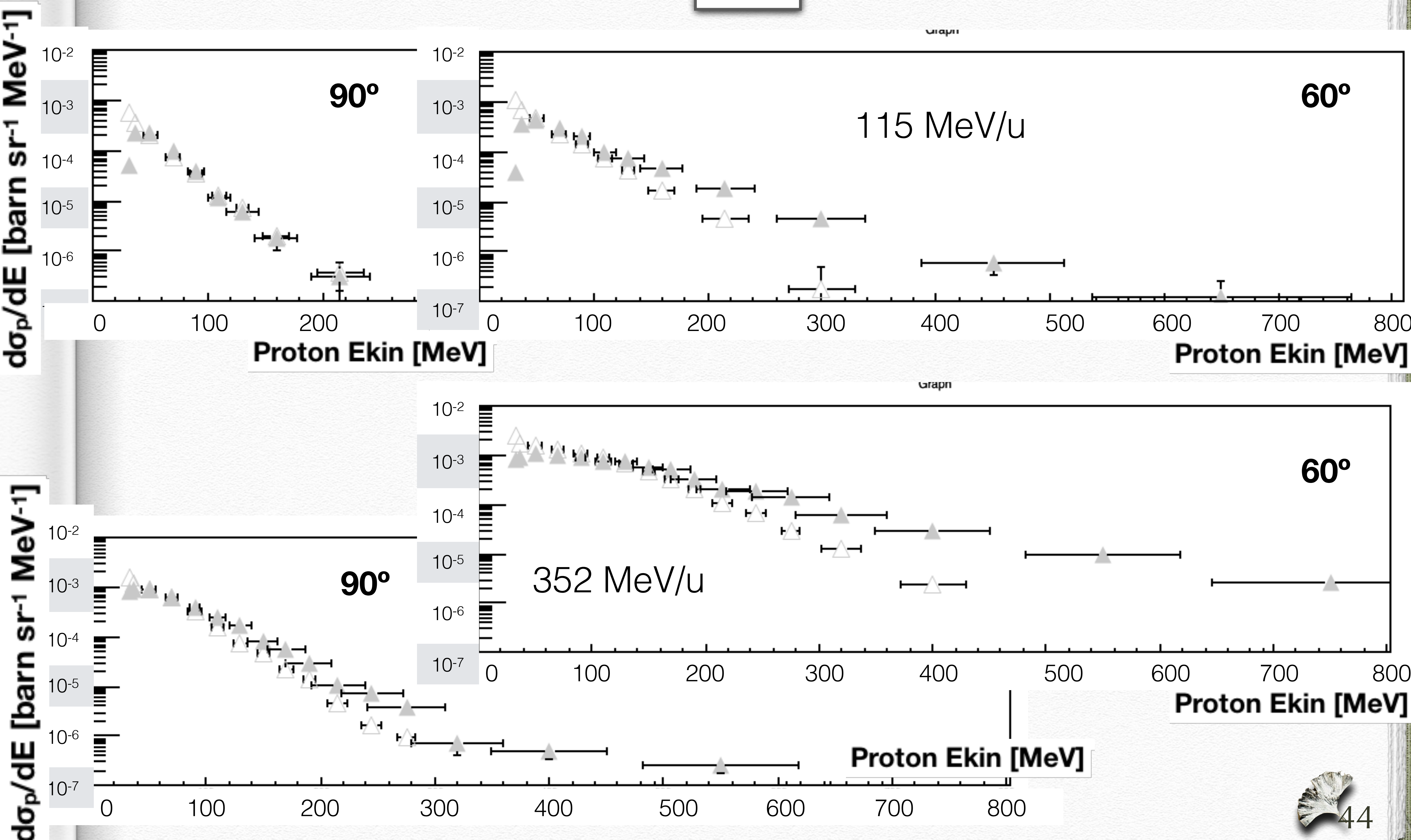

# Differential Cross Section for proton production from C on O, H, C vs Eproton

## - FLUKA (open) vs DATA (filled) -

**O**

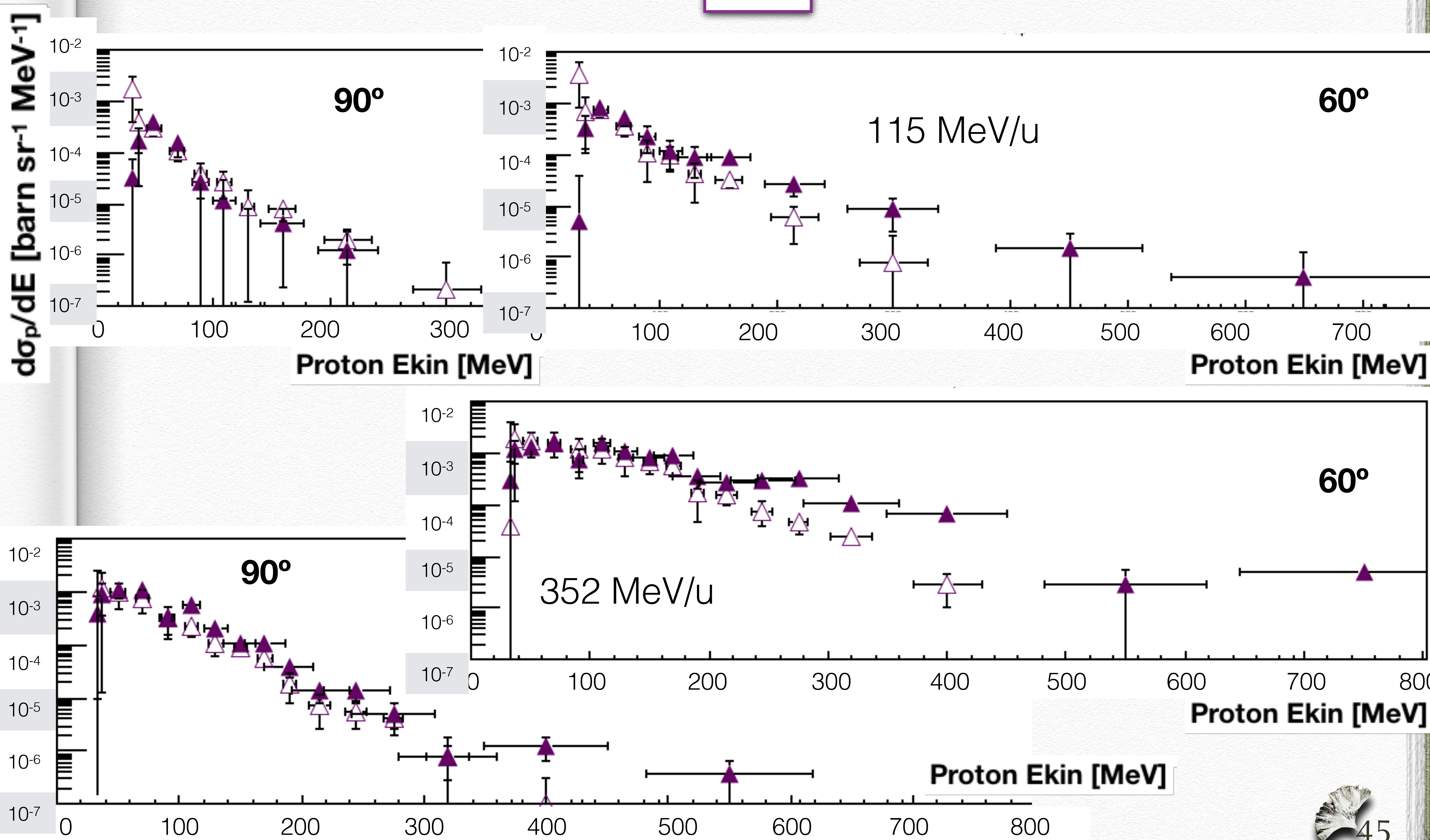

## Total Cross Section for proton production from C on O, H, C vs Ebeam

**- FLUKA (open) vs DATA (filled) -**

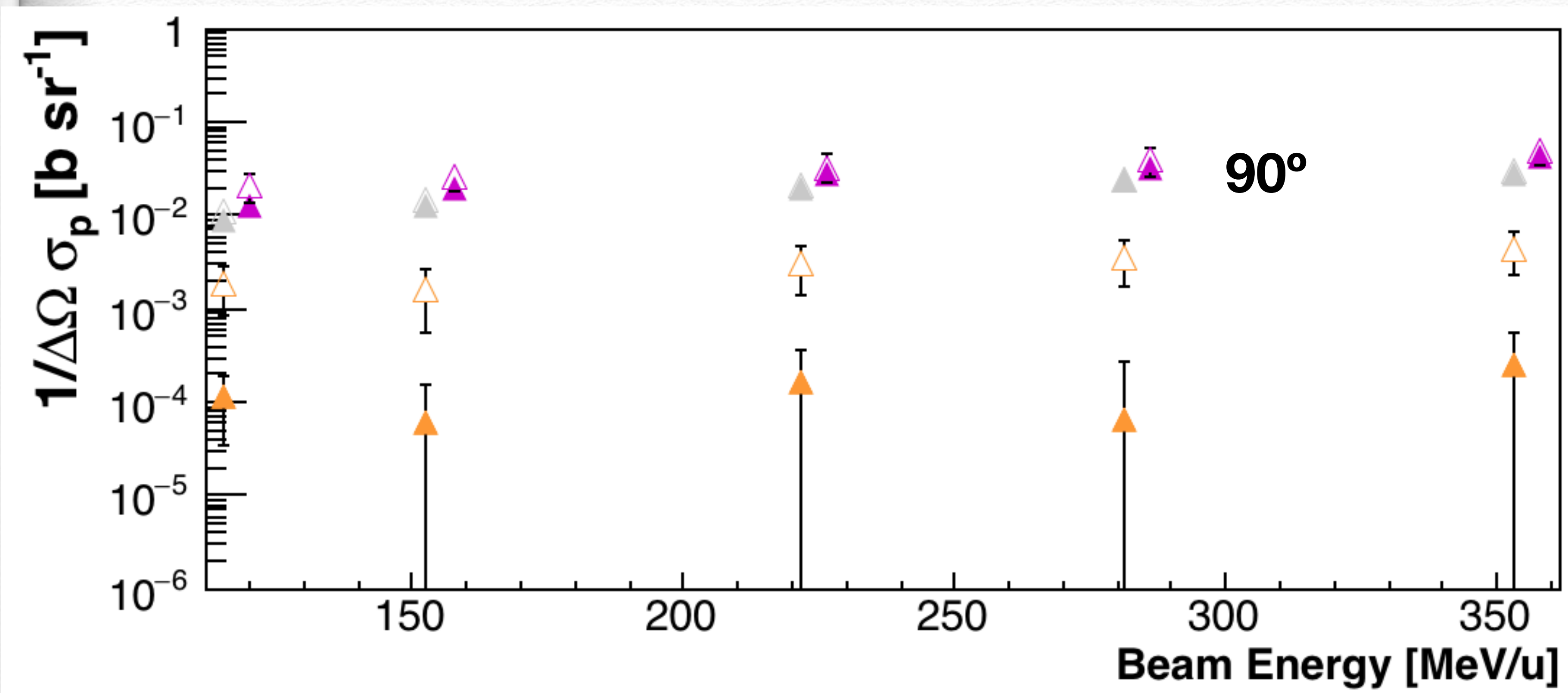


**C**

**O**

**H**

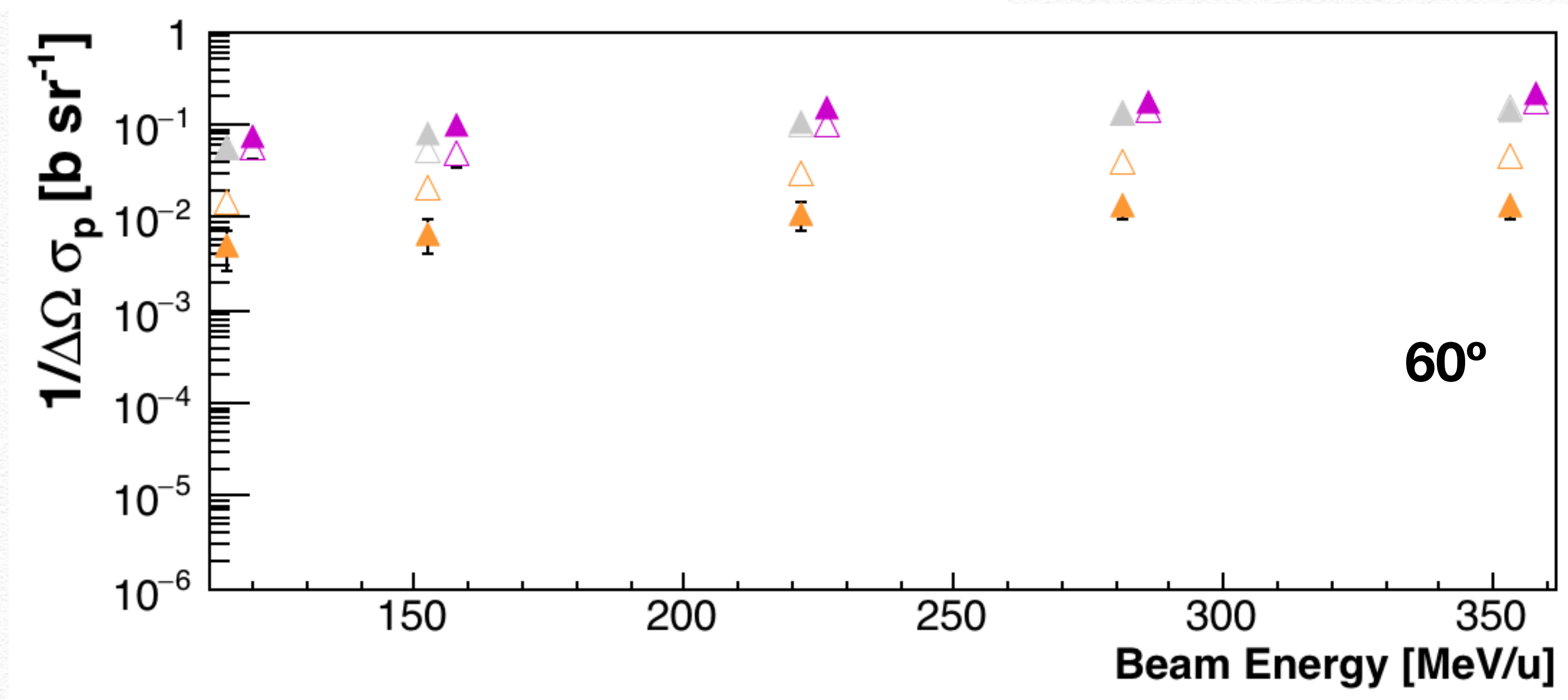


**Here DATA have been corrected for the contamination of deuterons in the proton signal**

## Total Cross Section for proton production from C on O, H, C vs ANGLE

**- FLUKA (open) vs DATA (filled) -**

**C** **O** **H**